



This work is protected by copyright and other intellectual property rights and duplication or sale of all or part is not permitted, except that material may be duplicated by you for research, private study, criticism/review or educational purposes. Electronic or print copies are for your own personal, non-commercial use and shall not be passed to any other individual. No quotation may be published without proper acknowledgement. For any other use, or to quote extensively from the work, permission must be obtained from the copyright holder/s.

WORK FUNCTION CHANGES OF CLEAN AND CONTAMINATED
METAL FILMS IN VACUUM
AND IN HYDROGEN

being
a thesis presented for the
Degree of Doctor of Philosophy
at the University of Keele.

by
R.C. Maddison, B.A., A.Inst.P., F.R.A.S.

Department of Physics,
University of Keele,
Keele,
Staffordshire.

April, 1964.



IMAGING SERVICES NORTH

Boston Spa, Wetherby

West Yorkshire, LS23 7BQ

www.bl.uk

BEST COPY AVAILABLE.

VARIABLE PRINT QUALITY

ACKNOWLEDGEMENTS

I wish to express my gratitude to:-

Professor D.J.E. Ingram for encouragement and the use of his laboratory and research facilities:

Dr. D.E. Davies for his guidance and helpful discussion at all stages of this work:

My thanks are also due to:-

My colleagues of the Physics Department, University of Keele, for helpful discussions during the course of this work:

Mr. F. Rowerth and his staff for assistance and advice in constructional work:

Finally, to Miss S. Lawson for her time and care in typing this thesis.

SYNOPSIS

This investigation is concerned with changes in the work functions of evaporated metal films caused by gas adsorption and variations in temperature. The importance of such changes is underlined by a description of the work function dependent discharge processes, and previous work in the field is reviewed.

The occurrence of cathodic insulating layers in vacua of the order of 10^{-9} mm.Hg. is demonstrated, and their origin is traced to the glassware of heated manifold components.

The variation of work function with film thickness is investigated and can be explained by the existence of sandwich layer structures of gas and metal and indicates a maximum depth beyond which film discontinuities cease to affect the surface work function.

Temperature variations in work function have been measured in vacua of 10^{-9} mm.Hg and 10^{-10} mm.Hg. for several single and superimposed metals and are attributed to temperature dependent adsorption of hydrogen, water vapour and oxygen together with both structural changes within the films and a temperature dependence of work function due to expansion and contraction. The temperature coefficient for the work function of silver is measured as $9.5 \times 10^{-5} \pm 11\% \text{ eV/}^\circ\text{C}$.

The diffusion of hydrogen through heated palladium is investigated as a possible proton source but the only ion emission appears to be that due to thermal desorption from the metal surface on initial heating.

CONTENTS

<u>Chapter I.</u>	<u>BASIC IONIZATION PROCESSES IN</u>	
	<u>GAS DISCHARGES</u>	
1.1.	Introduction	1
1.2.	Ionization Processes	2
	1.2.1. Gaseous Collision Processes	2
	1.2.2. Electrode Collision Processes	5
	1.2.3. Thermionic and Field Emission	11
	1.2.4. The Influence of Adsorbed Layers	13
1.3.	The Growth of Ionization in Uniform Fields	16
	1.3.1. Introduction	16
	1.3.2. The First Ionization Coefficient in Hydrogen	17
	1.3.3. Secondary Processes	21
1.4.	Paschen's Law	24
1.5.	Effect of the Cathode Work Function	27
1.6.	The Development of a Discharge in Time	31
1.7.	Conclusion	33
 <u>Chapter II.</u>	 <u>EFFECTS OF CONTAMINANTS AND SURFACE</u>	
	<u>NATURE ON WORK FUNCTIONS</u>	
2.1.	Introduction	36
2.2.	Method and Technique of Work Function Measurement	37

2.3.	Previous Work	43
2.3.1.	Structure of Evaporated Film	
	Electrodes	43
2.3.2.	Effects of Foreign Films	50
2.3.3.	Admission of Hydrogen as a Source	
	of Positive Ions	61
2.4.	Conclusion and Introduction to Present	
	Work	64

Chapter III. **DESCRIPTION OF APPARATUS AND EXPERIMENTAL**
PROCEDURE

3.1.	The Vacuum System	66
3.2.	The Ultra-High Vacuum System	71
3.3.	Vacuum Techniques	74
3.4.	The High Voltage Supply and Measurement	
	of Sparking Potentials	81
3.5.	Construction of Experimental Tubes	83

Chapter IV **EXPERIMENTAL RESULTS**

4.1.	Introduction	88
4.2.	Tube 1	89
4.3.	Tube 2	93
4.4.	Tube 3	94
4.5.	Tube 4	96
4.6.	Tube 5	98
4.7.	Tube 6	104
4.8.	Tube 7	105

Chapter V.

DISCUSSION OF RESULTS AND CONCLUSIONS

5.1.	Introduction	110
5.2.	Glass Decomposition and the Admission of Hydrogen	
5.3.	Effects of Discharges	
5.4.	The Production of Positive Ions from Heated Palladium.	
5.5.	The Stability of the Reference Surface	124
5.6.	Variation of Film Thickness	
5.7.	Effects of Cathode Cooling	
5.8.	The Superimposition of Different Metals	132
5.9.	Effects of Reduced Residual Gas Pressure	138
5.10.	Suggestions for Further Work	143

LIST OF FIGURES

- Figure 1 Potential energy of a metal in a vacuum.
- 2 The potential associated with the image force.
- 3 Details of potential energy near a metal surface
- 4 Potential energy diagram and electronic transitions
 for helium ions on molybdenum.
- 5 Effect of an accelerating field at the surface
 of a metal.
- 6 Schematic representation of significant gas-
 surface interactions.
- 7 Effect of adsorbed layers on potential near a
 metal surface.
- 8 Current Voltage characteristic of a gas discharge.
- 9 $\log I/I_0$, d curve for hydrogen at low pressures.
- 10 Previous determinations of the variation of
 α/p with E/p .
- 11 The variation of α/p with E/p for $E/p < 400$.
- 12 The variation of ω/α with E/p in hydrogen.
- 13 Minimum sparking potentials for hydrogen using
 different cathodes.
- 14 Variation of V_m with nature of cathode surface.
- 15 Variation of formative time lag with overvoltage
 in hydrogen at constant E/p .
- 16 Potential difference between two metals connected
 and separated in a vacuum.

- Figure 17 Contact Potential difference circuit and low frequency amplifier,
- 18 Reduction of potential energy near a surface projection.
- 19 Effects of impurities on cathode work functions.
- 20 Effect of a film of copper on the work function of nickel.
- 21 Changes in ϕ due to the use of a silver soldered palladium thimble.
- 22 The Vacuum system.
- 23 Internal spherical glass joint.
- 24 Pumping frame and measuring equipment.
- 25 High vacuum system and hydrogen producer.
- 26 Manifold and experimental tube.
- 27 Alpert ionization gauge.
- 28 Sparking potential circuit.
- 29 Typical electrode arrangement with Kelvin surface over cathode.
- 30 Typical electrode arrangement with sparking anode over cathode.
- 31 Change in ϕ with time Tube 1 (Copper)(a).
- 32 Change in ϕ with time after sparking.
- 33 Paschen curves for copper and silver in hydrogen.
- 34 Variation of ω/α with E/p for copper and silver in hydrogen.

- 35 Change in ϕ with time, tube 1 (b).
- 36 Palladium thimble and 'dummy' unit.
- 37 Variation of ϕ with time, Tube 2.
- 38 Change in ϕ with time Tube 3 (silver) (a)
- 39 Change in ϕ with time Tube 3 (b).
- 40 Design of Tube 4 and manifold.
- 41 Change in ϕ with time Tube 4 (a).
- 42 Change in ϕ with time Tube 4 (b)
- 43 Internal structure of Tube 5.
- 44 Photograph of Tube 5.
- 45 Change in ϕ with time Tube 5 (a).
- 46 Change in ϕ with time Tube 5 (b).
- 47 Change in ϕ with time Tube 5 (c).
- 48 Electrometer circuit for detecting positive ion emission.
- 49 Change in ϕ with time Tube 6.
- 50 Photograph of Tube 7.
- 51 Electrode and furnace layout, Tube 7.
- 52 Changes in contact potential difference and ϕ with time, Tube 7 (a).
- 53 Change in ϕ with time Tube 7 (b).
- 54 Change in ϕ with time Tube 7 (c).

CHAPTER I
BASIC IONIZATION PROCESSES IN
GAS DISCHARGES

1.1. Introduction

The sharp discontinuity in the conducting characteristics of an electrically stressed gas, normally called breakdown, has excited the interest of investigators since the discovery of the electron in 1897. The results of such investigations have led directly to the development of thermo-nuclear physics, arc rectifiers and switches, and numerous high voltage devices, but the study of the transition from insulator to conductor in even the most simple two electrode, single gas system is still far from complete.

The elementary processes occurring at this point of breakdown, which are important in understanding the breakdown mechanism, can be divided under two headings: (a) the gaseous collisional processes which may involve electrons, ions, photons or gas molecules, and (b) the electrode processes which may be photo-electric, thermionic or field emission, or impact processes involving positive ions, metastable or normal atoms.

An attempt is made in this thesis to see how the microstructure of the electrode surfaces can affect the important discharge parameters, and to investigate the changes caused by

condensed or adsorbed electrode films.

The investigation concerns, particularly, changes in the work functions of evaporated metal cathodes caused by, (a) the presence of adsorbed impurity layers, (b) the presence of positive ions on such insulating layers, (c) the presence of foreign metal films, (d) variations in the thickness of the cathode metal films and (e) the state of metal annealing.

1.2. Ionization Processes

1.2.1. Gaseous Collision Processes

Moving electrons can cause ionization by collisions with atoms, and the efficiency of the process depends on the kinetic energy of the electrons. Ionization will occur if this energy is greater than the ionization energy of the atom eV_i . The result of a collision is generally a positive ion and two slow electrons and the rate of ionization is directly proportional to the current, and is zero for $\frac{1}{2}mu^2 = eV_i$.

If the electron energy is less than eV_i then ionization cannot take place in a single collision but the atom may be raised to an excited state and subsequently ionized by another slow electron. For this the total incident electron energy must be greater than eV_i . This process requires a high concentration of electrons since the mean life of a normal excited state is of the order of 10^{-8} sec.

An important case arises if the excited state is a metastable level where the mean lifetime is of the order of

10^{-1} sec and the chance of a favourable collision is much greater than that for an excited state. The rate of ionization for such a double-impact process is proportional to the square of the current. If the gas contains atoms of another element having an ionization energy less than the potential energy of the metastable atom, then a collision of the second kind can occur in which potential energy from the metastable atom is used to ionize the impurity atom. Only small traces of impurity are necessary for this process to affect breakdown characteristics, (1), and it is important in work involving mixtures of gases.

A collision of the second kind may take place, for example, between a metastable neon atom Ne_m and an argon atom, A, to produce a neon atom and a positive argon ion, with the release of an electron.



Gas atoms and their positive ions can collide in two ways depending on their energies. If the ion is of low energy the interaction takes place slowly and an elastic collision occurs which is nearly adiabatic. Under these circumstances the ion loses half its total energy per collision. On the other hand, if the ion is energetic there will be insufficient time for the internal adjustment of the system and the collision will be inelastic. In this case either an electron or a photon will be produced, (2). It seems,

however, (3. 4), that the cross-section for this type of event is very low except for energies $\gg 50\text{eV}$ and the process is therefore important only for very low pressure discharges. A further possible electron release process exists for collisions involving negative ions in which electron detachment occurs, (2), but this is only important in gases having a high electron affinity and is not relevant to the present work in hydrogen.

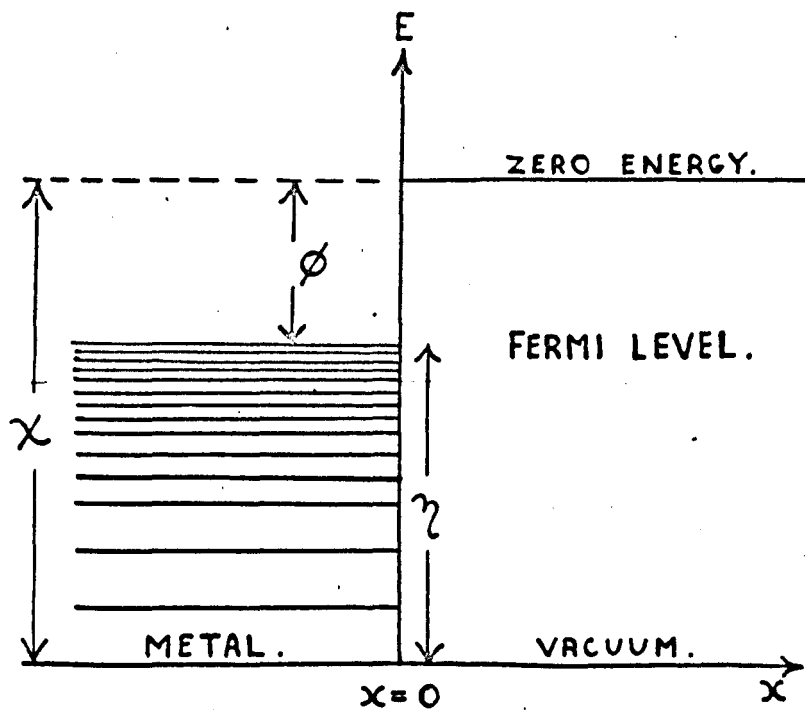
When an excited atom spontaneously reverts to its ground state a photon is emitted of energy $h\nu$, equal to the difference of energy between the two states. This photon can ionize an atom by 'collision' if its energy is of the order of the ionization energy of the atom. Unlike other collisional ionization processes the maximum cross-section for photo-ionization is for $h\nu = eV_i$ and is greater at higher pressures. The present investigation is concerned with discharges in pure hydrogen and since the ionization energy is greater than the energy of any excited state in this single electron system, photo-ionization cannot occur. If, however, impurity atoms, having high energy excited states, are present, then the process may become important. A low energy photon may liberate an electron already in an excited state, but because of the short life-time of excited states the cross-section for the event is very small.

In considering the possible conduction processes in a gas, the processes leading to loss of ionization must also be taken into account. Rapid deionization takes place when all ionization sources are removed and this is attributed to the processes of recombination, attachment and diffusion. Recombination of positive ions and electrons takes place by normal collision processes, the electron generally giving up most of its kinetic energy to a third particle or releasing it as a quantum of radiation. Most of this kinetic energy is absorbed by the wall of the containing vessel when the fast neutral particle impinges on it. If an electron attaches itself to a neutral particle to form a negative ion a normal recombination process may take place in which the excess energy is carried off by two neutral particles. Negative ions produced in this way, together with positive ions and electrons, may diffuse to the walls under the influence of concentration gradients. Neutralization can then take place at the surface with consequent dissipation of energy in the walls.

1.2.2. Electrode Collision Processes

The electrode processes to be described all depend in some way on the energy required to liberate an electron from the cathode surface, namely the cathode work function.

If the potential energy of an electron in a metal is lower than that of an electron above its surface by an amount χ , and if electron energies in the metal are distributed



Potential Energy of a Metal in a Vacuum.

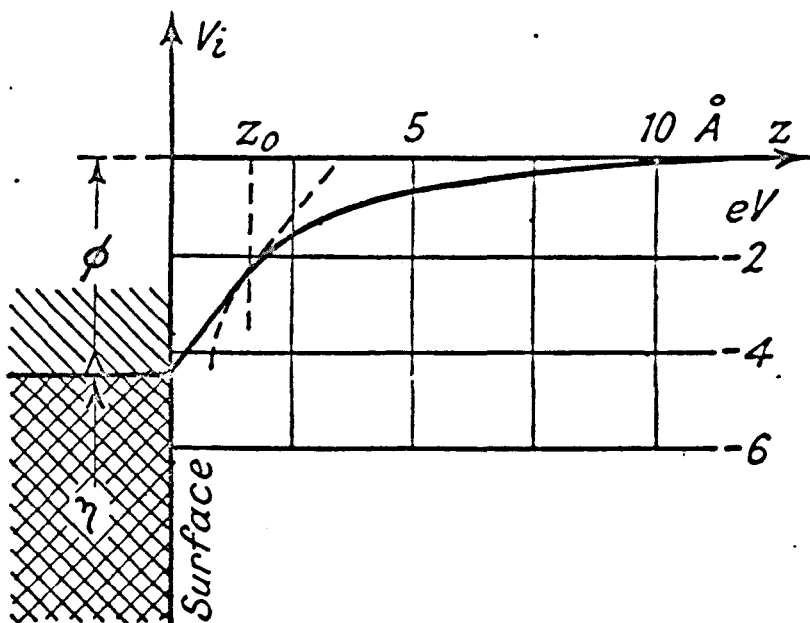
Fig. 1.

according to Fermi-Dirac statistics with the Fermi level at χ , then the surface barrier ϕ is the difference $(\chi - \eta)$ and is a measure of the energy required to remove an electron from the metal. The quantity ϕ is called the work function of the metal surface, Figure 1.

This potential barrier can be attributed to two causes, firstly the existence of an electrical double layer, and secondly an image force between the escaping electron and its mirror charge inside the metal.

Firstly, a few electrons that have escaped from the metal will form an electron atmosphere which, because of the electric charges, will have a greater density near the surface. At equilibrium the double layer formed will prevent more electrons from escaping. The fall of potential in the double layer can be shown, (5) to be (η/e) .

Outside the metal the electron density is very low and the particles behave like the molecules of a rarefied gas. At thermal equilibrium, with as many electrons being emitted from the surface as are absorbed by it, the energies are distributed according to the Maxwellian distribution. The energies of the electrons in this atmosphere can be assumed to be zero at the absolute zero of temperature. Within the metal energies up to η are present and equilibrium is attained when the potential drop in the double layer is equal to the maximum energy η within the metal.



The Potential V_i associated with the Image Force.

Fig. 2.

Secondly, a metal becomes polarized when an electron escapes from its surface so that an electrostatic force exists between the electron and its reflected positive image. If an electron is at a distance z in front of the surface, then the image force as calculated by Schottky, (6), using Coulomb's law is

$$F_i = \frac{e^2}{4\pi\epsilon_0(2z)^2}$$

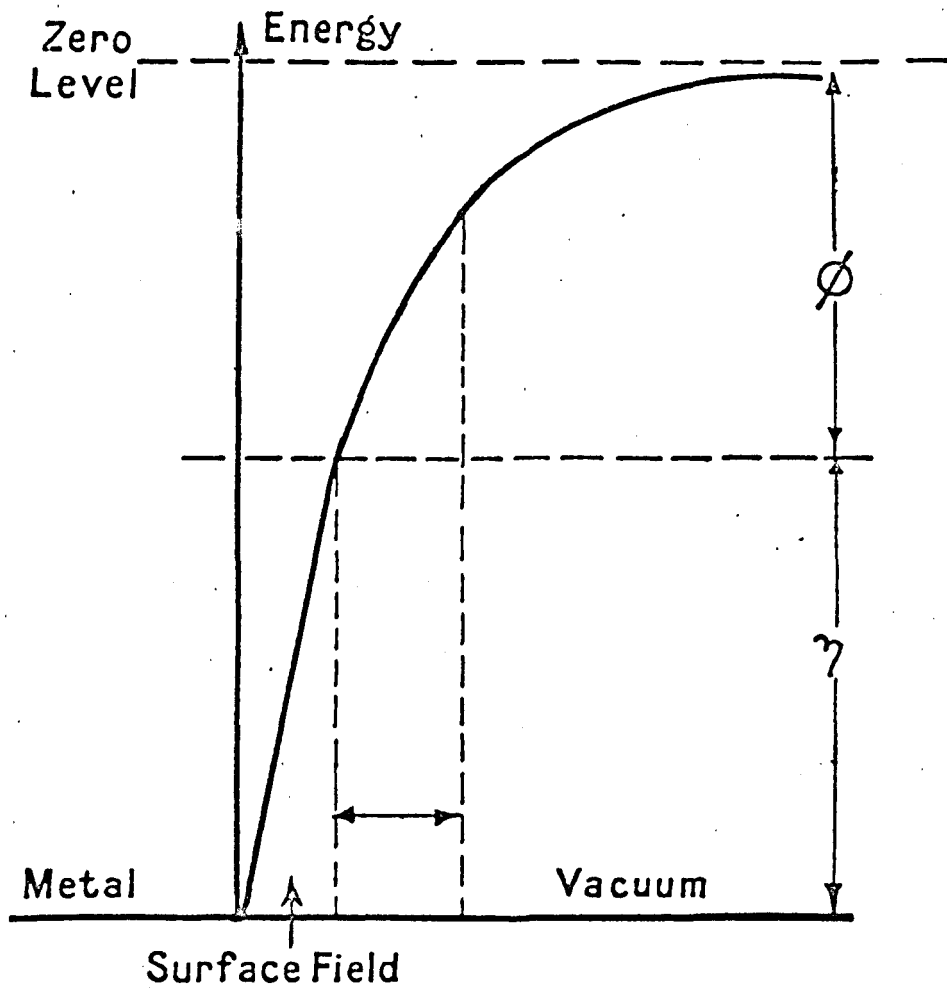
Where ϵ_0 is the dielectric constant for a vacuum, and the field strength corresponding to this force is,

$$E_i = \frac{e}{16\pi\epsilon_0 z^2}$$

The absolute value of the image force potential V_i , associated with E_i , is defined in such a way that it tends to zero as z approaches infinity, (7).

$$\text{then} \quad V_i = \int_z^{\infty} E_i(z) dz = \frac{-e}{16\pi\epsilon_0 z} \quad (1)$$

This equation was calculated assuming a uniform distribution of charge in the metal but for small values of z the influence of discrete charges becomes important. The shape of the image potential curve for small values of z is approximated by Schottky (Figure 2), by constructing a tangent to the curve at a critical distance z_0 so that the potential is assumed to decrease linearly with decreasing distance until at $z = 0$, V_i is the Fermi level. For $z > z_0$ the potential is



Details of potential energy near metal surface.

Fig. 3.

described by equation (1).

The work function may be expressed as the sum of these two parts, whence,

$$\phi = \frac{e}{8\pi\epsilon_0 z_0} = 7.2 \times 10^{-8} \cdot \frac{1}{z_0} \text{ eV.}$$

The critical distance z_0 is of the order of inter-atomic distances, i.e. about 10^{-8} cm, and if it is made equal to the lattice spacing, d , of the metal crystal then the work function obtained is nearly proportional to $1/d$. This implies that metals having large atomic volumes have small work functions and metals of high density have large work functions. This relationship is, in fact, observed.

The variation of potential energy near a metal surface can now be represented, (Figure 3), as a combination of the surface double layer effect and the image force.

Certain mechanisms are available for overcoming or reducing the surface potential barrier and thus promoting the emission of electrons. These may be classified as emission due to the following:-

- (a) The incidence of energetic positive ions, metastable or neutral atoms.
- (b) The incidence of radiant energy, i.e. photo-electric emission.
- (c) The absorption of heat energy from within the metal, i.e. thermionic emission.

Potential energy diagram and electronic transitions for helium ions on molybdenum *a* for direct AUGER neutralisation, *b* for resonance neutralisation followed by AUGER de-excitation.

- (d) The application of a strong electric field at the surface, i.e. field emission.
- (e) The building of a dipole layer on the surface having its positive side outwards.

The first two processes will be considered here as collisional processes and the others will be considered in subsequent sections as separate phenomena.

When positive ions are incident on a metal surface the processes of electron emission depend on the energy of the incident ions. If the ions are fast then the kinetic energy may be converted into heat which is sufficient to cause local thermionic emission, (8).

Oliphant and Moon, (9) found that the energy distribution of electrons emitted by fast positive ions is consistent with such a thermionic process.

It is also possible that the incident ion might cause the acceleration of electrons that are already nearly free in the metal, (10).

Another possible process for fast positive ions is that of direct Auger neutralization, (11). The fast ion may penetrate the potential barrier before capturing an electron and becoming an excited atom. It may then immediately give up its energy to an electron near the Fermi level, (Figure 4(a)) which may have sufficient energy to be emitted.

This is possible if $eV_i > 2\phi$. If the ion is slow it may be resonance neutralized by an electron from the filled band of the metal, having the same energy as an excited state in the atom, (12). Photo-electric emission may then take place as the excited atom returns to its ground state, (Figure 4(b)). If, however, the initial neutralization takes place within 10^{-7} cm of the metal the impact may take place before radiation can occur. In this case the excess energy of the atom may be given, by a collision of the second kind, to an electron in the metal which may then have sufficient energy to be emitted. For this to happen the energy of the excited state of the atom eV_{ex} must be greater than ϕ .

Neutral atoms may eject electrons from metals if they have sufficient kinetic energy. This process is similar to that for high energy positive ions, i.e. local heating leading to thermionic emission. The only condition for emission by metastable atoms is that $E_m > \phi$, where E_m is the energy of the metastable state. Since the only metastable state of hydrogen is of low energy, and is easily destroyed by very weak fields, the process is unimportant in the present work.

Incident radiation can cause the emission of an electron at absolute zero if the electron can gain an amount of energy equal to or greater than the work function, i.e. when $h\nu_0 \geq \phi$ where h is Planck's constant, and ν_0 is the threshold

frequency. The number of electrons liberated will be proportional to the intensity of the radiation at the required frequency. If the frequency is greater than ν_0 electrons can be liberated with kinetic energy greater than zero, but those electrons which have energy near to zero may include electrons from below the Fermi level. At room temperature it is possible that photo-emission will occur for frequencies less than ν_0 because of the finite probability of electrons in the metal having energy greater than the Fermi level.

The process of photo-electric emission may take place when radiation is produced by excited gas atoms returning to their ground states during discharges.

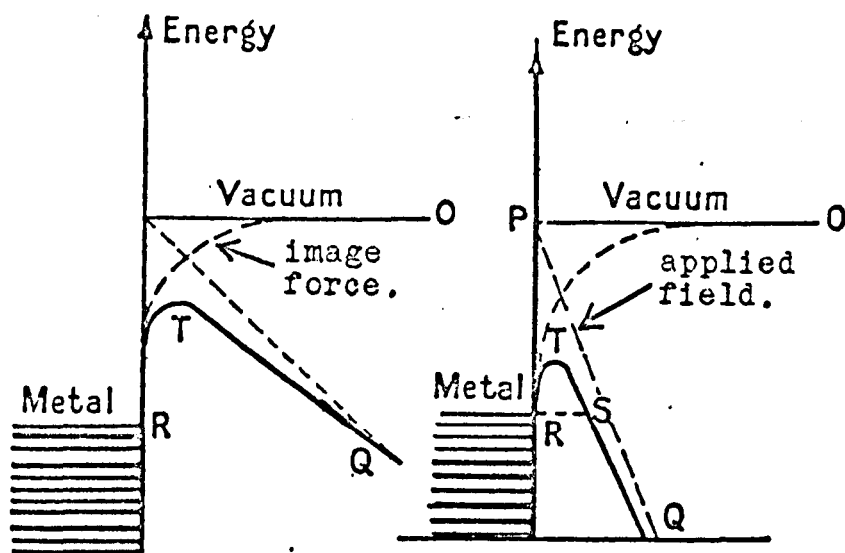
1.2.3. Thermionic and Field Emission

When a metal is heated to a sufficiently high temperature, its electrons may acquire sufficient kinetic energy to penetrate the potential barrier at its surface.

Richardson, (13) calculated a relationship between thermionic emission and temperature assuming that the electrons in a metal behave as if they are a perfect gas and that they have a Maxwellian distribution of energies. Later, however, Dushman, (14) derived a form of this equation which rested on sounder theoretical principles.

The Richardson-Dushman equation is:-

$$J = AT^2 \exp \frac{-b_0}{T}$$



Accelerating
field

High accelerating
field

Effect of an Accelerating Field at
the Surface of a Metal.

Fig. 5.

where J is the saturation current density, T the absolute temperature and b_0 is a constant of the emitting surface such that $b_0 k = \phi_0$ where k is Boltzmann's constant, and ϕ_0 is the thermionic work function. ϕ_0 is the work in electron volts necessary to remove unit charge of electrons from the surface. The constant A has the value $\frac{2\pi em^2 k^2}{h^3} = 60.2 \text{ amp/cm}^2 \text{ deg}^2$ where m is the mass of an electron. Modern theory suggests that this constant A should be doubled to take into account the spin of the electron. Experimental determinations of A for many metals are near the uncorrected value, but variations in the surface condition of the metals can account for the discrepancy.

Nordheim, (15, 16), obtained the same thermionic equation from statistical considerations and included the factor $(1-r)$ where r is the probability of reflection of emitted electrons.

Thermionic emission is negligible at the temperatures experienced in this investigation.

The application of a strong accelerating field at the surface of a metal reduces and thins the potential barrier to electron emission, thus effectively reducing ϕ , (Figure 5). The potential slope of the applied field must be added algebraically to that of the image force field thus leading to a reduction in ϕ where $\Delta\phi = e^{3/2} x^{1/2}$ and an emission of

$$I_a = I_0 \exp\left(\frac{e^{3/2} x^{1/2}}{kT}\right)$$

where x is the applied field, I_a and I_0 are the currents with and without the field respectively. This is the Schottky equation (17) which is accurate when applied to clean metals.

For high applied fields the potential barrier is reduced in thickness sufficiently for the wave mechanical tunnel effect to become important for electrons near the Fermi level. This field emission is independent of temperature but the required field is of the order of 10^7 volts/cm.

Field emission may be enhanced by surface contamination and the presence of gases. The theoretical work of Stern, Fowler and Gossling, (18), on this effect indicates that the reduced field necessary for emission under these conditions is of the order of 10^5 volts/cm, which is still greatly in excess of any fields encountered in this work. Very large fields may be built up by the accumulation of positive charges on insulating cathodic layers, but these are generally much less than 10^5 volts/cm since the insulation is not usually good enough to withstand high fields. Applied fields may also be exaggerated at the cathode surface by the existence of molecular irregularities such as projecting crystal corners and submicroscopic points, (19). This may cause a local increase of field up to a factor of ten for optically smooth surfaces.

1.2.4. The Influence of Adsorbed Layers

All gases form adsorbed layers on solid surfaces

but the binding forces involved may vary considerably.

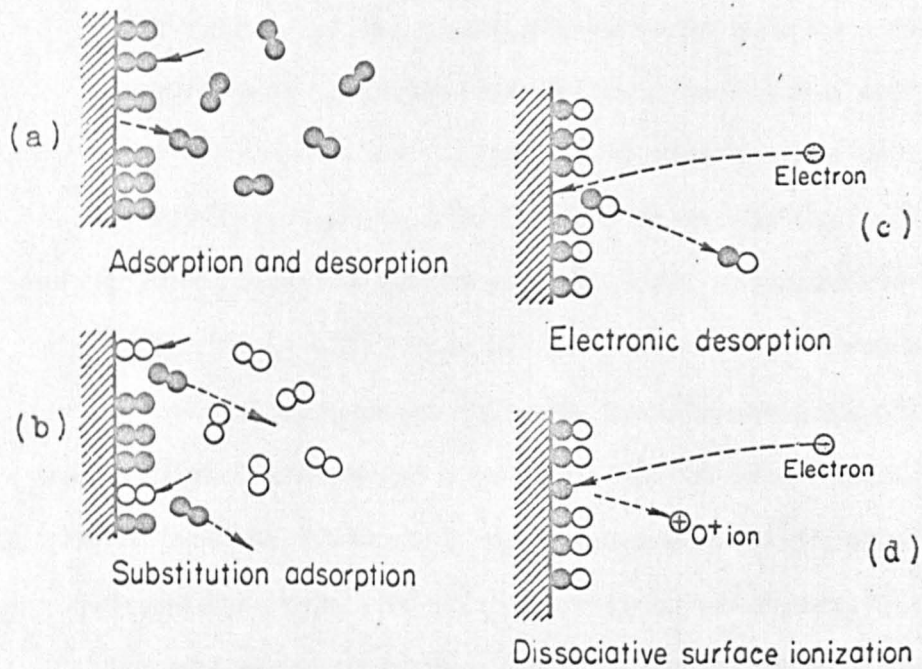
When an atom or an ion is subjected to an electric field the centres of positive and negative charge become separated and a dipole is formed.

At a surface image forces exist and an attractive force predominates which depends on the polarisability of the components.

If the difference of Gibbs free energies for the reaction between the components represents a total decrease in free energy of the system then a chemical bond may be formed in which electronic orbitals overlap and relatively stable compounds may be formed. Such chemisorption is generally irreversible and is increased by increasing temperature.

If, however, the difference of free energies for the reaction represents a total increase in free energy, and if no external electric field exists, then Van der Waals cohesive forces only can operate. These are formed by the continually varying field due to the electrons of one atom causing a continually varying dipole in the other atom. These forces are generally very weak, the process is reversible and the amount of adsorption increases with decreasing temperature.

The time taken for a gas to form a monolayer on a surface, as calculated from the random kinetic velocities of the gas molecules at room temperature, depends inversely on



Schematic representation of
significant gas-surface reactions

Fig. 6.

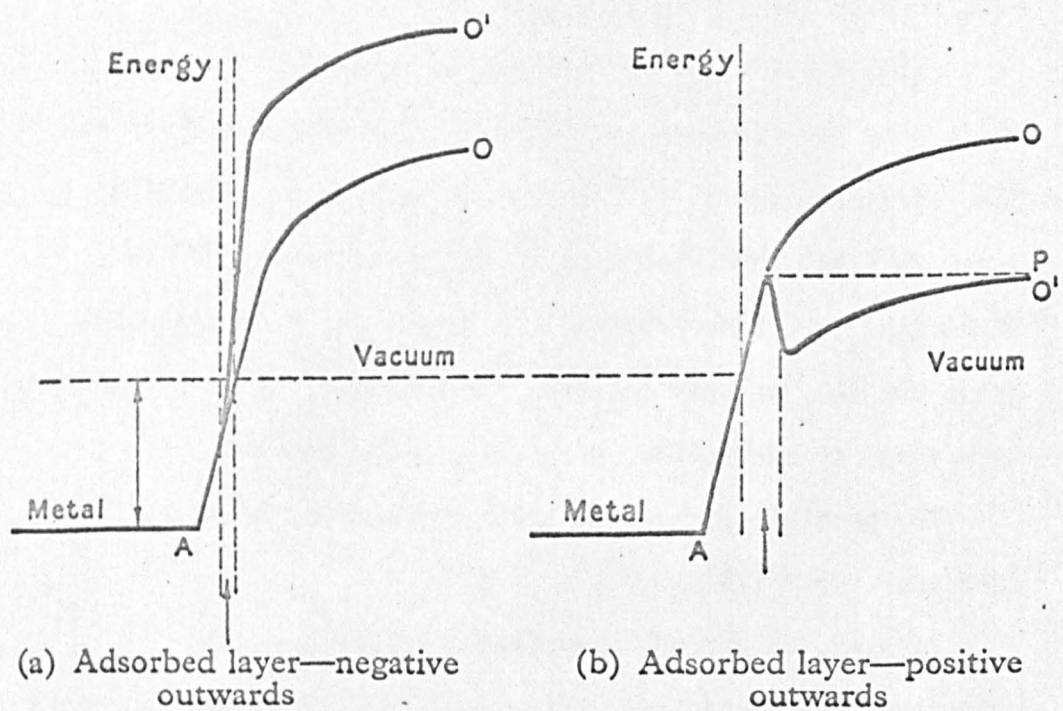
the pressure. Bloomer and Haine (20) have found the relationship for oxygen to be:-

$$\text{time} = 2.4 \times 10^{-6}/p \text{ seconds per sq.cm.}$$

where p is the pressure in mm.Hg., which indicates, for example, that at a pressure of 10^{-4} mm.Hg a monolayer will form in 2.4×10^{-2} sec. and that at 10^{-8} mm.Hg the time is 240 sec. These figures are correspondingly larger for non-adsorbable gases but they clearly indicate the necessity of using ultra-high vacua if adsorption effects are to be avoided.

The possible gas-surface interactions can be divided into four types (21):-

Firstly, as already described, the processes of adsorption and desorption acting concurrently and in equilibrium under any set of conditions, (Figure 6.(a)). Secondly, the process of substitutional adsorption, (Figure 6(b)). It has been found that some atoms or molecules adsorb preferentially on a surface and do so by displacing previously adsorbed molecules or atoms having lower binding energies. This process becomes important on the introduction of gases to a system when the surface nature may change considerably. Thirdly, there is the possibility of electronic desorption (22). An electron or positive ion incident on a surface may provide sufficient energy to desorb a weakly adsorbed particle, (Figure 6(c)). Finally there is the process of dissociative surface ionization (23. Figure 6(d)), in which adsorbed



Effect of Adsorbed Layers on the Potential
near a Metal Surface.

Fig. 7.

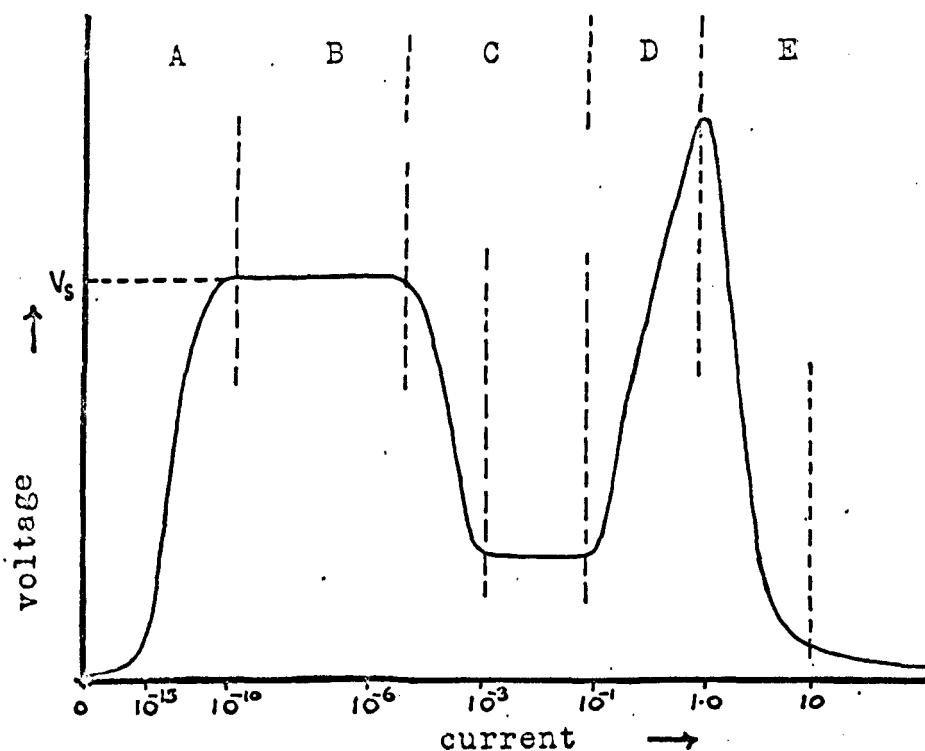
molecules may be dissociated by an incoming particle causing the release of an atomic ion.

Surface adsorbed layers modify the potential barrier at the surface and therefore change the potential energy of an electron passing through it. It can be shown that if n is the number of dipoles/cm², e the magnitude of the positive and negative charges of separation d , and M the dipole moment ed , then there is a change in work function of $4\pi neM$. If the dipoles have their negative charges outwards ϕ is increased; if the positive charges are outwards ϕ is decreased, (Figure 7).

1.3. The Growth of Ionization in Uniform Fields

1.3.1. Introduction

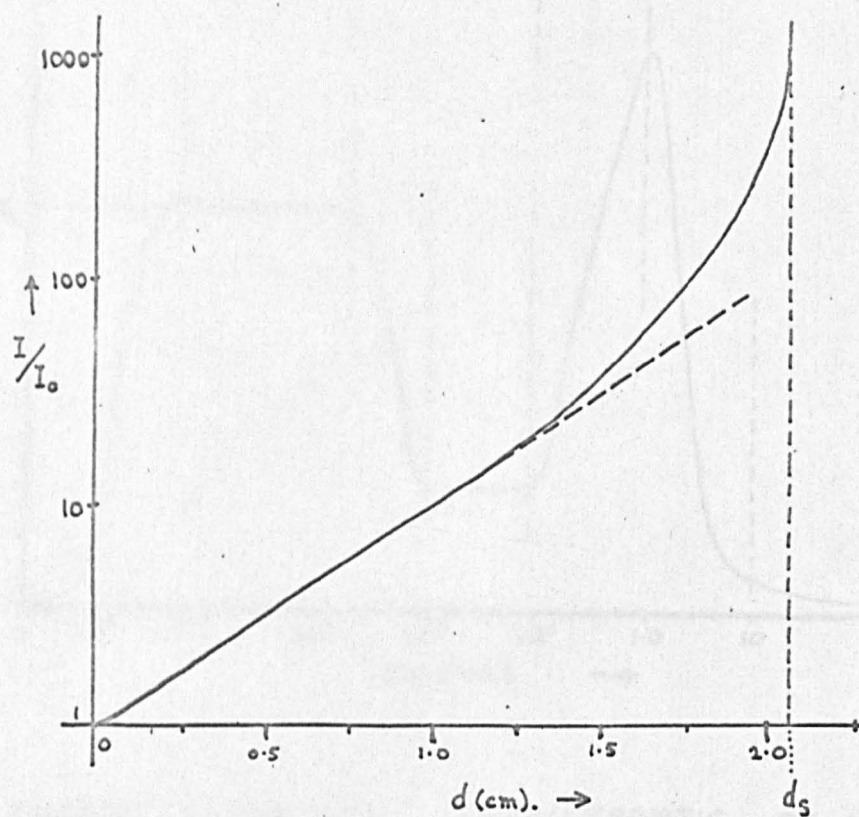
The current voltage characteristic for a gas discharge between two parallel plate electrodes is shown in Figure 8. If a small current I_0 , which is sufficient to ensure ionization in the gap, is maintained between the electrodes, and if a steadily increasing voltage is applied to the gap, the current will increase until some critical voltage V_g is reached, at which the discharge current I becomes independent of I_0 . As the voltage is further increased, the current is determined by the external circuit, in particular by the source impedance. If this impedance is low the voltage may be reduced as the current increases from about 10^{-6} amp into the glow discharge. A lower supply impedance would enable the



CURRENT — VOLTAGE CHARACTERISTIC OF A
GAS DISCHARGE.

- A - Townsend pre-breakdown.
- B - Townsend discharge.
- C - Normal glow.
- D - Abnormal glow.
- E - Arc.

Fig. 8.



Log I/I_0 , d curve for Hydrogen at Low Gas Pressures.

Fig. 9.

transition through the abnormal glow into the arc discharge region where a gap resistance of the order of a tenth of an ohm allows the passage of very high currents.

The present investigation is confined to the first part of the discharge characteristic, i.e. the Townsend pre-breakdown region and the self-maintained discharge with currents up to 10^{-7} amp.

The processes taking place under these conditions for uniform fields will be considered in more detail.

1.3.2. The First Ionization Coefficient in Hydrogen

The mean energies of electrons and ions moving through a gas under the influence of a field, E , are dependent upon the gas pressure p . An investigation of the manner in which the growth of current varies with electrode geometry and construction requires that the mean particle energies are kept constant, and this implies that for different pressures, the ratio E/p must be kept constant. It is also necessary that, in order to eliminate possible field distortion due to space charge effects, the currents used should not exceed 10^{-7} amps.

A typical curve for the variation of $\log I/I_0$ with d , for a given E/p , is shown in (Figure 9). For all values of E/p , but small values of d , the linear part of the curve can be described by:-

$$I = I_0 \exp. \alpha d,$$

where α is a constant depending on the gas and which is called the primary Townsend Coefficient. This coefficient is defined as the average number of electrons produced by ionizing collisions in the gas, per unit distance travelled in the direction of the field, by each primary electron. The distance, d , is defined as the geometrical electrode separation, d_g , minus the distance d_0 , required by an electron, immediately after its emission from the cathode, to acquire its mean energy.

If recombination and motion at right angles to the field are neglected an electron will acquire sufficient energy to cause ionization in a distance, λ where,

$$\lambda = \frac{V_i}{E}$$

The probability of a mean free path, L , being greater than λ is, from kinetic theory:-

$$\exp.\left(-\frac{\lambda}{L}\right)$$

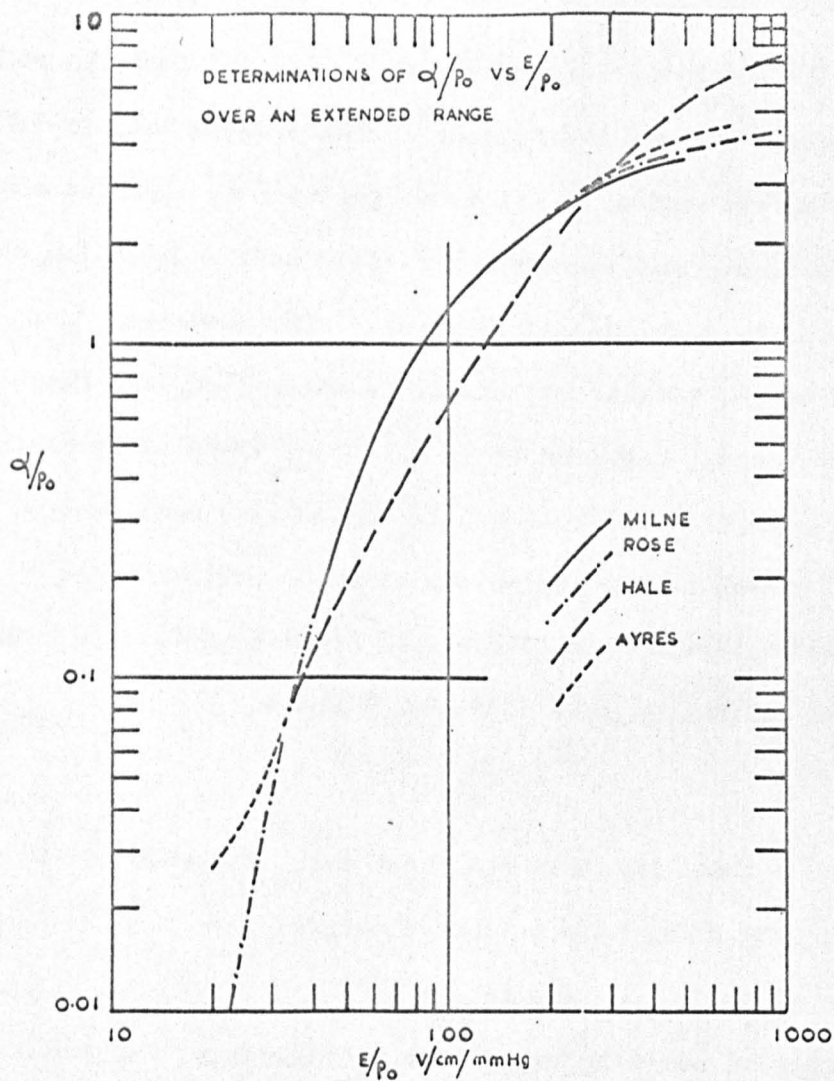
The number of ionizing collisions per electron, per unit distance, α , which is equal to the number of free paths multiplied by the chance that $L > \lambda$ can be expressed

$$\text{thus } \alpha = \frac{1}{L} \exp.\left(-\frac{V_i}{LE}\right) \quad (2)$$

Since $\frac{1}{L} = A p$, where A is a constant. Equation (2) can be written

$$\frac{\alpha}{p} = A \exp.\left(-\frac{AV_i p}{E}\right) \quad (3)$$

showing that α/p is a function of E/p , (24).



Previous Determinations of the Variation
of α/p with E/p .

Fig. 10.

It is found experimentally that the curves for α as a function of E/p , at different values of p , do not coincide but that the curves for α/p as a function of E/p for different pressure are coincident.

Equation (3) has been derived by making certain assumptions, for example, that the probability of ionization is zero for energies $< eV_i$ and is unity for energies $> eV_i$, but reasonable agreement with experiment is obtained by careful choice of the constant A .

For large values of d the processes of secondary emission, discussed in Section 1.2, become important and the upcurving part of the $\log I/I_0$, d curve can be described by:-

$$I = \frac{I_0 \exp \omega d}{1 - \omega/\alpha (\exp \omega d - 1)} \quad (4)$$

where (ω/α) is the generalised Townsend coefficient for secondary processes.

The earliest determinations of the variation of α/p with E/p , those of Townsend, (25), Ayres, (26), and Hale, (27), were not in very good agreement. Hale's values of α/p were much lower than Ayres' for the range of E/p between 40 and 300 and much higher than Ayres' for E/p greater than 400, (Figure 10).

It seemed that Hale's values were likely to be the most accurate owing to much improved vacuum techniques and rigid precautions against contamination, particularly from

mercury vapour. More recent determinations, however, (28, 29, 30, 31), indicate that Ayres' measurements were more reliable although he worked with a vacuum no better than 10^{-3} mm.Hg and used no freezing traps. The theoretical determinations of Emeleus, Lunt and Meek, (32), and Townsend (33), agree well with Ayres' determinations.

For the range of E/p between 50 and 200 the recent determinations of Rose, (34), Blevin, Haydon and Somerville, (35), and Milne, (36), agree well with those of Ayres. Rose used much improved vacuum techniques and obtained residual gas pressures less than 10^{-9} mm.Hg. The hydrogen used in these determinations was carefully purified by the formation of uranium hydride and its subsequent dissociation.

This comparison indicates that the contaminants likely to have been present for Ayres' measurements did not affect greatly the values of α/p .

The above determinations (29, 30, 31), for $E/p < 50$ were made in the absence of Hg vapour and under better vacuum conditions than those of Ayres', and although they are mutually consistent they differ markedly from Ayres' values. This difference may have been due to Ayres' poor purity conditions.

Milne, (36), Myatt, (37), and Fletcher, (38), in this laboratory have measured α/p in the range of E/p between 40 and 500 using evaporated metal electrodes and residual

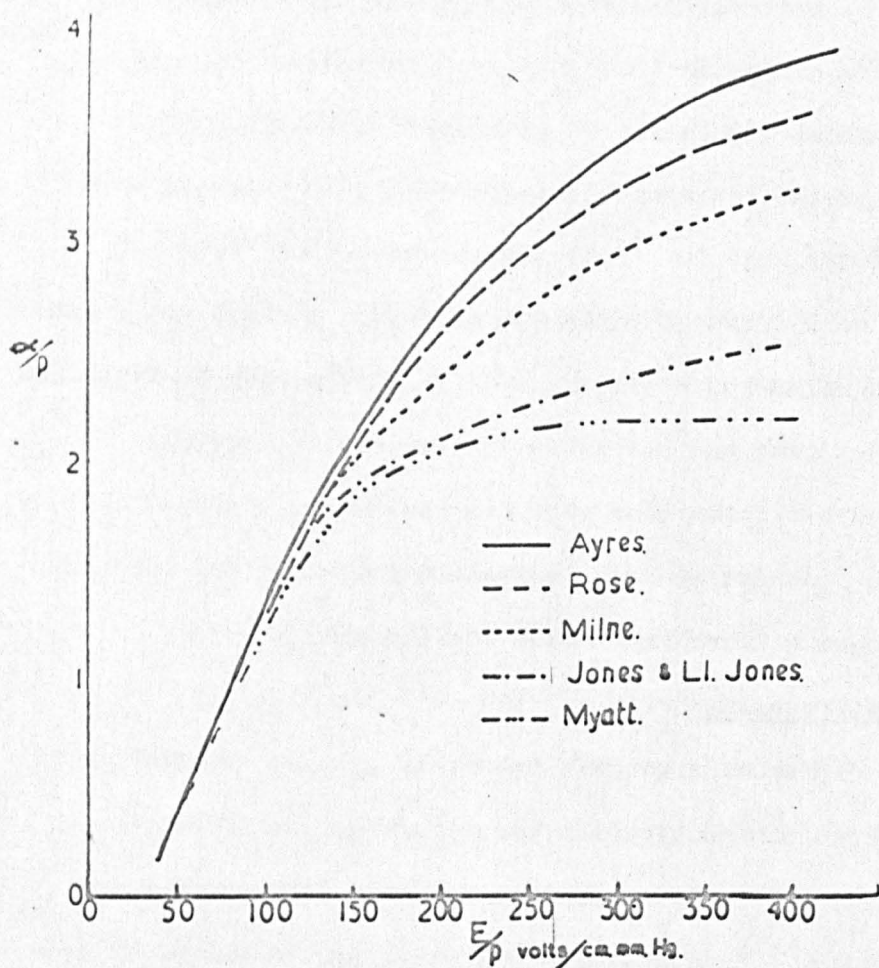
gas pressures less than 10^{-9} mm.Hg. The hydrogen used was obtained by electrolysis of barium hydroxide solution and purified by diffusion through palladium and the formation, and subsequent dissociation, of uranium hydride. (This uranium hydride technique is described in more detail later.)

It seems that for $E/p > 100$ the values of α/p decrease with increasing gas and electrode purity, (c.f. curves for Rose, Milne and Myatt, Figure 11). This may be explained by the fact that the ionization potentials of possible contaminants will be less than the ionization potential for hydrogen. A rise of mean ionization potential for the gas will produce a lower ionization coefficient.

1.3.3. Secondary Processes

The different secondary processes by which ionization may be produced and by which the upcurving portion of the curve (Figure 9), may be explained, have been described in Section 1.2.. Each of these processes may be described by a separate coefficient but measurement of these coefficients is extremely difficult since the processes act together and are not easily separated.

Gas ionization by positive ions and photons can be represented by coefficients β and k which are similar to the Townsend primary coefficient α . The cross-section for photoionization is very low and it can be neglected except at high pressures. The surface processes of photo-electric



Previous Determinations of the Variation of α/p with E/p for E/p less than 400.

Fig. 11.

emission and emission due to the incidence of excited and metastable atoms may be represented by coefficients δ and ϵ , again similar to α . Emission due to the incidence of positive ions is described by a coefficient γ , defined as the number of electrons liberated from the cathode per ionizing collision in the gas, and this process is highly dependent on the nature of the cathode surface.

The generalised coefficient (ω/α) can be approximately made up by a linear sum of the individual coefficients thus:-

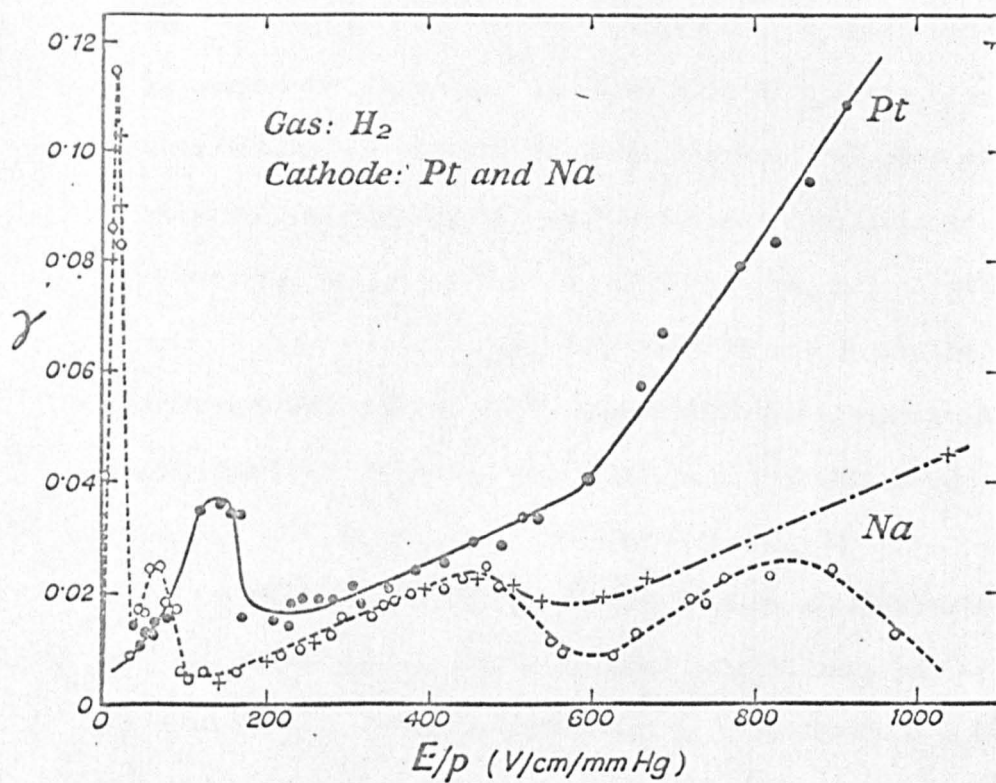
$$\omega = \beta + \alpha\gamma + \delta + \epsilon + k \dots$$

Unfortunately each of these separate coefficients leads to the same form of expression for the upcurving of the $\log I/I_0$, d curve, and, as mentioned earlier, it is impossible to estimate the relative importance of the various secondary processes from this curve.

The variation of ω/α with E/p may be investigated by measuring the discharge current for different values of E , p and d and substituting in equation (4).

This method, however, is very tedious and requires several days to build up the ω/α , E/p curve. It is certain that the condition of the cathode surface will not have remained constant during this time and since most of the secondary processes are extremely surface sensitive the final curve must be unreliable.

Hale's measurements by this method, (39), indicate that the nature of the cathode surface has a marked effect on



Values of γ as a function of E/p in hydrogen.

Fig. 12.

ω/α , (Figure 12).

For hydrogen at low pressures the important secondary processes are (a) the incidence of positive ions on the cathode, and, (b) photo-electric emission. The efficiencies of both these processes are dependent on ϕ for the cathode surface.

Hagstrum, (40 - 44) has measured the secondary coefficient for the incidence of positive ions, taking extensive precautions to ensure clean surfaces. He has shown that emission is virtually independent of the ion kinetic energy in the range from 10 to 1,000 volts and is thus highly dependent on ion potential energy. The presence of gas layers on the surface reduces the coefficient for low energy ions, the effect being greatest for oxygen due to its high electronegativity.

The steady increase in ω/α at high E/p , (Figure 12), is thought to be due to predominant emission by positive ions, (45, 46). At low E/p photo-electric emission should be dominant and the photon absorption in the gas at very low values of E/p should practically eliminate the process. The shape of Hale's curves can be explained in this way but his results are probably unreliable at very high and very low values of E/p (see section 1.3.2.).

A simpler, but more restricted, method of determining the variation of ω/α with E/p is from the sparking potential curve.

The method depends on accurate knowledge of the variation of α/p with E/p for exactly similar conditions as for the sparking potential measurements and is, therefore, of limited application.

It can be seen from the current growth curve, (Figure 9), that for a given E/p there exists a value of gap distance d_s corresponding to an infinite current. For this condition, see equation (4),

$$1 - \frac{\omega}{\alpha} (\exp \alpha d - 1) = 0 \quad (5)$$

and this is known as the sparking criterion.

For a given value of gap distance and gas pressure there is a potential V_s , called the sparking potential which, if applied across the gap, will maintain a current in the gap which is independent of the externally generated current, I_0 . If V_s can be measured and if values of α are known for the same conditions, then ω/α may be easily found. It is usually convenient to define V_s as the potential that will cause a self-maintained current of 10^{-7} amps. Under these conditions the field is not distorted by space charge effects. The values of ω/α obtained in this way are similar to those obtained from the current growth curve (39, 47-51).

1.4. Paschen's Law

At very low gas pressures both the collision frequency and the probability of ionization are low. It follows that

as the pressure is lowered further the electron energies must be increased in order to maintain the level of ionization required for a self-maintained discharge. Thus V_s will increase as the pressure is lowered below a certain value. At much higher pressures the electron mean free paths are small and much energy is lost in frequent low velocity collisions. In order to maintain a constant level of ionization with increasing pressure it is therefore necessary to increase the energy gained per mean free path from the field. This is achieved by increasing the field with a consequent increase in V_s . It can be seen that the values of V_s pass through a minimum as the pressure is varied, for a given value of d .

The work of de la Rue and Muller, (52), indicated that the sparking potential depended on the product pd . Later work in CO_2 and H_2 by Paschen, (53), confirmed that the value of V_s appeared to be a function of pd only.

The statement:-

$V_s = f(pds)$ is known as Paschen's law and typical curves of V_s against pd are shown in (Figure 13) for low values of pd .

The breakdown voltage is dependent on the cathode material, (Figure 13), the greatest effect being in the region of the minimum.

This minimum sparking potential V_{sm} depends on the

state of the cathode and on its secondary coefficients and is a useful indicator in the investigation of surface phenomena in gas discharges.

Deviations from Paschen's law have been found for large values of d which can be explained by electron losses from the gap by diffusion. Townsend and McCallum, (54), working in Neon, and Llewellyn-Jones and Morgan, (55), working in Hydrogen, found that, for a fixed value of pd_g a higher value of V_g is required than that predicted. This effect is small if the gap diameter is small compared to its width. It has also been found by Davies, Dutton and Llewellyn-Jones (56, 57), that ω/α depends on pressure on the range 250 - 450 mm.Hg. This indicates a deviation from Paschen's law which may be due to collisions of the second kind, in which neutral atoms destroy excited molecules thus reducing the number of photons produced. Deviations have also been observed in this laboratory by Davies and Smith, (58) working in mercury vapour.

Using values of α and ω/α obtained from the current growth curves, the sparking distance can be calculated from equation (5) for a known E/p . The measured and calculated Paschen curves are found to be in general agreement indicating that the same basic processes are operating both for low currents and under breakdown conditions.

1.5. Effect of the Cathode Work Function

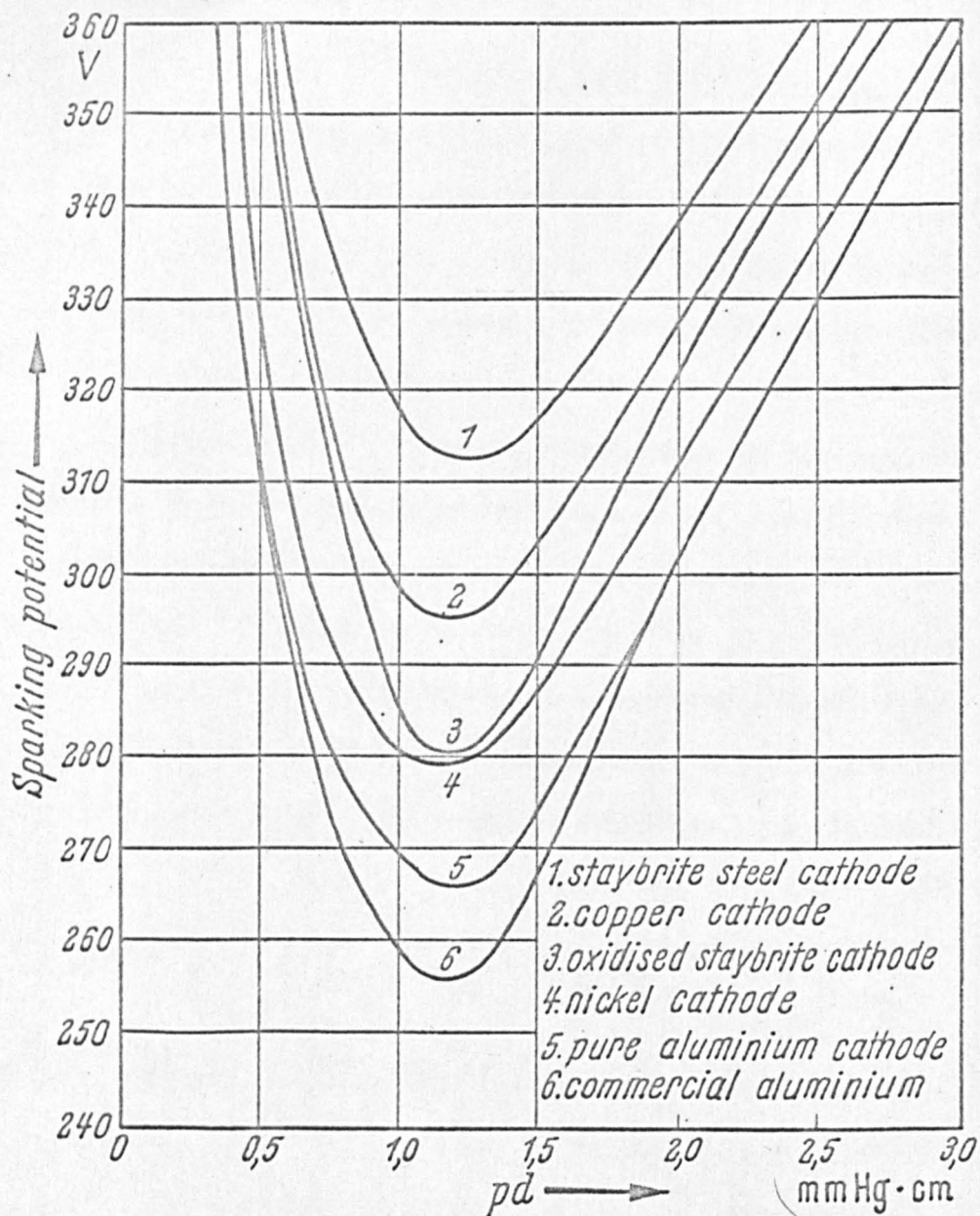
The work of Carr, (59), in 1903 showed that under his pressure conditions there were no differences between the sparking potentials for the fifty metals he studied. Townsend, (60), deduced from these measurements that the predominant secondary process must be that due to positive ions acting in the gas, but no experimental evidence was forthcoming to support this. In re-checking Carr's results for more varied conditions, a great amount of work has been done on the dependence of V_s or ω/α on the cathode surface. If a change in the cathode produces a change of $\Delta(\omega/\alpha)$ in the secondary coefficient and a corresponding change ΔV_s in the sparking potential then, according to Llewellyn-Jones and Henderson, (47), :-

$$\Delta V_s = \frac{\Delta(\omega/\alpha)}{(\omega/\alpha)} \cdot f \frac{V_s}{d_s} \quad (6)$$

It is characteristic for most gases that $\frac{V_s}{p \cdot d_s}$ changes very little for high values of p .

This shows that at high pressures, cathodes with different values of ω/α should have Paschen curves that are almost parallel and that near V_{sm} the fractional change $\frac{\Delta V_s}{V_s}$ should be greater and easier to observe.

Carr's failure to observe changes in V_s with cathode material can be attributed to his experimental conditions.

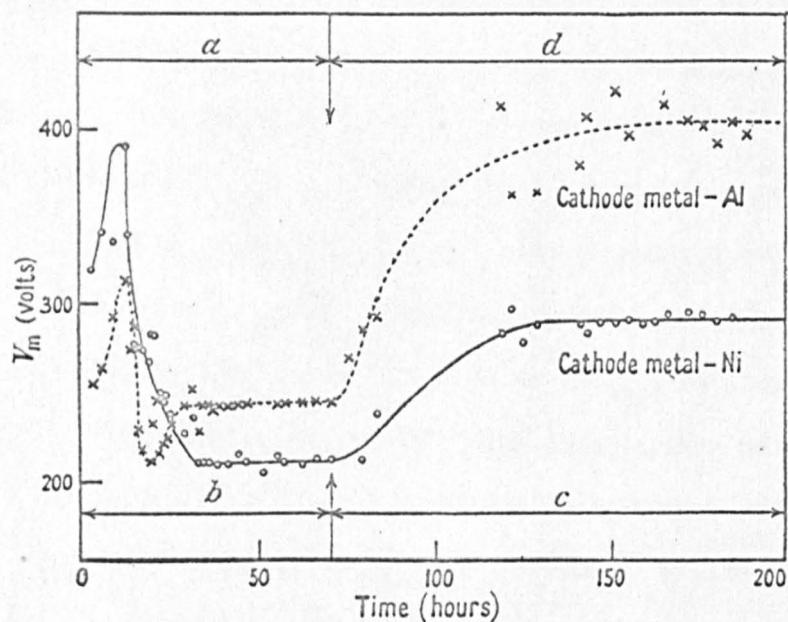


The minimum sparking potential of hydrogen with different cathodes.

Fig. 13.

At high pressures $\frac{\Delta V_s}{V_s}$ would be small and would fall within his experimental error and at low pressures the electrode surfaces, which were not outgassed, would each be covered by similar oxide and adsorbed gas layers which would mask any small changes due to differing materials. Llewellyn-Jones and Henderson, (47), have drawn Paschen curves for six different cathodes in the same sample of hydrogen, (Figure 13). They found a marked dependence of V_{sm} on cathode material, but for values of $pd_s > 100$ the curves were practically indistinguishable. At low values of $P.ds$ the differences were observed only for very clean, de-gassed surfaces, each metal being covered by similar thin layers of hydrogen which were not sufficient to mask the effect of the bulk metal, (c.f. Carr's results). It appeared from these measurements that, for all the metals except nickel, V_{sm} depended on the work function ϕ .

Jacobs and La Rocque, (50. 61) suggested a method of calculating V_{sm} for values of ω/α and ϕ from their work in argon. The values of ω/α obtained from minimum sparking potentials of several different cathodes in argon were plotted against the work functions and the minimum breakdown potentials. Provided the work function of any cathode is known, it is possible to estimate, from the two curves, a value of V_{sm} for that cathode in argon. However, Hale and Huxford, (62), pointed out that the measurements of Bowls, (63), and Ehrenkrantz, (64), did not apply and that the values for iron



Variation of V_m with time during: (a) cleaning of Al cathode, (b) deposition of Al film on Ni cathode, (c) cleaning of Ni cathode, and (d) deposition of Ni film on Al cathode [150]

Fig. 14.

and nickel did not satisfy the relationship.

In 1951, Llewellyn-Jones and Davies, (51, 65), undertook an investigation of the dependence of V_{sm} on cathode conditions in which the composition of the cathode was varied by sputtering different metals on to it. It was found that the normal outgassing procedure of baking at 400°C was inadequate and that, in order to obtain clean surfaces, the electrodes had to be subjected to a glow discharge in hydrogen.

An interesting outcome of this work is that as the second metal was deposited on the first, values of V_{sm} were obtained which were characteristic of neither metal, (Figure 14). This indicates a modification of the effective work function of the cathode by the presence of the thin foreign film, the direction of the modification depending on the relative electronegativities of the metals. It is important, therefore, to determine values of V_{sm} for pure metals, under conditions which eliminate the possibility of foreign metal films, i.e. where both electrodes are of the same metal and stringent precautions are taken against back diffusion of mercury vapour from the vacuum system. It is likely that cleaning by a glow discharge in hydrogen will produce a hydrogen saturated surface which would lead to irregular work function measurements. It is, therefore, an unsuitable process for use in ultra-clean and ultra-highly evacuated systems.

In 1959 Davies and Fitch, (66), investigated the effect of a discharge on the sparking potential for copper in hydrogen. They found that a current of 10^{-7} amps flowing for 10 seconds lowered the sparking potential by 30 volts, the effect decaying in about 30 minutes.

By following the cathode work function, using the Kelvin vibrating capacitor method, they also found that a reduction in ϕ of 0.3 eV occurred corresponding to the change in V_s , this effect also decaying in about 30 minutes.

This variation in ϕ could be explained by the existence of a thin insulating layer, possibly an oxide layer, on the cathode. This would prevent some positive ions, formed during the discharge, from being neutralised at the cathode. The presence of such a positive layer would reduce the work function and the effect would decay as the positive charge gradually leaked away.

A similar investigation was carried out by Davies and Hopkins, (67), using oxide coated cathodes. A linear relationship was found between V_{sm} and ϕ . The result indicated that a change in ϕ of 1 eV corresponded to a change in V_{sm} of 60 volts. Gozna, (68), has shown that for copper and nickel cathodes different values of ϕ , caused by positive ion layers, lead to a change in V_s of 45 volts per eV change in ϕ .

The experiments of Davies and Fitch, Davies and

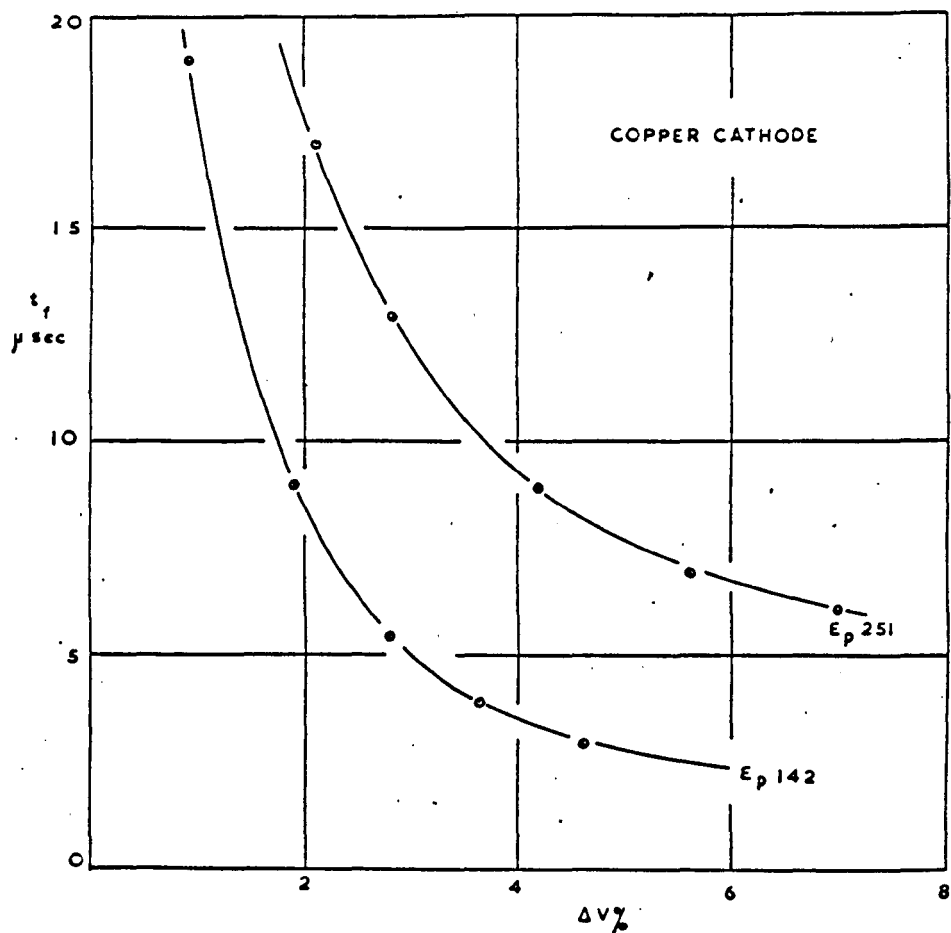
Hopkins, and Gozna were all carried out under similar conditions, with reproducible surfaces. It is interesting to note that the calculations of Jacobs and La Rocque, referred to earlier, indicated a change in V_s of 40 volts per eV change in cathode work function. These experimenters were interested in estimating values of V_{sm} from known values of ϕ for cathodes in commercially produced electron tubes. Their anodes and cathodes were of the same metals in the same gas atmospheres and it was impossible for them to measure cathode work functions. Although the conditions and materials for the two sets of experiments were different, and no serious comparison can be made between them, the figures obtained are remarkably consistent.

1.6. The Development of a Discharge in Time

When a potential, greater than the sparking potential, is applied across a gap a certain time will elapse before the breakdown processes can commence, i.e. a certain time is required before an electron will appear in the gap. This time is called the statistical time lag and it may be completely eliminated in the laboratory by illuminating the cathode with sufficient ultra-violet light. The time required for breakdown to occur after the appearance of the first electron is called the formative time lag.

Work has been carried out by Llewellyn-Jones and de La Perelle, (69), on the emission of electrons from various

FORMATIVE TIME LAGS



Variation of Formative Time Lag with Overvoltage
at Constant E/p in Hydrogen.

Fig. 15.

electrode surfaces by measuring the statistical time lags. Voltages, which were greater than the sparking potential, were applied across a gap for short times and breakdown occurred as soon as an electron appeared in the gap. Statistical time lags were obtained from the results of many such experiments and it was found that the presence of tarnish films, oxides and metallic dust on the surfaces enhanced electron emission by the tunnel effect. It was found also that the first breakdown of each test took place after a long statistical time lag and that, due to the presence of a positive ion layer, subsequent lags were much shorter.

The results of other early workers, (70), showed that the formative time lag was of the order of 10^{-7} seconds. This was thought to indicate that the emission of electrons from the cathode by positive ions is negligible since most positive ions are formed near the anode and at least 10^{-5} sec is required for them to traverse the gap.

It has also been found that the formative time lag depends on the overvoltage applied to the gap, (71), i.e. the excess voltage above V_g for the gap, and it also depends on the nature and relative importance of the secondary processes taking place. Figure 15 shows typical curves obtained when formative time lag is plotted against overvoltage for constant values of E/p .

The transit times of the positive ions taking part

in the γ process are 100 times greater than those for the electrons produced by the δ process. When the applied voltage is of the order of the sparking potential, several transits are required to cause breakdown and the formative time lag for the γ process will be 100 times greater than for the δ process. This implies a dependence of formative time lag on the nature of the cathode surface.

Accurate measurements of formative time lags have made it possible to assess the relative importance of the various secondary processes. The theoretical work of Dutton, Haydon, Llewellyn-Jones and Davidson, (72), on formative time lags in hydrogen has provided a means of making such an analysis concerning the γ and δ processes.

The measurements of Morgan, (71), using this technique, indicate that for $E/p \approx 50$ photo-electric emission is most important. For higher values of E/p , up to about 300, positive ion effects increase and become of equal importance. Fisher and Bederson, (73), also suggest that for air the dominant process is photo-electric emission.

Formative time lags are being measured in this laboratory (74, 75), using refined electronic instruments and techniques and these may provide a more accurate assessment of these processes.

1.7. Conclusion

It is evident, from the preceding discussion of

the low pressure discharge, that the mechanisms involved depend critically on the nature and material of the cathode surface. It has been shown that sparking potentials and statistical time lags depend on the effective work functions of the surfaces and that the presence of insulating layers alters these work functions.

Many of the secondary processes taking place in gas discharges are highly surface sensitive and it is, therefore, necessary, when studying such discharges, to have clean and accurately reproducible electrode surfaces. Comparison of previous work has been difficult since the vacuum and purification techniques available have been so diverse and have given rise to such a wide variety of surface conditions, but modern ultra-high vacuum techniques are now available and recent measurements are showing a higher degree of consistency.

Previous measurements of the Townsend primary ionization coefficient α have shown little agreement because of the diversity of experimental conditions. In order to explain the processes of breakdown an accurate knowledge of the value of α under given conditions is required.

By confining the present work to the use of evaporated metal electrodes, it is hoped to obtain reproducible systems for which the primary ionization coefficient is known, since workers in this laboratory have followed the variation of α/p with E/p in hydrogen using such electrodes.

In the present work the occurrence and nature of insulating layers on clean, evaporated metal cathodes is investigated. The dependence of cathode work function on thickness, temperature and previous history is described together with the effects of the superposition of foreign metal films. The work is restricted to such surface effects in hydrogen and under vacuum and previous work in the field will be reviewed in the next chapter.

CHAPTER II

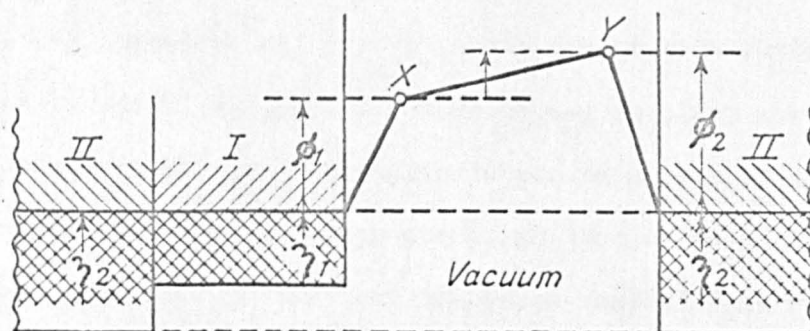
EFFECTS OF CONTAMINANTS AND SURFACE NATURE ON WORK FUNCTIONS

2.1. Introduction

In order to investigate the work function variations of clean electrodes in gas discharges, it is necessary (a) to have as low a residual gas pressure as possible in the vacuum system, (b) to have a method of preparing fresh metal surfaces immediately prior to testing, which does not introduce impurity, (c) to have an efficient method of introducing the very pure test gas to the system, and, (d) to have a method of measuring work functions which is sensitive and reliable for all surface conditions and which is independent of the discharge gas.

Throughout this work ultra-high vacuum techniques have been employed giving residual gas pressures between 10^{-10} and 10^{-8} mm.Hg. Metal surfaces have been evaporated on to glass substrates in the experimental tubes, and hydrogen, in a state of high purity, has been admitted to the experimental tubes by diffusion through heated palladium. A method of measuring relative work functions has been used which is independent of the discharge gas and which indicates the average work function of the entire cathode at any temperature.

The advantages and disadvantages of these techniques



Potential Variation between two Directly Connected Metal Electrodes.

Fig. 16.

will be discussed later in the light of the experimental results.

2.2. The Method and Technique of Work Function Measurement

The method of measuring work functions directly by following cathode emission characteristics as either the temperature or the illumination are varied cannot be used in this work. Thermionic emission is negligible at room temperature and metal annealing properties could not be investigated. The photo-electric effect does not lead to a sufficiently accurate measurement because emission is reduced gradually as wavelength is increased and it is difficult to observe a sharp threshold for the work function.

The only practicable methods are those involving a knowledge of the work function of a reference surface, and the measurement of the contact potential difference, (c.p.d.) existing between it and the test surface.

Since changes in work function, rather than absolute values, are to be followed, the only difficulty lies in the assumption that the work function of the reference surface remains constant throughout the tests. This assumption is discussed in more detail later.

Figure (16) shows the variation of potential energy of an electron between different metal surfaces both in contact and separated in a vacuum.

When two metals are in contact electrons will flow between them until the two Fermi levels (γ_1 and γ_2) coincide.

At equilibrium a potential difference will exist, in the metal and at the junction, which is equal to $\gamma_1 - \gamma_2$. This is known as the galvani potential.

In a vacuum, however, a potential difference ($V_{1,2}$) will exist between the outer limits of the surface potential barriers (X and Y) which is equal to the difference in work functions: (See Figure 16).

$$\text{i.e. } V_{12} = \phi_1 - \phi_2$$

This potential difference is known as the contact potential difference and the relationship is exact when both metals are at the same temperature.

If a large temperature difference exists then differences in contact potential difference exist, due to the thermo-electric effect, which may amount to a few millivolts.

A method of measuring contact potential differences which was developed by Anderson, (76), and which has been used extensively, is the retarding potential method. For this method a narrow beam of low velocity electrons from a normal gun arrangement is directed on to a reference surface and the current is plotted as a function of the retarding potential between the gun and the surface. A similar curve is obtained from the test surface, which is exactly substituted for the reference surface, and the difference between the characteristics is equal to the change in retarding potential caused by the

contact potential difference, (77).

This method has the advantage that small areas of surface may be studied using narrow electron beams, but it has the disadvantage that it can only be used at very low pressures. Even at low pressures work functions may be altered by the effects of electrons trapped in adsorbed gas layers, and the electron beam may ionize gas atoms and lead to the production of positive ion layers on the cathode.

The method chosen for this work is Zisman's modification of the Kelvin method, (78). For this the cathode and reference surfaces are made to form a small condenser. If one of the surfaces is made to vibrate with respect to the other, the value of the capacitance of the system will fluctuate and there will be a consequent oscillating charge flow in the circuit linking the surfaces. The magnitude of this charge flow will depend on the contact potential difference. If the resistance in the circuit is high enough a small oscillating voltage will be produced by the charge flow and this can be amplified and monitored. It is possible to 'back-off' the contact potential difference at source, and accurately measure it, by introducing a small voltage in series with the electrodes and of opposite polarity.

The method is most suitable for this type of work since its operation does not interfere with the nature of the surfaces, i.e. there is no bombardment or irradiation of the

surface. No ionization is produced and the technique can be applied in the presence of any gas and at any temperature.

The only disadvantage of this method is that the average work function of the entire surface is measured. The existence of partial monolayers cannot easily be detected and the effects of patchy surfaces, presenting areas whose work function may differ by a few tenths of an electron volt due to differing crystal faces, may be apparently eliminated. However, it is possible to measure contact potential differences to within ± 0.005 V, an error which is small compared to the signals monitored.

In this investigation the reference surface was a gold film evaporated on to a borosilicate glass substrate and it was made the vibrating component of the system. Gold was chosen as the reference surface since, (a) it can be obtained in a very pure state, (b) it is chemically relatively unreactive, and, (c) it is likely to maintain a steady work function throughout the time of an experiment. The work function of gold should be unaffected by the presence of hydrogen, (79). It is of utmost importance, when studying changes in one surface, that the reference surface should remain constant. There is a difference between the values quoted for the true work function of gold but this seems to be due to differences in the conditions under which they were obtained. Anderson, (76), gives a value of 4.83 eV when

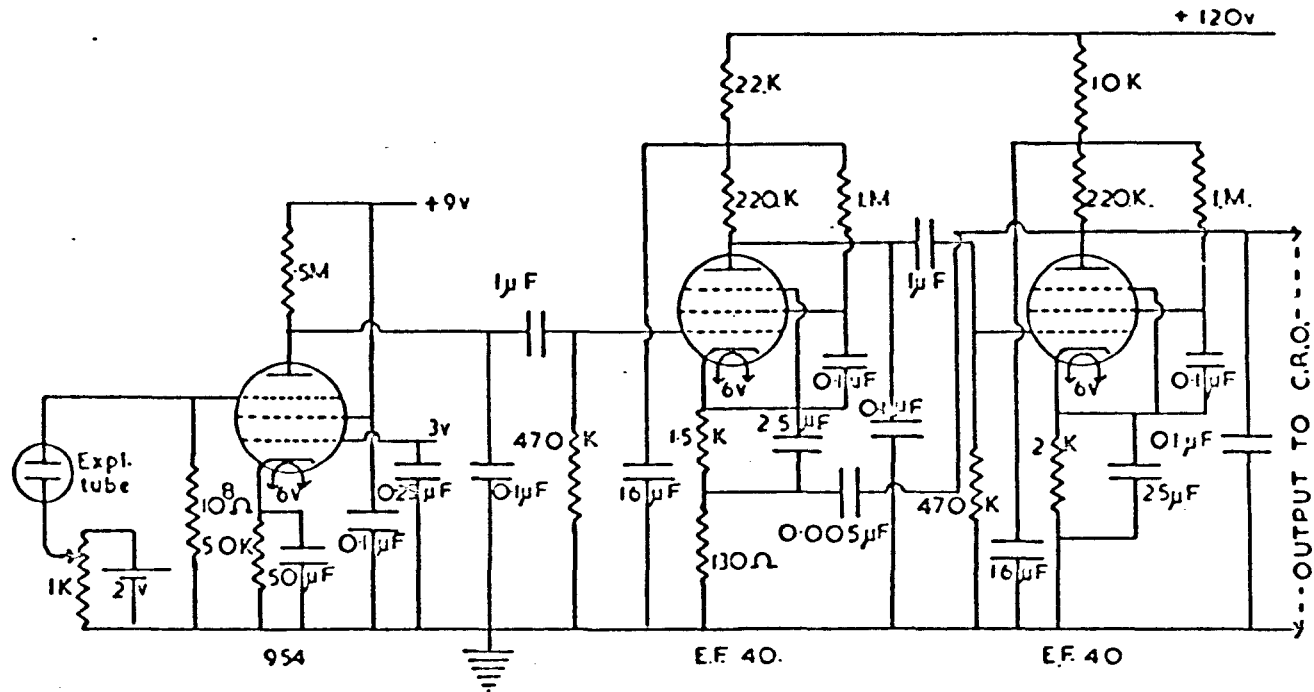
measured with respect to barium. These measurements were for a thick gold film on tantalum and are probably not reliable owing to the extreme reactivity of the reference surface and the consequent ease of formation of foreign films. The figure given by Rivière, (80), was obtained under similar conditions to those used in the present investigation and relates to a tungsten surface. Tungsten is very much more stable than barium, as a reference surface, and the figure of 4.70 eV for gold will be quoted throughout this work. Since changes in work function only are to be measured, an exact knowledge of the work function of the reference surface is not essential.

The work of Gozna, (68), using one gold reference surface and several fresh gold cathodes, indicates that, although an insulating layer may be formed on the reference surface, its work function remains constant to within ± 0.006 eV throughout an experiment lasting several days.

Because the magnitude of the varying capacitance was low, and because its frequency of between 20 and 30 c/s was so near to the mains frequency, great care was taken to screen the electrode system and leads, thus reducing distortion. Field distortion between the electrodes due to possible charge build-up on the glass envelope was reduced by coating the inside of the tube with a layer of aquadag which was maintained at earth potential.

For maximum sensitivity a low frequency amplifier

FIG. 17.



CONTACT POTENTIAL DIFFERENCE CIRCUIT AND LOW FREQUENCY AMPLIFIER

was used having a gain of about 10,000 and a high input impedance, ($10^8 \Omega$), (Figure 17). The signal was fed on to the grid of an electrometer valve, (type 954), and then through a two stage amplifier employing E.F.40 pentodes and a negative feedback system. The power supplies were dry batteries so that maximum stability could be obtained. Because of the low frequency input signal, large coupling condensers were used. The output was displayed on a Cossor type 1035 oscilloscope with a range of 50 mV, and the reversible backing-off potential was supplied by accumulators across a 1000 ohm potentiometer and was monitored on a calibrated Crompton multi-range meter. Every part of this system was enclosed in metal boxes for electrostatic shielding and all leads were of coaxial cables, (75 ohm), coupling loops being reduced to a minimum. It was also found necessary to mount the amplifier on a table not mechanically connected to the pumping frame - thus reducing vibration effects in the circuit.

Electrical contact to the pinch leads at the base of each experimental tube was made through a set of coaxial sockets fixed into a cylindrical aluminium can and the entire experimental tube was surrounded by aluminium foil which was taped to the rim of this can. The complete shield was maintained at earth potential.

To make measurements, as soon as the cathode film had been deposited, the reference electrode was moved over it

(see Chapter III), and the screening foil placed in position. It was possible to measure work functions within one minute of deposition using this arrangement.

The reference electrode, (see Chapter III), was made to vibrate by tapping the tube and the small oscillating voltage produced was displayed on the oscilloscope. This oscillating display could be eliminated by suitable adjustment of the 'backing-off' voltage and the contact potential difference could be read directly from the Crompton voltmeter.

2.3. Previous Work

2.3.1. Structure of Evaporated Film Electrodes

A great amount of work is at present being carried out on the structure and properties of metal films less than 10^9 \AA in thickness, but very little work is reported on the thickness range $10 - 2000 \text{ \AA}$. Since the history of a metal film i.e. its crystal structure and its state of annealing etc., largely influences its surface properties, the work in this field will be reviewed.

The method of depositing a metal film, particularly when the film is being condensed on to the surface of an insulator, appears to affect the continuity of the film for thicknesses up to about 100 \AA , depending on the metal, (81).

If no electrical measurement is made on the film during its growth, the mutual repulsion of the condensing

aggregates on the substrate, caused by electrostatic charging in the evaporation process, will promote the building of metal islands until these become sufficiently large to touch and cover the substrate. Electrical measurement of the surface, or even contact with a sufficiently large isolated conductor, allows some charge to leak away and the effect is practically eliminated. This effect is important in that sufficient energy may be given to the substrate by the condensation process to cause decomposition and gas evolution from the exposed metal-substrate boundary. Such decomposition products, particularly in the case of glass, (82), may form adsorbed insulating layers on electrodes.

The roughness of an electrode surface, which may be due primarily to the roughness of the substrate, is a factor which may facilitate field emission (see Section 1.2.3.), and which determines the amount of adsorption that can take place.

The work of Crowell, Norberg, et al, (83), shows that a properly prepared and clean evaporated metal film is certainly porous. Different types of adsorption site exist, which lead to different values of the magnetic moments of the adsorbed dipoles and a more complex relationship with the work function. For example, two adsorption sites A and B, giving rise to magnetic moments M_A and M_B , lead to a modification of the work function expressed by:-

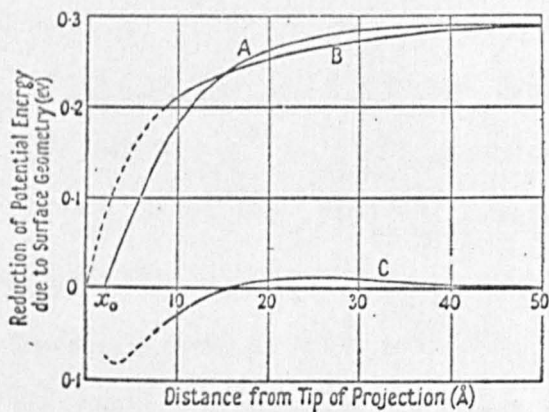
$$\Delta\theta = 4\pi N_s (\pm M_A \theta_A \pm M_B \theta_B)$$

where N_s is the total number of adsorption sites and $\theta = \theta_A + \theta_B$ is the fraction of these sites occupied by adsorbed particles (c.f. Section 1.2.4.). The \pm sign refers to the orientation of the dipoles.

Measurements have recently been made by Kivel, Albers, Olsen and Johnson, (84), of the surface roughness of microscope cover glasses (Corning code 2915), using a radioactive tracer technique to obtain adsorption isotherms from aqueous solution. The true surface area of 1sq.cm. geometrical area of glass was 2.5 sq.cm. Ultra-high vacuum treatment of flame polished borosilicate glass electrodes, including baking at 450°C for some time, is bound to cause surface decomposition and dehydration, (82), which is likely to lead to an increase in roughness factor. The figure of 2.5 quoted above must be regarded as low from the point of view of the present work.

Surface areas of nickel-iron alloy evaporated thin films were also determined and the figure obtained was 2.8 sq.cm. This figure is higher than expected but may indicate the importance of the nature of the substrate surface. In this case the substrate was the Corning glass described above.

The effects of an irregular metal surface on the work



Components of change of potential energy along the axis of a surface projection 60 Å high and of 30 Å base diameter : A, reduction of image potential; B, compensating patch potential; C, net change of potential energy.

Fig. 18.

function have been investigated by Morant and House, (85), by considering a surface projection in the form of a spheroidal boss, and by plotting fields associated with it using an electrolytic trough.

It has been shown by Lewis, (86), that the microgeometry of a surface effects only the image potential of an electron above it and that this image potential is lower for distances up to about 100 \AA above a surface projection than it is for a plane surface.

Morant and House have shown that the modification of the image potential is almost exactly compensated by the patch field associated with the projection, (Figure 18). This patch field may be visualised as a distortion of the electron cloud outside the metal by the contact potential differences existing between the projection and other parts of the surface. The shape of the surface barrier is unaffected by projections for distances greater than about 15 \AA .

The main effect of surface geometry on electron emission is the enhancement of an applied electric field thus facilitating field emission, (Section 1.2.3.).

Measurements made in the United States by Farnsworth and Schlier, (87), show that films of copper, up to a thickness of about 25 atomic layers and deposited on to a clean titanium crystal substrate, are made up of crystallites

which grow epitaxially and which are oriented with respect to the titanium. If, however, the copper is deposited on titanium having a surface of chemisorbed oxygen, the crystallites are completely disoriented. It is known that different faces of the same crystal have work functions that differ by a few tenths of a volt, (88), due to different lattice spacings, and from this it would be expected that deposition of a metal on to a single crystal of the same metal would lead to epitaxial growth and no change in work function. Farnsworth, Blackmer and Chung Fu Ying, (89, 90, 91), have shown, however, that silver deposited on one face of a silver single crystal substrate leads to a work function that is 0.3 eV lower than that of the bulk metal. They have also found that films of gold and silver deposited on substrates at room temperature, have work functions which are lower than those of the bulk metals and that some variation is observed for different substrates, e.g. quartz, single crystals, glass etc.. If the films prepared in this way are annealed at temperatures of about 200°C the work functions increase to the bulk metal values. An explanation of these effects is that large densities of lattice defects are frozen into the films on condensation and that these disappear on annealing. Different substrates may lead to different preferred orientations of the small crystallites concerned.

Recently a short investigation was made into the

dependence of the work function of an evaporated copper film on the film thickness, (92). Ultra-high vacuum techniques were employed and work functions were measured by the Kelvin method. Contact potential differences were obtained, at various stages of copper deposition, between the copper film and a gold reference surface. The thickness of the final copper film was of the order of 1,500 Å and contact potential differences of 0.063, 0.173, and 0.265 volts were measured during deposition. The work function of the film therefore, decreased as the thickness was increased and it was found that the work function of the final film was in reasonable agreement with other published values for copper. For this work the films were deposited on flame polished glass at room temperature and it must be assumed that lattice defects were present on the surfaces. It is likely that these defects in the final film would have caused a lowering of the work function, (91), to a value below that for the bulk metal, but this was not observed. It is possible that either the final film was not sufficiently thick to see the levelling off in work function, or the film was covered by a chemisorbed layer. No explanation was given of the high work functions obtained for thin films but it is probable that electrical contact was made through a tungsten rod of relatively high work function. The decrease in ϕ with increasing film thickness may then have been due to a progressive

covering of the exposed contact.

Farnsworth and Chung Fu Ying, (90), referred to earlier, also report a decrease in work function with increasing film thickness for thin gold films.

An investigation of the variation of photo-electric work function with film thickness for aluminium, silver and gold has been carried out by Garron, (93). Films up to about 800 \AA in thickness were investigated with reference to the depth within a film from which photo-electrons are emitted. The films used were unannealed and the values of $\phi_{P,E}$ measured must be minima for the surfaces. Comparison of results is, therefore, not possible but it is interesting that high values of $\phi_{P,E}$ are obtained for films $< 50 \text{ \AA}$ and steady values are obtained for films $>$ about 150 \AA , the minimum being at a thickness of about 50 \AA .

The Kelvin method has been used by Rivière, (80), in a series of experiments to measure the contact potential differences of seven evaporated metals, and work functions were obtained relative to a tungsten surface. A value of $4.565 \pm 0.025 \text{ eV}$ was assumed to be accurate for the tungsten surface and is the normally accepted figure obtained from thermionic emission characteristics corrected for room temperature. The metal films were evaporated on to glass substrates coated with a layer of platinum which was obtained by baking a 'liquid bright platinum' layer. Ultra-high

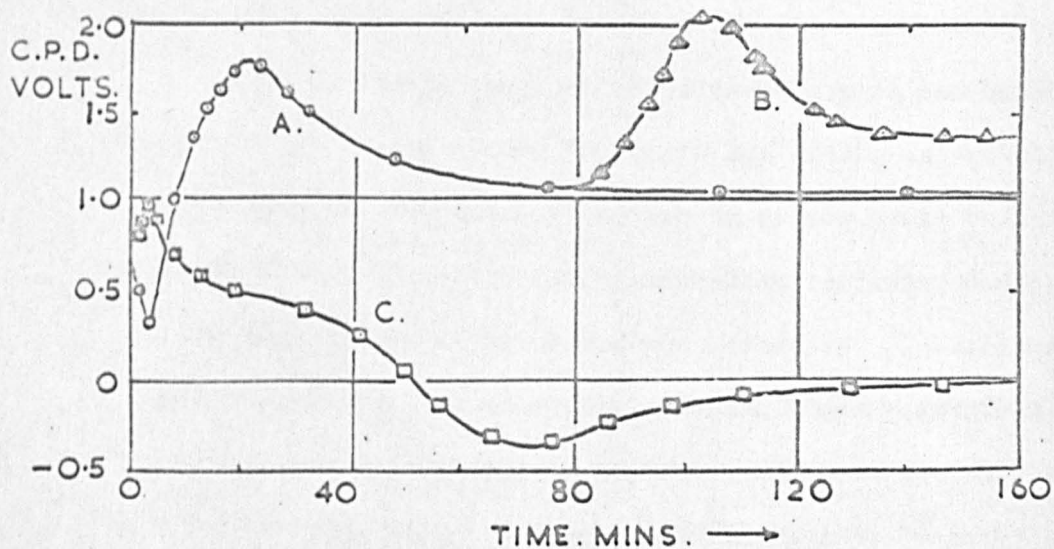
vacuum techniques were employed and residual gas pressures of the order of 10^{-8} mm.Hg. were obtained. Metal evaporation was continued until the walls of the containing vessel became opaque and it was possible to measure contact potential differences within one minute of deposition. For the metals studied there was no change in the measured value of the contact potential difference over a period of four weeks from deposition. Since the maximum error in measurement was ± 0.02 volts and since the films were not annealed, it must be inferred from the constancy of the contact potential differences that either all adsorbed layers were formed before measurement began and no annealing took place, or, what is more likely, that a slow annealing process at room temperature was exactly compensated by a slow formation of adsorbed layers.

Impurities are likely to have been present immediately after deposition due to thermal effects of the evaporation on the glass system.

2.3.2. Effects of Foreign Films

Work function changes caused by the adsorption of contaminants likely to be encountered in a conventional vacuum system have been investigated by Davies and Cozna, (94), (Figure 19).

The impurities considered were Apiezon vacuum oil B, silicone fluid D.C. 703, and mercury vapour. It is



Change in Work Function of a Copper Cathode on Exposure to : (A) Apiezon 'B' oil ; (B) Warmed Apiezon 'B' oil ; (C) Mercury Vapour.

Fig. 19.

uncertain how vacuum oils react with surfaces and it is therefore impossible to measure values of work functions relative to standard surfaces. The figures quoted are changes in contact potential difference.

At residual gas pressures of the order of 10^{-8} mm.Hg. the oil vapour was admitted to the manifold from a separate ultra-high vacuum system by means of a thin glass breaker. The pressure above the oil was limited by its own vapour pressure at room temperature. On opening the breaker there was a small fall in contact potential difference between the copper and gold surfaces which was followed by a rise of 1.06 volts during the next twenty minutes. A steady value of 1.11 volts was obtained after about three hours. When the vapour pressure of the oil was raised by warming, the maximum value of contact potential difference became 2.03 volts and the final steady value, 1.4 volts.

These changes can be explained if the oil vapour initially adsorbs preferentially on one of the electrodes and if adsorption is complete on both surfaces only after some time. It was found to be extremely difficult to measure the pressure in the system because of the ionization and oil decomposition caused by the operation of the ionization gauge. A rapid fall in contact potential difference of 0.44 volts was observed when the ionization gauge heater was turned on. It was probable that ions produced in the gauge

diffused into the experimental tube since the manifold system was as small as possible.

Measurements made using silicone fluid D.C. 703 in a completely new vacuum system were similar to those made with Apiezon B oil, but the changes in contact potential difference were much smaller.

When the experimental tube was exposed to clean mercury vapour there was a small increase in contact potential difference followed by a drop of nearly 1 volt, the final value after $2\frac{1}{2}$ hours being zero.

Both copper and gold form amalgams and gold amalgam is formed more easily than copper amalgam. The observed changes in contact potential difference can be explained if a layer of amalgam is produced on the gold electrode first. An increase in work function would be expected if the amalgam surface was made up of mercury atoms held between gold atoms thus producing a closely packed skin of amalgam on the gold. The contact potential difference would fall as both surfaces became amalgam surfaces and would finally disappear when both surfaces were covered with mercury films.

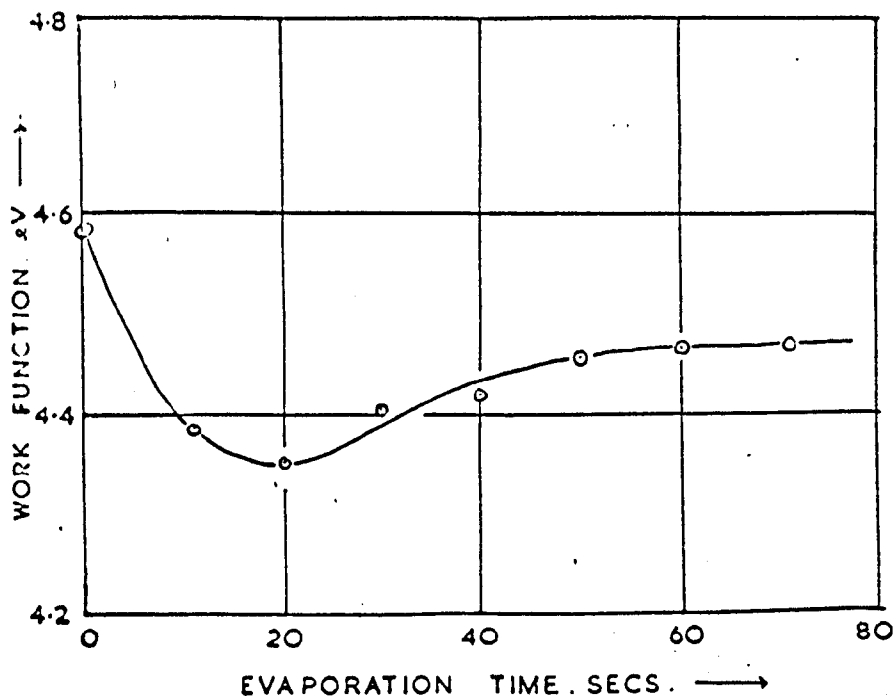
The work of Bills and Evett, (82), concerning the decomposition of pyrex borosilicate type glasses is particularly relevant to this work, since pyrex vacuum systems have been used throughout. It appears that, as water vapour is evolved from the glass during the normal beakeout procedure,

the surface structure becomes unstable and breaks away in fairly large aggregates containing sodium and potassium, (95). It has been established that such decomposition can be caused by radiation from an exposed heater filament in the glass system and can also be produced by the collision of ions with the walls of glass ionization pumps and gauges. It is probable, therefore, that impurity layers may be formed from glass decomposition products since, (a) the film electrodes used in this investigation are formed by evaporation within the glass tubes, (b) the metal films condense on to glass substrates, the films being initially in the form of many islands, and, (c) ionization pumps are employed having long, exposed tungsten heaters.

The importance of maintaining very low residual gas pressures during metal deposition has been demonstrated by Sachtler in his work on nickel films, (96). Measurements were made of the changes in work function of nickel accompanying film exposure to 2 mm.Hg. pressure of pure hydrogen. It was found that, for films prepared at residual gas pressures of the order of 10^{-8} mm.Hg. such exposure led to an increase in work function but for films prepared at 10^{-6} mm.Hg exposure led to a decrease in work function.

These results can be explained by considering the nature of the dipole layer formed in each case.

Under extremely clean conditions the hydrogen will be



The Effect of a Film of Copper on the
Work Function of Nickel.

Fig. 20.

chemisorbed as a hydride and will behave as a negative ion. The dipole layer thus formed will have its negative side outwards and will cause an increase in work function. If, however, the nickel surface is contaminated by a thin insulating layer of oxide or other material, the hydrogen will be physically adsorbed in a manner determined by the relative electronegativities of the adsorbent and adsorbate. In this case nickel is electronegative relative to hydrogen and will tend to accept electrons from the hydrogen. The resulting dipole layer will be positive side outwards and will lead to a reduction in work function.

Davies and Gozna, (94), investigated the effect of depositing a film of copper on nickel by following the change in work function of the composite surface with copper evaporation time, (Figure 20). The work function of the nickel surface was initially 4.58 eV but this value fell to 4.36 eV and finally became 4.48 eV, which is characteristic of a complete copper film.

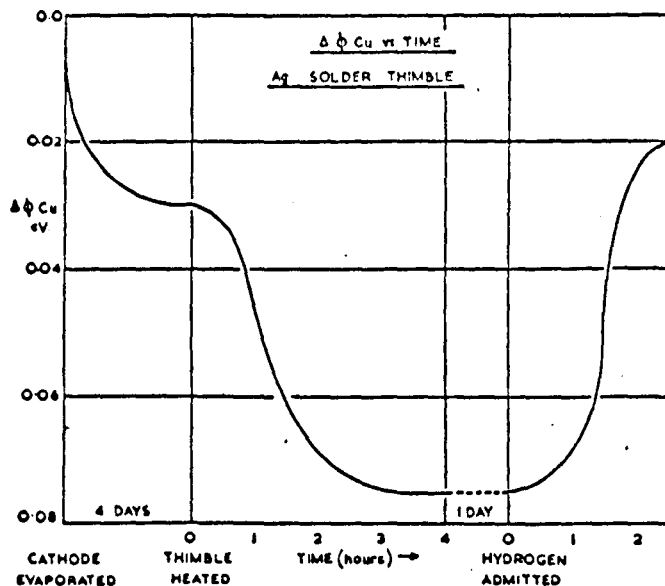
Nickel is electronegative with respect to copper and a thin film of copper would tend to lose electrons to the nickel. This would lead to a positive outer layer and would produce the observed decrease in work function.

Davies and Fitch, referred to earlier, (66), using evaporated copper films on glass substrates followed changes in cathode work function using the Kelvin method

at residual gas pressures of the order of 10^{-6} mm.Hg.

It was found that during the first twenty minutes after evaporation the work function of the copper fell by 0.05 eV. This was attributed to the adsorption of hydrogen liberated from the copper bead during evaporation. (The beads were prepared by hydrogen furnacing and must have contained some of the gas.) Physical adsorption of hydrogen together with metal annealing would account for this effect in the absence of any chemisorption process. It has been shown by Allen and Mitchell, (97), that copper and gold films do not chemisorb hydrogen at room temperature. After this initial change the work function remained constant indefinitely, but an increase of 0.14 eV was observed on admitting hydrogen to the system. The hydrogen was admitted by diffusion through heated palladium tubes, sealed by lead and soda glasses and a graded seal into the pyrex manifold. It was subsequently found that the palladium tubes had been stopped with silver solder and the increase in work function was attributed to the diffusion of oxygen through the silver, (98), followed by preferential chemisorption on to the copper surface, (97). Later work was carried out using palladium tubes stopped with gold and the effect was very much reduced but still present.

Gozna, (99), was able to repeat this work using a silver soldered thimble and to show a separate effect by



Variation of Work Function with Time while using a Silver Soldered Palladium Thimble.

Fig. 21.

heating the thimble in the absence of hydrogen, (Figure 21).

After evaporating the copper surface its work function dropped by 0.03 eV to reach a steady value after a period of four days. With a residual gas pressure of 10^{-8} mm.Hg. in the manifold, and of 10^{-6} mm.Hg. in the hydrogen system, the palladium thimble was heated and a further drop in work function of 0.04 eV was observed during three hours. This was attributed to desorption of hydrogen from the palladium and subsequent physical adsorption on the copper surface. Using the palladium thimble as a diffusion tube for a hydrogen pressure of 10 mm.Hg., an increase in work function of 0.05 eV was observed which was thought to be due to diffusion of oxygen through the silver as before. In later work Gozna placed a platinum stopped thimble in parallel with the silver stopped thimble and was able to show that when hydrogen was admitted through the platinum stopped thimble the work function dropped, as would be expected.

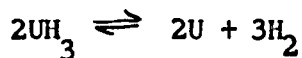
The presence of an insulating layer on the cathode was established by Davies and Fitch, (66), by following the changes of work function immediately after passing a discharge of 10^{-7} amps for ten seconds. The effect of the discharge was a 0.3 eV lowering of the work function followed by a recovery during the next thirty minutes, and the effect was found to be reproducible.

The explanation put forward is that positive ions

produced by the discharge are deposited on a cathode insulating layer, thus forming dipoles having their positive ends outwards. The effect of this would be a lowering of the work function. The original work function would be gradually regained as the positive ions became neutralized. Confirmatory evidence was supplied by the fact that the original work function could be regained, at any time, by illuminating the cathode with ultra-violet light. It was also found that when a reverse discharge was passed between anode and cathode the work function increased. Such a change would be produced if a layer of electrons was present on the cathode insulating layer. Under these circumstances no change was expected or detected in the sparking potential since the operative part of the cathode would be the part having the lowest work function, i.e. a part not covered by an electron layer.

This work indicates that an insulating layer is formed on the cathode which is not due to the diffusion of oxygen from the hydrogen systems. Gozna also observed these effects, (99), and built a further experimental tube in which all the electrodes were of gold and for which hydrogen was purified by the uranium hydride technique. Uranium, in the form of reactor grade turnings, can be outgassed thoroughly at 900°C by heating under vacuum in a silica tube. If this clean uranium is heated to 250°C, and then cooled in hydrogen

very pure uranium hydride is formed according to the reversible reaction:-



Excess hydrogen may be pumped off and the uranium hydride opened to the manifold. Controlled amounts of hydrogen may then be liberated by gently heating the hydride. The measurements of Rose (100) show that impurities exist to the extent of 2 parts per million and that these are chiefly rare gases. It is known that all other compounds of uranium do not dissociate except at very high temperatures.

This method, without palladium thimbles, has been used by Gozna to show that insulating layers, which will retain positive ions, can still be formed on cathode surfaces. Since oxygen is not chemisorbed on gold, (97), the cathodic layers in this case could not have been oxide layers. It is possible that such layers are formed from glass decomposition products, and it is hoped to show, in this thesis, that such a process is taking place in these systems.

The effects of surface films and positive ions on cathode emission has been investigated in a little more detail by Llewellyn-Jones and Morgan, (101). The metals studied were nickel, tungsten, copper and iron with clean, oxidized and tarnished surfaces.

Large numbers of statistical time lags were obtained

for different values of the electric field, E_m , applied to the discharge gap, and the values of electron emission, I , under these conditions could be calculated from a sufficiently large number of measurements, (69). The results showed that the relationship between I and E_m was:-

$$I = A E_m^2 \exp.(-D/E_m)$$

where A is the ordinate intercept and D the slope of the experimental curve.

Comparison of this equation with the Fowler-Nordheim equation, (102),

$$I = 3.85 \times 10^{12} \frac{SE^2 \xi^{\frac{1}{2}}}{(\xi + \phi) \phi^{\frac{1}{2}}} \exp. \left[\frac{-6.8 \times 10^7 \phi^{3/2}}{E} \right]$$

by equating:

$$\frac{D}{E_m} \quad \text{to} \quad \frac{6.8 \times 10^7 \phi^{3/2}}{E} \quad \text{and}$$

$$AE_m^2 \quad \text{to} \quad 38.5 \times 10^{12} \frac{SE^2 \xi^{\frac{1}{2}}}{(\xi + \phi) \phi^{\frac{1}{2}}}$$

yields estimates of the effective work function ϕ and the emitting area of the source of initiatory electrons, S . E is the microscopic electric field at the cathode surface and is described by a local field intensification factor, M , given by $M = E/E_m$. I is measured in electrons per second and ξ is the energy of the Fermi level for the cathode assumed to be $\approx 5\text{eV}$. The most reasonable value of M for the surfaces used was 10.

Figures obtained for the oxidized electrodes were $\phi = 0.5$ eV and $S = 10^{-14} \text{ cm}^2$. These are consistent with the view that the electrons were obtained from sites on the oxide surface formed by groups of negative ions with detachment energies ≈ 0.5 eV and areas of molecular dimensions $\approx 10^{-14} \text{ cm}^2$ rather than from the metal itself (69, 101). The thickness of the oxide films in these cases was of the order of 10^{-5} cms.

For tarnish films (i.e. thin oxide films) of the order of 10^{-7} cm in thickness the experimental relationship between I and E_m was the same as for thicker films but comparison with the Fowler-Nordheim equation led to values of $\phi \approx 0.01$ eV and $S \approx 10^{-20} \text{ cm}^2$ which clearly have no physical significance.

A consideration of the potential energy system associated with a layer of positive ions on the tarnish led to a relationship of the same form as that obtained by Stern, Gossling and Fowler, (18), for a thin metal film of work function ϕ_2 on a base of work function ϕ_1 , where $\phi_2 < \phi_1$.

In their case the relationship was:-

$$I = 38.5 \times 10^{12} \frac{\xi^{\frac{1}{2}} S E_h^2}{(\xi + \phi_1) \phi_1^{\frac{1}{2}}} \exp \left[\frac{-6.8 \times 10^7 \phi_2^{3/2}}{E_h} \right] \frac{\phi_1 \exp(-6.8 \times 10^7 \psi)}{\phi_2}$$

where E_h is the enhanced value of the applied field at the surface and ψ is given in terms of the film thickness, a , by:-

$$\psi = a \left[\frac{\phi_1 + \phi_2 + (\phi_1 \phi_2)^{\frac{1}{2}}}{Q_1^{\frac{1}{2}} + \phi_2^{\frac{1}{2}}} \right]$$

Comparison of the experimental relationship with this equation gave estimates of the field set up across the tarnish layer by positive ions, which was of the order of 10^7 V/cm., and was within the range of fields required for field emission, (18).

The emitting areas appeared to be about 10^{-7} cm² which were in agreement with estimates of the areas of deposition of positive ions produced by the measuring sparks, (103).

2.3.3. Admission of Hydrogen as a Source of Positive Ions

Most of the work on hydrogen discharges carried out in this laboratory has employed the diffusion properties of palladium as a means of purifying the test gas. Hulubei in 1934, (104), showed that, under certain circumstances, such diffusion produced positive ions and the process could be regarded as a possible proton source for nuclear accelerators. In view of the important effects of ions on cathodic insulating layers described above, an investigation of the process became necessary.

Hulubei applied an electric field, which could be varied from 200 to 200,000 V per cm., to the exit side of a heated palladium tube and claimed to have observed positive ion currents of up to 750 μ A, which could be maintained for

at least one hour. The proton yield varied from one sample of palladium to another, depending on the previous physical treatment and state of the metal surface and increased with temperature and applied electric field. Unfortunately the temperature range is not given but it is likely, from a consideration of the high diffusion rates quoted, that the lowest temperature would be about 800°C.

Wolfke and Rolinski, (105), detected an explosive emission of ions from warmed palladium charged with hydrogen by electrolysis, but were unable to detect any ionization resulting from diffusion through the metal at temperatures between 700° and 1200°C. On the other hand, Goldmann, (106), was unable to detect any ion emission from electrolytically hydrogenated palladium. Sugiura, (107), and Kollath, (108), were able to detect ions formed by diffusing hydrogen through a heated tube which was bombarded by electrons, but they were able to show that the ion energies were consistent with their formation from gas which had left the metal and not surface formation of ions by the palladium.

In all this work poor vacuum conditions must have led to contaminated surfaces and the palladium temperatures were so high that any surface layers would have been evaporated in ionic form. The burst of so-called 'fresh emission' at the commencement of an experiment probably corresponds to thermal desorption of such adsorbed layers.

High palladium temperatures might also have led to thermionic emission of protons from the metal, (109), and thermionically emitted electrons could form protons by collisions with gas atoms on the exit side of the metal.

Stansfield, (109), using much better vacuum conditions and cleaner surfaces, was unable to detect any ionization in the hydrogen leaving palladium, either when the gas diffused through the metal or was evolved by warming electrolytically saturated metal.

The more recent work of Bachman and Silberg, (110), however, using a mass spectrometric method, has shown that for a temperature of 700°C , an inlet pressure of 11 cm. Hg and a collection potential of 3 volts, ion currents of the order of 10^{-10} amps could be detected.

In the work described measurements have been confined to diffusion of hydrogen through pure palladium.

It has been pointed out by Crompton and Elford, (111), that hydrogenated palladium exhibits a phase change at about 150°C and that, if this is not taken into account, it can result in distortion of the palladium which will eventually lead to micro-fissures which are porous to impurities.

A silver-palladium alloy has been developed, (112), which does not exhibit this phase transition and which may be heated and cooled in hydrogen without any harmful effects on the metal or the purification characteristics.

2.4. Conclusion and Introduction to Present Work

Most of the work described in this chapter has been concerned with the effects of thin impurity layers on thin metal electrodes, especially the effects of these layers on surface work functions. It has been established that an insulating layer forms on a clean surface very rapidly but the nature and origin of this layer is not known. Further layers have been formed by the normal operation of palladium diffusion tubes and these have been attributed to the diffusion of oxygen through soldered metal junctions.

The effects of positive ions on insulating layers have been described and the suggestion, (113), that the purification of hydrogen by diffusion through palladium might be a source of such ions is to be investigated.

Decomposition of the glass in the vicinity of the palladium tubes has been suggested as a possible source of impurity and it is hoped to investigate this in the present work. The original insulating layer may be explained by such decomposition caused by the presence of heaters in the experimental tubes and ionization gauges.

Bulk metals appear to have different surface properties from thin films of the same metals and the properties of such thin films appear to depend on their thickness and state of annealing.

Because of the importance of obtaining accurately

reproducible electrode surfaces, and consequently reproducible secondary gas ionization processes, the variation of work function with film thickness will be investigated together with the effects of gas adsorption on work function.

A strong dependence of secondary processes on electrode nature has been demonstrated and, in order to understand the processes taking place in the gas discharge, it is most important to understand what causes the observed variation of surface properties.

- Fig. 22.

CHAPTER III

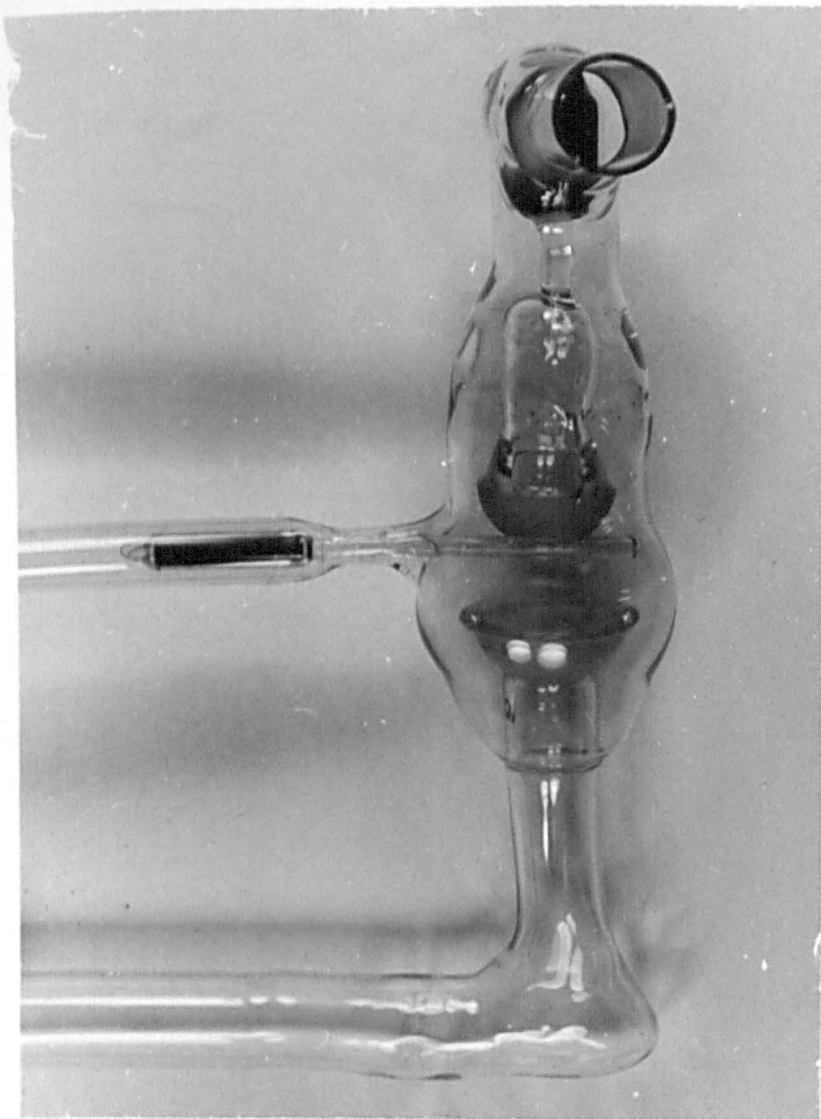
DESCRIPTION OF APPARATUS AND

EXPERIMENTAL PROCEDURE

3.1. The Vacuum System

The vacuum system, (Figure 22), was built in two separate sections, one to provide a clean method of exhausting the manifold and experimental tubes and the other to obtain a low residual gas pressure in the hydrogen producer and purifier. The clean system consisted of a three stage mercury diffusion pump which was backed by a high speed Edwards rotary pump. Greased taps were eliminated above the diffusion pump because they are difficult to outgas and they may have constituted a source of impurity. All glass parts of the system, including the mercury pump, were of pyrex and wide bore connecting tubes were used to obtain maximum pumping speed.

Before assembly the glassware was rigorously cleaned by soaking in nitric acid and washing with distilled water, methylated spirits and acetone. The diffusion pump mercury was cleaned in acid and subsequently distilled under vacuum. In order to prevent contamination by oil and water vapour a large reservoir containing P_2O_5 was introduced above the backing pump, and any mercury vapour diffusing towards the manifold was condensed by two liquid nitrogen freezing traps above the



Internal Spherical Glass Joint.

Fig. 23.

diffusion pump.

In later work it was found to be beneficial to introduce another mercury diffusion pump, in series with the first, in order to reduce the final pressure by about one third, thus increasing the efficiency of the ultra-high vacuum system.

The vacuum system was to be joined to the manifold by a series of constrictions and breakers. After evacuating the system, the manifold could be isolated by carefully closing a constriction. Reconnection could be made by breaking a thin 'pig's tail' type of internal seal using a glass covered iron slug.

To facilitate leak detection in the building of the manifold, a magnetically operated, internal, ground glass-spherical joint, of the type suggested by Yarwood, (114), was used as a temporary seal, (Figure 23). The closed conductance of such a tap was found to be too high to allow its use under experimental conditions and bakeable metal Alpert taps were not available.

The ultimate pressure obtained with this system was about 10^{-7} mm.Hg and it was measured by means of a Penning gauge situated above the liquid nitrogen traps. This type of gauge consists of two nickel plates, 1 cm. apart, forming the cathode, and a ring anode situated between them. A potential of 2KV is maintained between the anode and cathode,

which are in a magnetic field of about 600 oersteds perpendicular to the plates. The discharge current could be conveniently measured with a multi-range micro-ammeter, and the calibration curve for these conditions in hydrogen is shown in Appendix I. For low pressures it was found necessary to trigger the discharge in the gauge by using a high frequency Tesla coil. The lower limit of the gauge is about 10^{-7} mm.Hg when it 'blacks out' and passes no current.

The hydrogen producer was evacuated by means of an oil diffusion pump which was backed by the same rotary pump used in the high vacuum system. A mercury diffusion pump was not used in this system since palladium readily forms an amalgam and since further freezing traps would have been required. Ultimate pressures below 10^{-7} mm.Hg were not anticipated and the vapour pressure of oil in the system under these conditions is negligible. Further difficulties would have arisen in the use of an oil manometer to measure gas pressures. Any oil contamination in the hydrogen system would not have been communicated to the manifold. All glass parts of this system were cleaned thoroughly before assembly and were flame outgassed after assembly.

Hydrogen was produced by the slow electrolysis of barium hydroxide solution and was dried thoroughly by storing in a reservoir containing pure P_2O_5 . Suitably arranged taps made it possible to admit the hydrogen to another

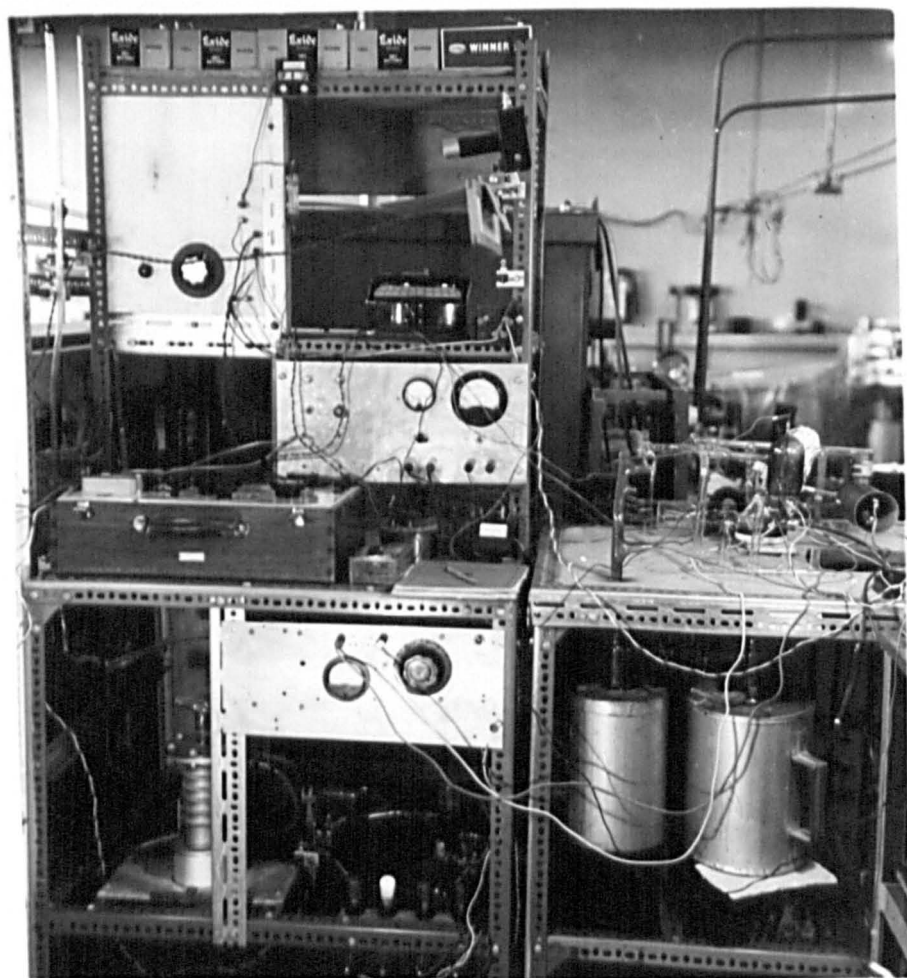
reservoir from which it could be passed into the manifold via the palladium diffusion unit.

The hydrogen pressure was measured by means of a 3 metre manometer, containing apiezon B oil, inserted between the hydrogen reservoir and the low pressure port of the oil diffusion pump. Changes in oil level could be measured to within 0.01 mm. with a cathetometer which was suitably position and levelled.

It was found necessary to outgass the manometer oil, using a cool flame and a hair drier for about three days. The calibration of the oil manometer is shown in Appendix II.

To facilitate the removal of large quantities of hydrogen from the system, without harming the oil diffusion pump, a by-pass could be opened linking the reservoir directly to the backing pump.

Hydrogen was admitted to the manifold by diffusion through two palladium thimbles arranged in parallel with one another. For later work these palladium thimbles were replaced by palladium-silver alloy thimbles which have a better performance, (112). The thimbles were platinum soldered to short lengths of platinum tube sealed into lead glass beads, which were joined by graded seals into the pyrex system. (The alloy tubes were sealed by copper housekeeper joints directly on to pyrex.) The insides of the thimbles were open to the manifold and the outsides were



Pumping Frame and Measuring Equipment.

Fig. 24.

sealed into a side arm of the hydrogen reservoir so that direct heating would cause diffusion of hydrogen into the manifold.

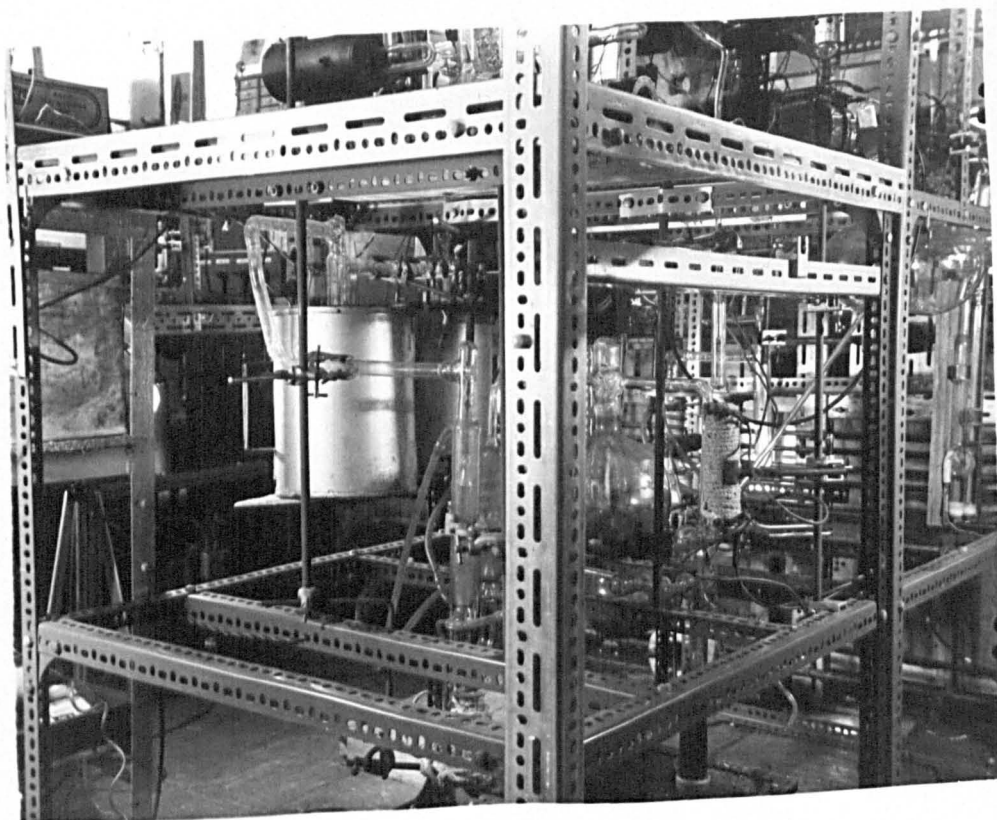
Initially a small oven, operating at 250°C , was placed around the entire thimble unit and the palladium was heated by radiation and convection in the hydrogen. It was not possible to operate at higher temperatures because of the low melting point of lead glass.

As a result of some of the work to be described, this oven was replaced by a safer and more efficient system, (see later).

Palladium absorbs very large quantities of hydrogen and, in order to maintain constant pressures, the heater was switched on for the duration of an experiment. Gas pressures were measured when the manifold and hydrogen systems were in equilibrium, times of four to five hours being required for this to occur. A Penning gauge was fitted to the hydrogen system to measure residual gas pressures prior to operation.

The manifold, ultra-high-vacuum system and experimental tubes were arranged to be above an asbestos table in such a way that a large oven could be lowered over them enabling prolonged baking at 450°C . All metal parts in this system could be outgassed using an eddy current heater.

The Penning gauge in the pumping system and the palladium diffusion unit were positioned beneath the asbestos



High Vacuum System and Hydrogen Producer.

Fig. 25.

table.

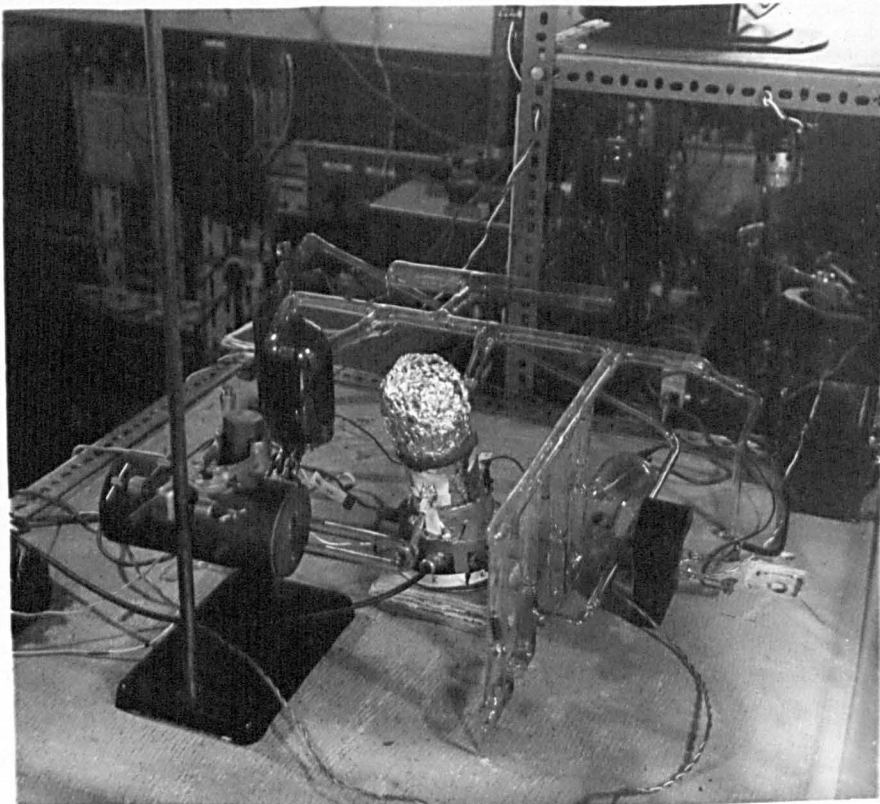
Photographs of the vacuum systems and manifold are shown in Figures (24, 25 and 26).

3.2. The Ultra-High Vacuum System

After the initial evacuation and outgassing of the manifold and its contents, a sealed system having a residual gas pressure of 10^{-7} mm.Hg remained which would have kept clean metal surfaces for less than a second. In order to study the properties of clean surfaces it is necessary therefore to reduce gas pressures until monolayers are formed in several minutes or a few hours, and this implies gas pressures of the order of 10^{-10} mm.Hg.

In work carried out by Bayard and Alpert, (115), on the measurement of pressures below 10^{-8} mm.Hg, a modification of the conventional ionization gauge was developed which was found to act also as a pump. The operating ranges of conventional gauges were found to be limited by photo-electric emission from the collector electrodes due to the incidence of soft X-rays produced in the gauges. For the modified design the collector electrode became a thin wire down the centre of the gauge presenting a very small area to incident radiation.

The pumping action of this gauge is thought to be due to the incidence of positive ions on the glass envelope and subsequent trapping of the neutral molecules. It is



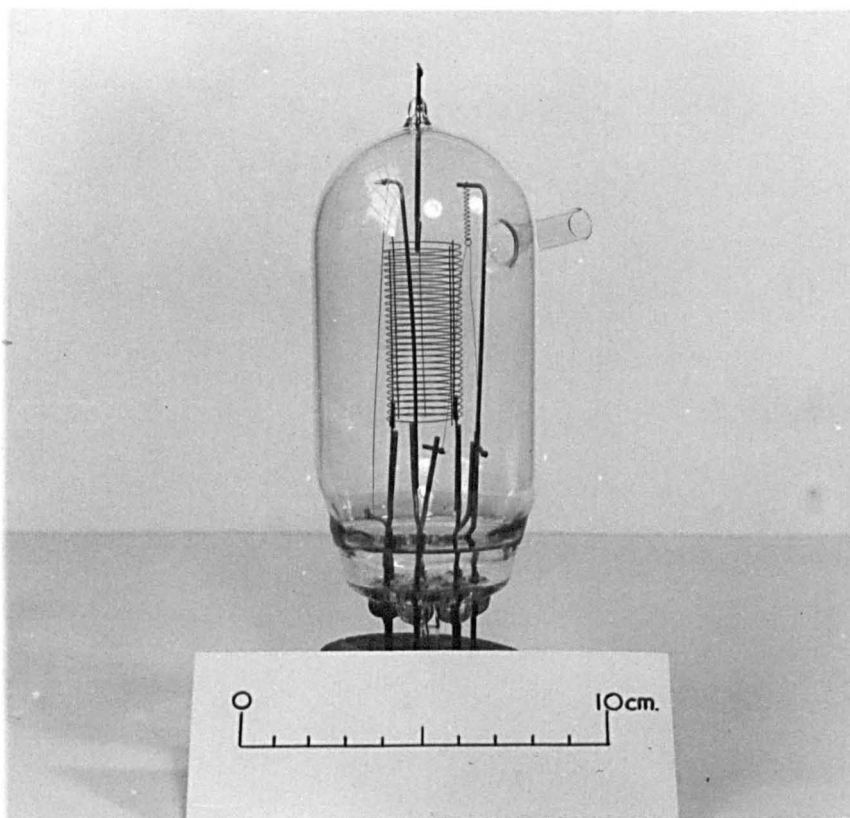
Manifold and Experimental Tube.

Fig. 26.

found that there can be an initial pumping speed of about 2 litres per minute but this gradually decreases as the trapping vacancies in the envelope become occupied. In order to obtain maximum efficiency it is, therefore, necessary to start pumping at as low a pressure as possible.

Barium getters were used in the present work to reduce the manifold pressure by an order of magnitude before operating the Alpert pump. Care was taken to arrange the getters in a side arm which could not 'see' directly into the experimental tube. In this way it was possible to prevent any barium contamination of the surfaces.

The filament of the Alpert pump was of 0.125 mm diameter tungsten wire spot welded through nickel on to a commercially produced seven lead pinch. This filament was mounted outside a helical grid 2 cm. in diameter, 4 cm. long, having six turns per cm. The collector electrode was made by electrolytically etching a thin tungsten wire in sodium hydroxide solution and mounting it on a tungsten glass seal over the centre of the grid. It was important to ensure good vacuum properties for the tungsten glass seals and they were made by gently oxidizing tungsten rods and running thin glass sleeves over the black oxide. These sleeves were heated until a rich copper coloured chemical seal was formed between the oxide and the pyrex. The section of the collector electrode not surrounded by the grid was shielded by a thin



Alpert Ionization Gauge.

Fig. 27.

glass tube, thus reducing the area of wire presented to radiation and also increasing the electrical leakage path formed by any metal evaporated from the filament. A photograph of a completed Alpert pump is shown in Figure 27.

During operation of the pump the electron current to the grid was measured with a milliammeter, the grid being maintained at 120 volts above the filament. The positive ion current was measured using a 'Vibron' electrometer with the collector maintained at 60 volts below the filament. Under these conditions, and by calibration against a Penning gauge an indication of the order of magnitude of the pressure in the manifold could be obtained from the relationship:-

$$P = \frac{1}{S} \frac{I_p}{I_e}$$

where p is the pressure in mm.Hg, I_p is the positive ion current and I_e the electron current. The sensitivity, S , of this type of gauge was 10, (116), and it was possible, using a single Alpert pump to obtain pressures of the order of 10^{-9} mm.Hg. For recent work it has been possible to use commercially produced Alpert type pumps, (Mullard I.O.G. 12 gauges), of an improved design. These tubes are furnished with a conducting layer on the inner envelope wall, which can be maintained at collector potential, thus accelerating the positive ions and improving the pumping action.

With a grid potential of + 140 volts and a collector

potential of -28 volts, relative to the filament, the sensitivity of these gauges is 12.

3.3. Vacuum Techniques

When the high vacuum and hydrogen systems had been satisfactorily erected, the manifold and ultra-high vacuum system was added between them. The palladium diffusion unit linked the hydrogen system and manifold and a closed breaker or internal spherical ground glass tap separated the latter from the high vacuum system. With this arrangement it was possible to evacuate the manifold in such a way that back diffusion of mercury vapour was unlikely.

The hydrogen system was pumped down first using the mechanical pump, and when the pressure had fallen to 10^{-3} mm.Hg the oil diffusion pump was switched on.

After four days of continuous pumping and heating the manometer oil had thoroughly outgassed and the residual gas pressure was 10^{-6} mm.Hg.

At this stage small quantities of hydrogen were produced by electrolysis, dried overnight with P_2O_5 , and flushed through the heated system. This was repeated five times and the system evacuated and assumed to be clean. Tests were made to estimate the leakage rate of this system by isolating the pumps and following the pressure with a Penning gauge over a few days. No increase in pressure was observed while the high vacuum system was being prepared - a

period of seven days.

The high vacuum system was prepared initially in the same way as the hydrogen system, by pumping to 10^{-3} mm.Hg and flaming with a hand gas-torch. Any major leaks could be detected using a high frequency spark tester.

Because of the importance of preventing the entry of mercury vapour into the manifold it was essential to clean thoroughly the freezing traps and glass tubing above the diffusion pumps, and to ensure an adequate supply of cooling water to the diffusion pumps. It is important to realise that mercury has a relatively high vapour pressure at room temperature and that molecules will diffuse into the manifold if they are not prevented by suitable trapping.

Each freezing trap was baked at 450°C , with the diffusion pump running, by surrounding it with a small cylindrical oven. When the trap nearest the diffusion pump had been thoroughly outgassed it was surrounded by liquid nitrogen while the second trap was baked. After this treatment the first trap was again heated while the trap in contact with the manifold was cooled. This procedure prevented mercury vapour from diffusing into the manifold connection.

As soon as an experimental tube had been annealed it was coupled to the manifold and carefully positioned so that the electrode positions could be obtained with ease, (see Section 3.5.). With the diffusion pump off, the

completed manifold was exhausted to about 10^{-3} mm.Hg by breaking the 'pig's tail' seal using a glass covered iron slug. At this time the freezing traps were at room temperature so that any water vapour introduced to the system by glass blowing could be readily pumped away. This was necessary because ice has an appreciable vapour pressure at liquid nitrogen temperature and would have constituted a source of contamination. As the water vapour was pumped away the freezing trap nearest the diffusion pump was cooled and the diffusion pump started. After about three hours the second trap was cooled and the first one allowed to warm to room temperature. In this way any residual water vapour condensed in the traps could be pumped away. After a further two hours both traps were cooled and the system was fully operational.

The pressure was monitored during this period of pumping with a Penning gauge, and the ultimate pressure obtained depended on the presence or absence of any small leaks. If a pressure of 5×10^{-7} mm.Hg was unobtainable leaks were suspected and three methods of detection could be employed. The use of a high frequency 'Tesla' coil in darkness caused either puncturing of the glass at weak points or the enlarging of existing leaks, both effects providing spark channels which were easily visible. The use of a small cool flame caused an increase in the leakage rate of a fault, which led to a sudden detectable change in

pressure, and the use of a highly volatile liquid, usually carbon tetrachloride, led to a similar increase in pressure as the liquid evaporated on being drawn through the leak. After the vacuum system had been isolated, by closing the spherical tap or a constriction, any leaks could be repaired and the outgassing procedure started afresh. It was found that tungsten to glass seals were the most common leak sources and special care was taken in their construction.

At this stage the entire manifold system was enclosed in a furnace and heated to 450°C . A slow stream of hydrogen was admitted, by heating the palladium to 250°C , in order to reduce any oxides formed in the last stages of glass blowing and in order to flush out any other gaseous impurities. After baking and flushing for about twelve hours the furnace was removed and all hydrogen pumped out of the hydrogen system. The palladium was maintained at 250°C in order to remove as much hydrogen as possible from the metal.

Most of the metal components of the manifold, i.e. Alpert gauge grid, metal evaporator shields, getters, Penning gauge plates, etc., were outgassed using an eddy current heater at temperatures of about 800°C until no further gas was evolved. The Alpert filament was heated to white heat and left at that temperature for about an hour while the evaporation beads, (Section 3.5) were heated until their surfaces had been kept mobile for at least ten minutes. Because of the possibility

of evaporation during the outgassing of these beads the appropriate electrode surfaces were carefully shielded.

Care had to be exercised in the outgassing of the barium getters since any overheating would have initiated the barium deposition reaction. This reaction appeared to be endothermic and difficult to stop if once initiated. When no further gas was evolved the oven was replaced and the system baked for another twelve hours. The outgassing routine of baking followed by metal outgassing was repeated three times until no gas evolution could be detected with either the Penning gauge or the Alpert gauge.

The commercially produced Alpert gauges were also outgassed by linking the grid and collector electrodes and drawing a filament current of 75 mA for several hours.

The first stage of evacuation was thus completed.

Before sealing the manifold from the vacuum system the palladium was allowed to cool and the constriction gently softened until the pressure steadied at about 10^{-7} mm.Hg. A getter was then evaporated using the eddy current heater, so that any gas evolved during sealing the constriction would be readily taken up. The Alpert gauge was adjusted for a grid current of about 1mA thus limiting its pumping action while being used as a gauge. At this stage the constriction was closed and the manifold completely separated from the pumping system. Two more getters were fired immediately after

sealing and the Alpert gauge was turned off. The system was left for six hours while the getters were most effective.

After getter pumping, during which the pressure fell to about 5×10^{-8} mm.Hg, the Alpert pump was turned on and operated at a grid current of 10 - 15 mA for maximum efficiency. A period of between two and three days was required for the Alpert pump to achieve a pressure of the order of 10^{-9} mm.Hg. If small leaks still existed in the system the pressure would not fall below 7×10^{-8} mm.Hg. Under these circumstances the manifold had to be gradually dismantled until the leak had been eliminated and then the system had to be opened, reconstructed, exhausted and processed as before. This proved to be an extremely lengthy process but leak-free systems were eventually obtained holding residual gas pressures of the order of 10^{-10} mm.Hg.

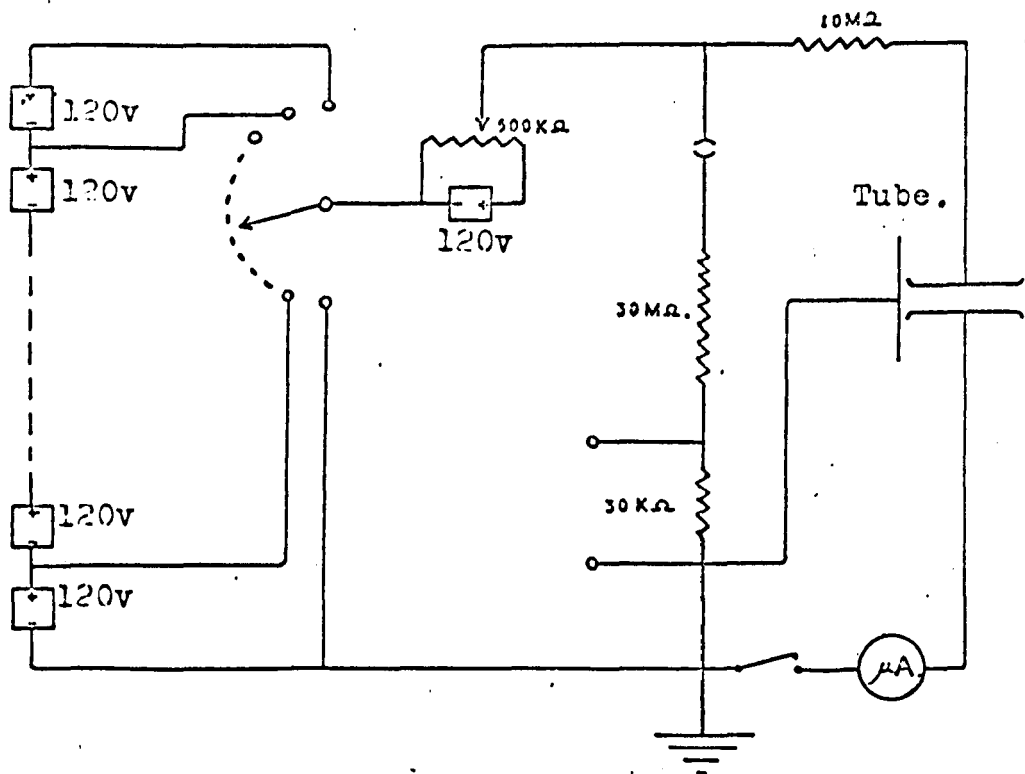
If care was taken in the use of the Alpert pump and it was not made to pump high gas pressures, i.e. pressures greater than 10^{-5} mm.Hg., then it could be used in more than one experiment after baking at 450°C although the subsequent pumping efficiency would be decreased. If, however, large amounts of gas had been pumped it was not possible to outgas completely by baking, (117), and subsequent pumping efficiency was very low.

When the system had been thoroughly evacuated and prepared the electrode surfaces were deposited. The

measuring electrodes were deposited first so that their surface properties would become stable before measurements were made on a cathode. Each electrode was deposited slowly, with the remaining electrodes shielded, by heating the appropriate metal bead until it melted and began to evaporate. Heating too rapidly might have caused the bead to fall from its support and heating too slowly might have caused the tungsten seals to become hot, with a consequent danger of breaking. Measuring electrodes were deposited to thicknesses of about 3-4000 Å, (films usually become opaque at about 2000 Å, (118)).

Since an investigation was to be made of changes in work function with film thickness some method of estimating thicknesses had to be developed. Within the last few months a method has been developed employing the effect of mass loading on the resonant frequency of a quartz crystal oscillator, (119). Unfortunately this device was not available initially and a method based on the optical properties of metal films was used.

Figures are available for the thicknesses of metal films corresponding to opacity in the visible region of the spectrum, (118). From these, and a measurement of optical absorption for the translucent films it is possible to make an estimate of the film thickness. For this investigation observations were obtained corresponding to one third, two



Sparking Potential Circuit.

Fig. 28.

thirds and total optical absorption using a pair of crossed polarisers for comparison. This method must be subject to an error of at least 20% but it was possible to correlate changes in work function with changes in film thickness.

3.4. High Voltage Supply and Measuring of Sparking Potentials

Because of the difficulty of constructing a high stability power pack the high voltage was drawn from a bank of eight 120 volt batteries connected in series as shown in Figure 28.

Increasing voltages could be tapped off in steps of 120 volts by means of a selector switch and a fine adjustment could be made using a 500 kilohm potentiometer placed across a single 120 volt battery. A high resistance chain (30 M Ω) was placed in parallel with the output of this system, and the output voltage could be measured across a tapping of the chain using a potentiometer and standard cell. The chain was of fifteen 2 M Ω resistors, which were individually calibrated against a standard megohm, sealed into a long glass tube for protection. Voltages were monitored across an accurately calibrated 30 kilohm resistor at the end of the chain, using a Cropico potentiometer (type P.3.) and standard cell. With this arrangement sparking potentials could be determined to within ± 1.0 volt. The current detector was a mirror galvanometer with a lamp and scale. A current of 10^{-8} amps giving a deflection of 2 cm.

As a safety precaution the press key used in the sparking potential determinations was mounted in a perspex box and it was impossible to touch any of the terminals.

The breakdown potential was defined as the potential difference required for a self-maintained discharge of 10^{-7} amps to pass between the electrodes. In order to determine this potential the cathode was illuminated with ultra-violet light which could be interrupted by means of a shutter placed over the quartz window of the experimental tube. The potential difference was increased in steps of about 1 volt and the pass key was closed for ten seconds after each increase.

When the galvanometer indicated a discharge of 10^{-7} amps, i.e. a deflection of 20 cm. on the metre scale, the ultra-violet light was interrupted and any change in the current was noted.

If the current ceased to flow the potential difference was increased slightly and the shutter reopened. A current of 10^{-7} amps which was unaffected by the absence of ultra-violet illumination, corresponded to a potential difference equal to the sparking potential which was then measured with the Cropico potentiometer.

Different pressures of hydrogen were admitted to the tube by heating the palladium and waiting until the pressures on each side of it were in equilibrium. The hydrogen

pressure was measured using the 3 metre oil manometer and a cathetometer, and it was found that times of between four and five hours were required for equilibrium to occur. The pressure was measured before and after each test and the palladium thimbles were heated continuously.

3.5. Construction of Experimental Tubes

The first experimental tubes were built in such a way that sparking potential and work function measurements could be made in the same sample of gas and under the same conditions. Each tube was designed for a particular set of measurements, for example, later tubes had cathodes which could be cooled to liquid nitrogen temperatures and units for evaporating different metals on to the same cathode. The tubes will be individually described in the appropriate parts of Chapter IV, but the common features are summarised below.

The electrodes were made by running molten pyrex into a carbon mould and pressing to form buttons about 2 cm in diameter and 3 mm thick. A tungsten rod was gently oxidized and pressed through each molten glass disc to form tungsten seals, the rods acting both as supports and electrical contacts to the surfaces. After positioning the rods the discs were carefully annealed. The surface of each electrode was prepared by grinding with three grades of carborundum powder and cerium oxide followed by thorough cleaning and light flame

polishing to produce flat and microscopically smooth faces. The last stage in this process oxidized the ends of the tungsten rods and this oxide was electrolytically etched away in sodium hydroxide solution. After a final cleaning any discontinuity between the tungsten rod and the electrode surface was eliminated by applying a small drop of aquadag at the junction. This also had the effect of protecting the tungsten against further oxidation during subsequent glass blowing operations.

Each cathode was fixed by a short glass rod on to the central stem of a commercially produced seven lead pinch and was positioned about 2 cm off centre. The anodes, Kelvin electrodes or evaporation shields, were fixed to a vertical pivot, together with a glass covered iron slug, in such a way that the cathode could be shielded, open to metal evaporation or exposed to the Kelvin electrode by magnetically deflecting the iron slug. Each pivot was held in a glass frame by two pointed rods and the frame was fused to the central stem of the pinch. It was possible to hold the pivots magnetically in any position between two stable positions, thus exposing the cathode for deposition of the metal surface from above. One stable position was with the Kelvin electrode over the cathode, thus enabling damping of the oscillating system to be a minimum. The other stable position was for either a sparking anode or a cathode evaporation shield. Each Kelvin

electrode was supported on the end of a spring made by diagonally spot-welding two tungsten strips to two short lengths of nickel wire. The spring system was adjusted so that the Kelvin electrode could oscillate vertically with a frequency of between 20 and 30 c/s.

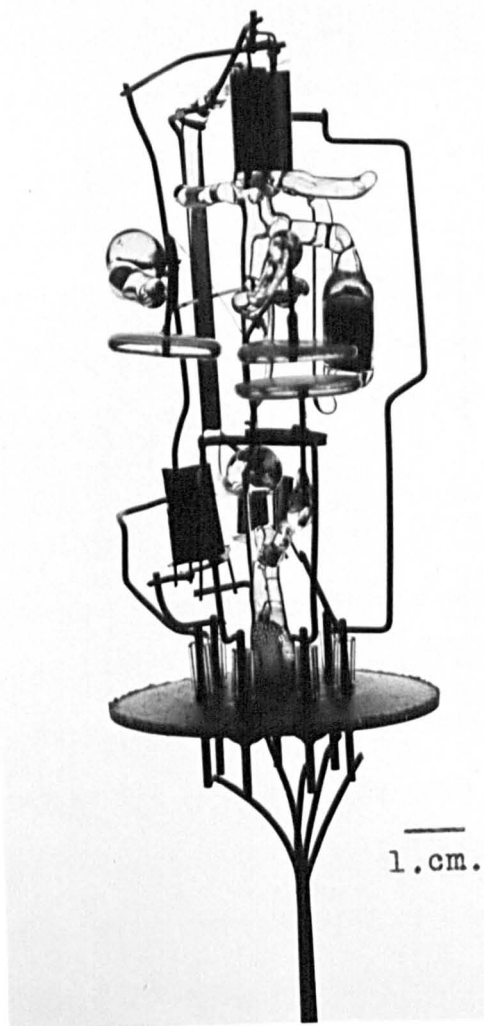
Electrical contact to the moveable electrodes was made by spiral nickel tapes welded to the tungsten points supporting the pivot. These tapes were soft and did not impede the movement of the pivot in any way. Nickel leads to all electrodes were spot welded to seals on the pinch after short glass cones had been slipped over the seals to protect them against any short circuiting caused by evaporated metal. The Kelvin electrodes, and any other moveable flat surfaces, were made parallel to the cathode by introducing a spacer of known thickness and softening the upper electrode support. No spacings greater than 5 mm. were used in this investigation.

The metal beads from which the surfaces were evaporated were made from lengths of Johnson and Matthey 0.3 mm. diameter copper, silver or gold wire, and were melted on to the points of 0.5 mm. tungsten V shaped filaments. Each bead was prepared by melting in a stream of hydrogen until the mobile surface appeared to be clear and uniform. This corresponded to the removal of all reducible impurities. Any hydrogen absorbed by the beads could be driven off in the outgassing processes during evacuation of the completed tube.

The beads were mounted opposite the faces of the appropriate electrodes and as near to them as possible without impeding the pivot action. Each bead was enclosed in a nickel cylinder which was closed at one end, and which confined the beam of evaporating metal to the area of the appropriate electrode. Great care was taken to prevent metal being evaporated from one bead and condensed on another. The electrical leads to the evaporators were made from the pinch, one lead being common and maintained at earth potential.

The pyrex envelope was prepared by joining two side arms, one for evacuation by coupling to the manifold, the other to hold a quartz window through which the cathode could be illuminated with ultra-violet light. After cleaning with acid, distilled water, methylated spirits and acetone an aquadag layer was painted and dried on to the inside of the clean envelope. Contact to this shield was by means of a tungsten spring which was spot welded on to the common lead of the pinch, and its function was to act as a means of preventing charge build-up on the glass surface and to provide some measure of electrostatic shielding.

When the pinch and electrode system had been correctly aligned within the envelope, the temperature was slowly raised until a drop seal was formed between the pinch and envelope. It was found to be most important to maintain



Typical Electrode Arrangement with
Sparking Anode over Cathode.

Fig. 30.

uniform heating and great care was taken to ensure that a good vacuum-tight seal was made. The tube was slowly annealed to reduce strains in the glass and was then coupled to the manifold and evacuated.

Photographs of a typical electrode system, in the two stable positions, are shown in Figures 29 and 30, and a completed tube and manifold can be seen in Figure 26.

CHAPTER IV

EXPERIMENTAL RESULTS

4.1. INTRODUCTION

Of the seven experimental tubes constructed the first three were for the investigation of changes in work function with film thickness, and of the occurrence of cathodic insulating layers during the admission of test gases. The fourth tube was used in an attempt to isolate contaminants arising from the glass vacuum system and to observe changes in cathode work function caused by deliberate slowing of the film annealing processes. Tube number five was designed to investigate annealing processes for films deposited on substrates of different crystal structure and the resulting cathode was used in an attempt to detect proton emission from hydrogenated palladium. The remaining tubes were used to confirm the results from earlier tubes and to detect any changes in the work function of the reference surface. Effects of annealing in the temperature range $-190^{\circ}\text{C} \rightarrow +250^{\circ}\text{C}$ under very good vacuum conditions were also studied.

The experimental tubes will be described in chronological order and the results analysed together in Chapter V.

4.2. Tube 1.

The admission of hydrogen to the experimental system by diffusion through palladium has been suspected as a source of contamination, (66, 99), and in order to investigate the effect a 'dummy' palladium thimble unit was constructed and placed in parallel with the existing unit. The dummy unit was similar in all respects to the normal unit except that it contained no palladium, i.e. the lead glass graded joint was made into a vacuum seal. This dummy unit was cleaned and outgassed in exactly the same manner and at the same time as the normal unit and it could be heated by a similar oven.

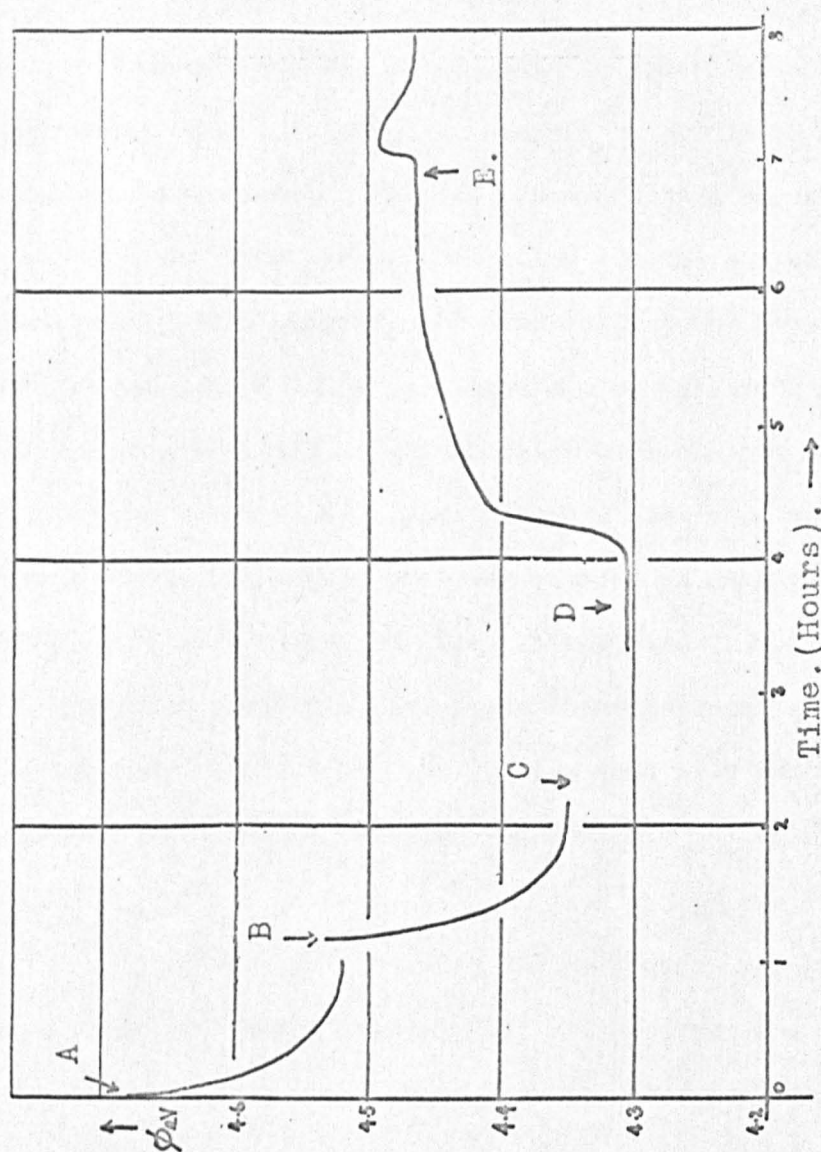
The sparking anode and Kelvin electrode were of copper and gold respectively and the surfaces were deposited as soon as the residual gas pressure had reached a value of 5×10^{-9} mm.Hg.

During deposition the pressure rose to 8×10^{-9} mm.Hg. and regained its former value about half an hour after the films had been put down.

After deposition of these electrodes a period of an hour elapsed before the formation of the cathode so that stable reference surfaces could be obtained. The pressure again rose to 8×10^{-9} mm.Hg. during cathode deposition.

The copper cathode was deposited slowly until about 30% of the light incident on the electrode was absorbed by the metal, an absorption corresponding to a film

Change in ϕ with Time. - Tube.(1). Copper Cathode.



- A.- First film deposited.
- B.- Second film deposited.
- C.- Third film deposited.
- D.- Dummy heater switched on.
- E.- Palladium heater switched on.

Fig. 31.

thickness of between 550 and 600 Angstrom units.

A metal having a high work function has a Fermi level of lower energy than that of a metal having a low work function. If these metals are connected electrically a contact potential difference will exist, the metal of low work function being positive with respect to the other metal. A positive potential must, therefore, be applied to the metal of high work function, relative to the other metal, in order to 'back-off' this contact potential difference.

The contact potential difference between the cathode and gold reference surface was measured 50 seconds after the cathode had been deposited and was found to be 0.02 volts, a positive potential being applied to the reference surface.

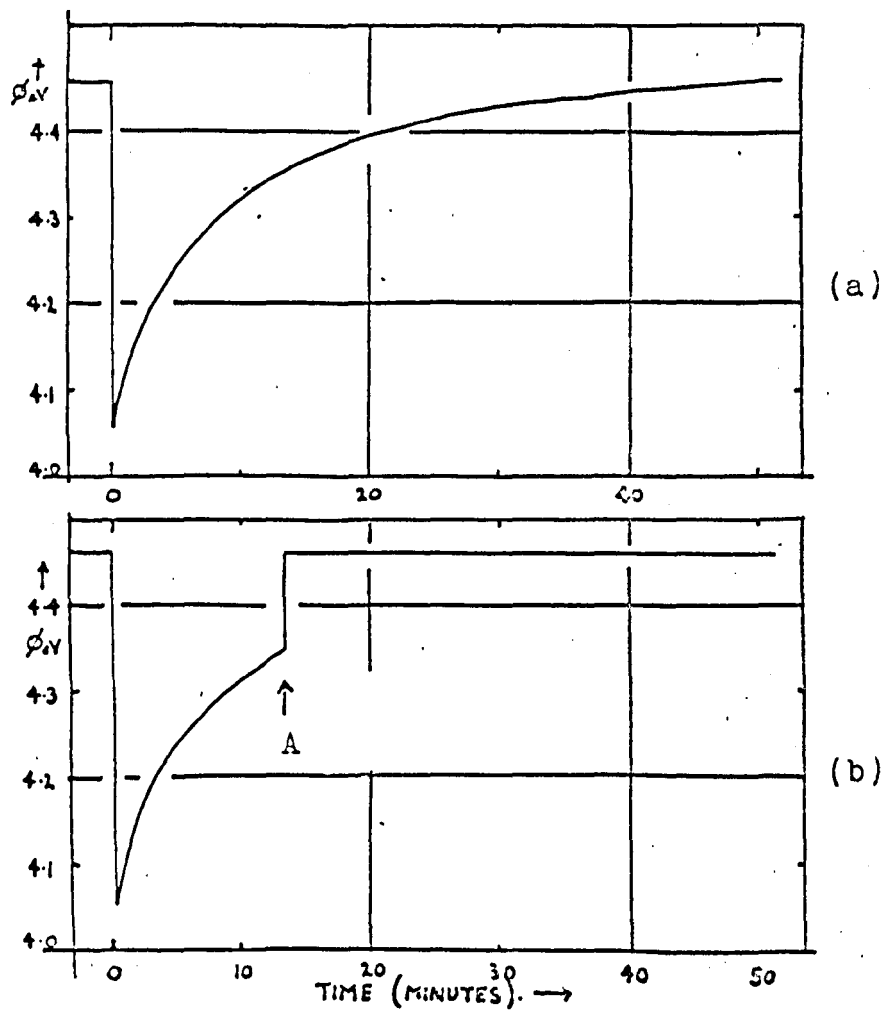
The work function of gold was assumed to be constant at 4.70 eV, (80), and the work function of the cathode must have been 4.68 eV. Unless stated otherwise all results will be expressed as changes in cathode work function.

During the first hour after deposition the work function gradually fell and steadied at a value of 4.52 eV, (Figure 31). On attaining this steady state a second copper film was deposited giving a total optical absorption of about 65% and corresponding to a film thickness of between 1100 and 1200 Angstrom units. The work function immediately after deposition was 4.53 eV and this fell to a

steady value of 4.35 eV in one hour. A further copper film was put down giving an opaque surface of about 1700 angstrom units in thickness, (118). The initial work function was not observed, due to a fault in the equipment, but the final steady value was 4.305 eV. At this stage, when the cathode surface had been steady for two hours, the dummy thimble unit heater was switched on. After 30 minutes, (the time taken for the oven to reach about 250°C), a small increase in pressure was noted, the final pressure being 5×10^{-7} mm.Hg. after a period of four hours. When the heater was switched off the pressure slowly dropped, due to Alpert pumping, and reached a steady value of 5×10^{-8} mm.Hg.

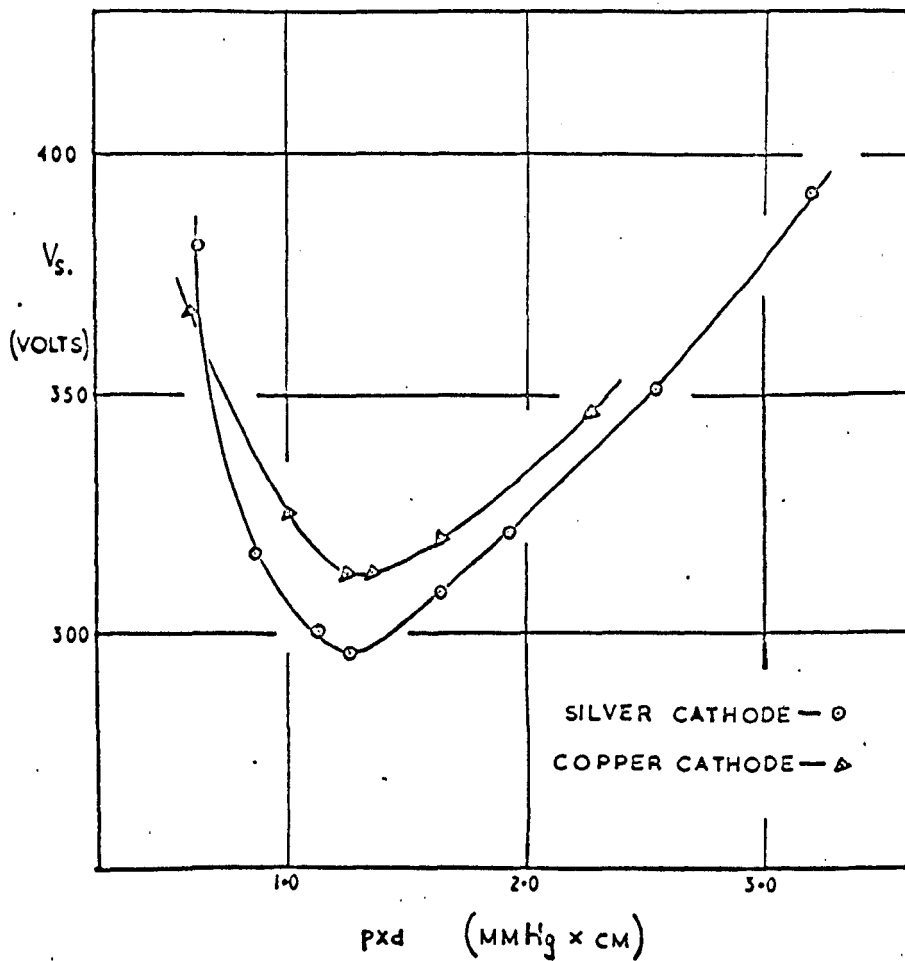
As soon as the oven had reached 250°C during heating and the pressure had begun to rise, a change in work function was detected. An increase of 0.095 eV took place in the first ten minutes and this was followed by a gradual increase of 0.06 eV during $1\frac{1}{2}$ hours, the final value being 4.46 eV.

Hydrogen was admitted by heating the palladium tubes to 250°C, a change in pressure being first detected twenty minutes after switching the oven on, corresponding to a palladium temperature of about 200°C. At this point an increase in ϕ of 0.03 eV was detected over a period of five minutes, which was followed by a gradual decrease to the original value in one hour.



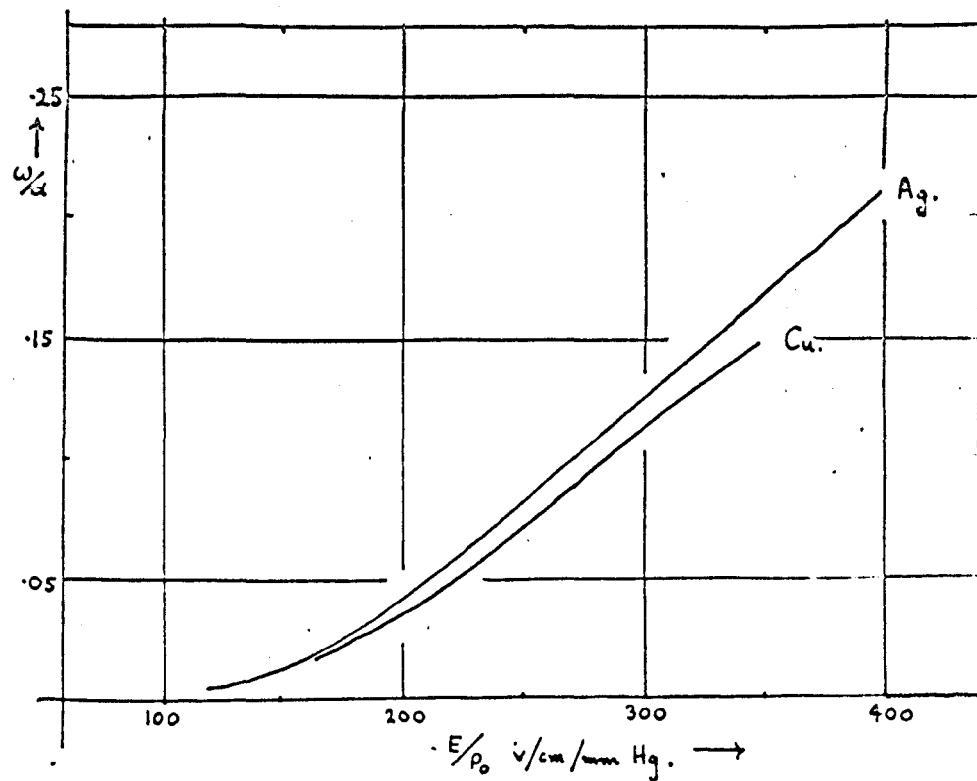
Change in ϕ with Time after Sparking.
 (A.- Ultra-Violet light switched on.)

Fig. 32.



Paschen Curves for Copper and Silver in Hydrogen.

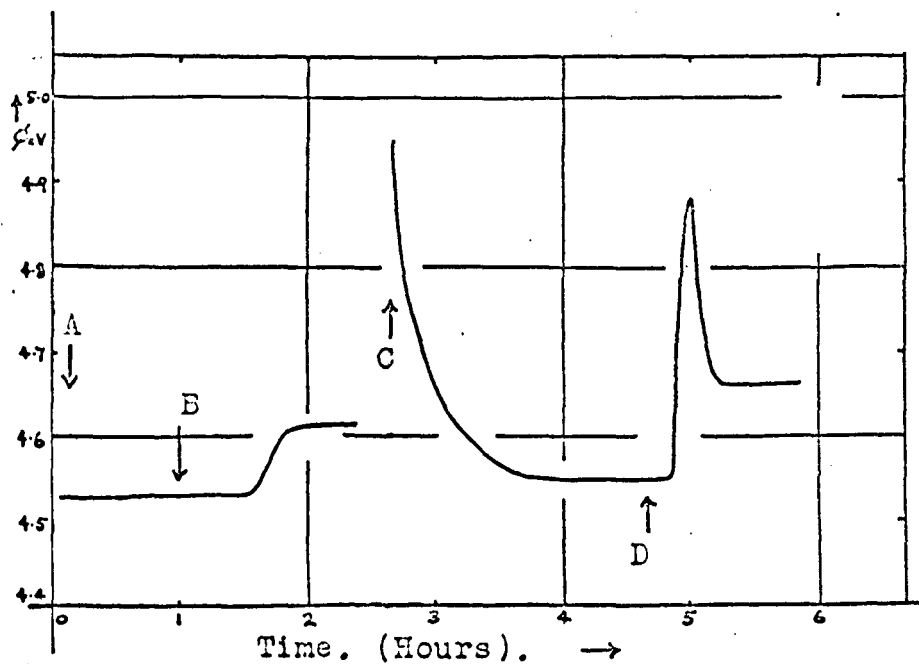
Fig. 33.



Variation of ω/α with E/p for Cu. and Ag. in Hydrogen.

Fig. 34.

Change in ϕ with Time. - Tube.(1). Copper Cathode.



- A.- Fourth film deposited.
- B.- Dummy heater switched on.
- C.- Fifth film deposited.
- D.- Palladium heater switched on.

Fig. 35.

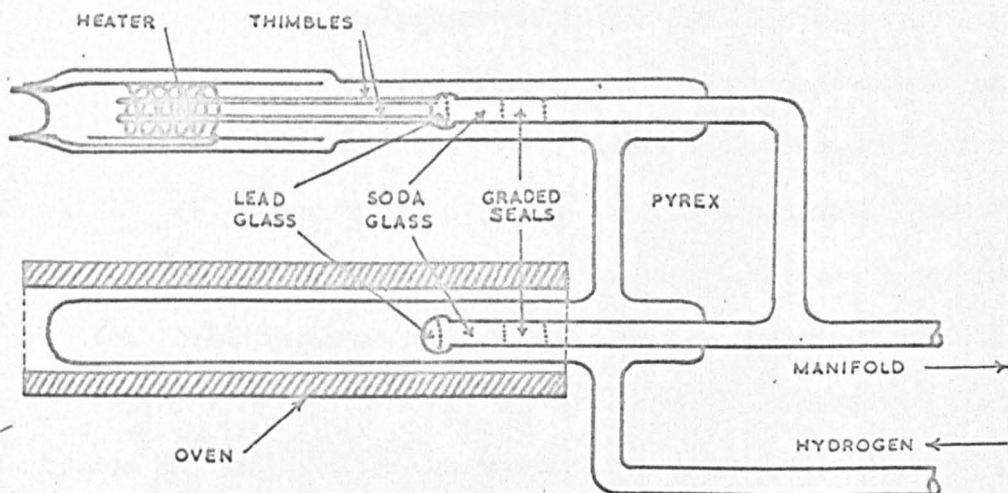
When the hydrogen pressure had steadied and both sides of the palladium were in equilibrium a sparking potential was determined. The effect of the discharge on the cathode was a decrease in ϕ of 0.4 eV, the original work function being regained after about 50 minutes, (Figure 32(a)). Several sparking potential measurements were made for different hydrogen pressures, the cathode work function being reduced by each discharge and recovering after between thirty and fifty minutes. In one case the contact potential difference increased to 10 volts after a current of 10^{-6} amp had passed for ten seconds, but in each case the normal work function could be immediately regained by illuminating the cathode with ultra-violet light, (Figure 32(b)).

The values of V_s and pressure obtained for the particular gap distance of 0.35 cm. were used to obtain a Paschen curve, (Figure 33), and the variation of (ω/α) with (E/p) , (Figure 34), was calculated using Myatt's figures for the variation of (α/p) with (E/p) , (37).

After re-evacuation and processing a fourth copper film was deposited, its work function settling at 4.53 eV in about forty minutes.

The effect of heating the dummy thimble unit was repeated and an increase in ϕ of 0.08 eV was detected which compared with 0.095 eV in the first test, (Figure 35).

The work function of the fifth copper surface was



Palladium Thimble and Dummy Diffusion Unit.

Fig. 36.

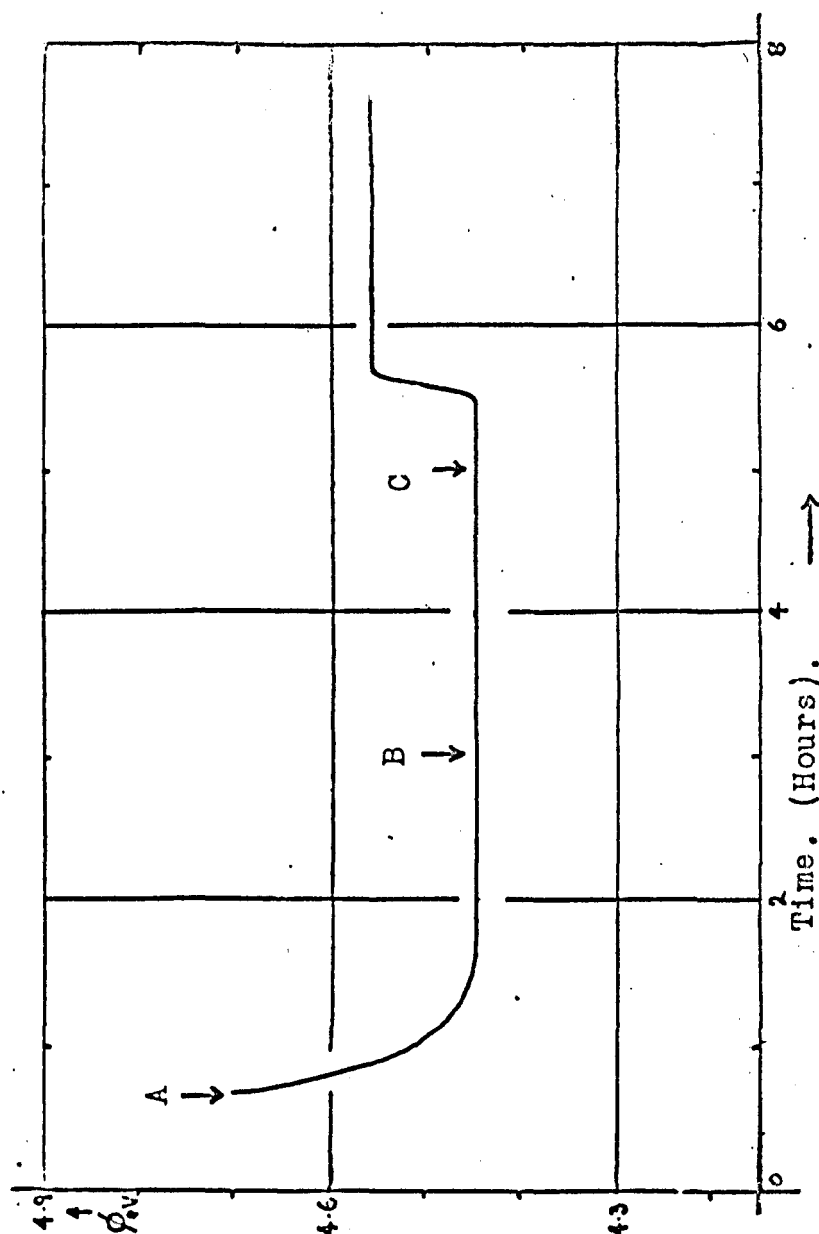
originally 4.95 eV but this became 4.55 eV in eighty minutes. When the surface had become steady the palladium diffusion unit was heated and hydrogen admitted. Within thirty minutes ϕ increased to 4.88 eV and then decreased to 4.66 eV, the total change taking place in 15 minutes and amounting to an increase in ϕ of 0.11 eV. Insufficient copper remained in the evaporator to enable further measurements to be taken with this tube.

4.3. Tube 2.

Because of the earlier difficulty in admitting hydrogen to the manifold without heating any of the glassware near the palladium, a simple modification was made to the method of heating employed. A small tungsten heating coil was wound on a short alumina cage and placed in the hydrogen around the ends of the palladium tubes, (Figure 36). The amount of heat carried down the tubes by conduction was small and the glassware linking the palladium tubes to the manifold remained near room temperature during operation. The ends of the tubes could be heated to temperatures greater than 250°C quickly by radiation and local convection in the hydrogen and equilibrium between the two sides of the system could be obtained within two hours.

The second tube contained a gold reference electrode and a copper sparking anode similar to tube 1, but the cathode was of silver.

Change in ϕ with Time.- Tube.(2).Silver Cathode.



- A.- Silver Surface Deposited.
- B.- Modified palladium heater switched on.
- C.- Dummy heater switched on.

Fig. 37.

Difficulty was experienced during the deposition of the silver film and the variation of ϕ with thickness was not observed, a thick film being obtained in a residual gas pressure of 10^{-7} mm.Hg. The cathode work function immediately after deposition was 4.70 eV, but this decreased to 4.45 eV in one hour, (Figure 37).

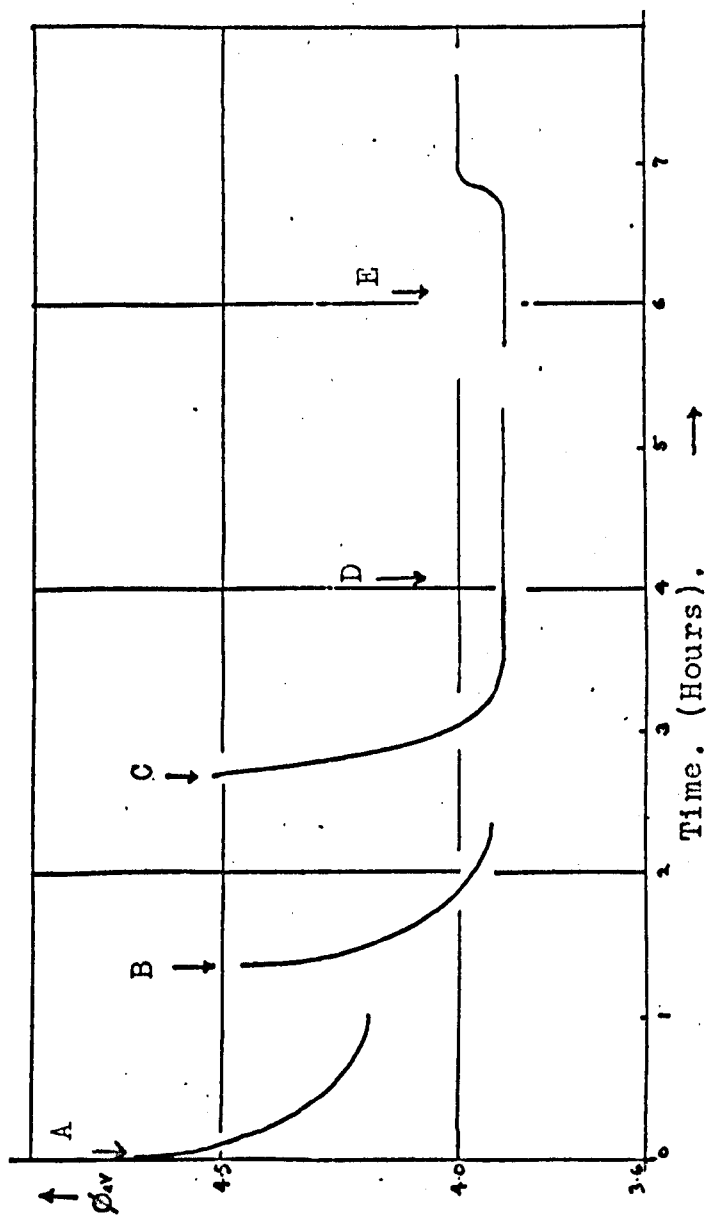
There was no detectable change in ϕ as hydrogen was let into the manifold by heating the tungsten coil and the steady surface condition was maintained in the presence of hydrogen for over ninety minutes. When the oven surrounding the dummy thimble had been switched on for twenty minutes ϕ increased by 0.11eV and remained at this value.

Unfortunately an electrical contact failed after this test and no further measurements were obtained from the tube.

4.4. Tube 3.

Before evacuating tube 3 a device for introducing small quantities of pure oxygen was constructed and fitted to the manifold. The device consisted of two tungsten filaments surrounded by alumina tubes which were coated with a paste of barium peroxide in collodion solution. After evacuation of the system, and before the final baking process, the filaments were flash heated to about 700°C in order to decompose the cellulose binding compound and outgas the metal parts. Pure oxygen is formed by the decomposition of barium

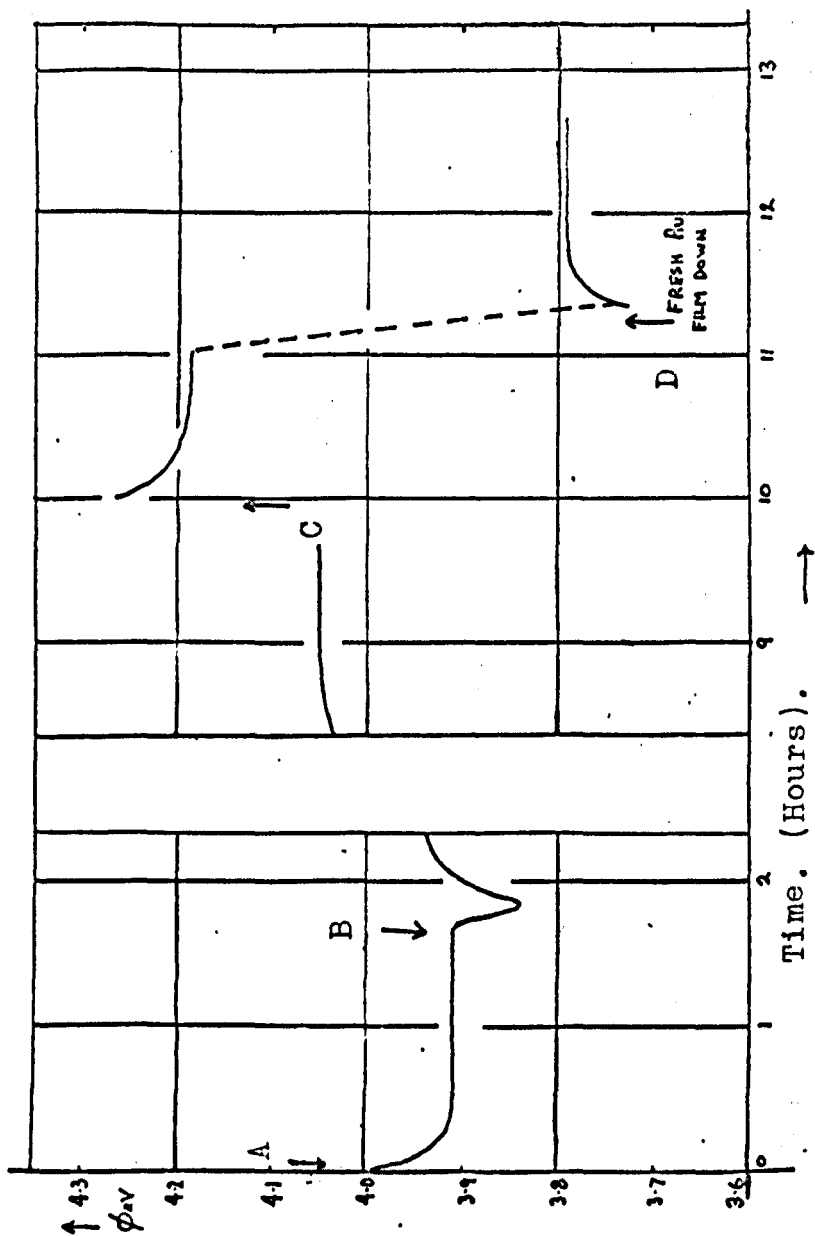
Change in ϕ with Time.- Tube.(3). Silver Cathode.



- A.- First Silver film deposited.
- B.- Second silver film deposited.
- C.- Third silver film deposited.
- D.- Palladium heater switched on.
- E.- Dummy heater switched on.

Fig. 38.

Change in ϕ with Time. Tube. (3).



- A.- Fourth silver film deposited.
- B.- Oxygen admitted.
- C.- Fifth silver film deposited.
- D.- Fresh Kelvin surface deposited.

Fig. 39.

peroxide at temperatures of the order of 700°C.

Both the sparking electrode and the kelvin electrode in this tube were of gold, the silver cathode being deposited when the residual gas pressure was about 10^{-8} mm.Hg.

The variation of ϕ with silver film thickness was investigated as for copper in tube 1, and similar 'aging' effects were observed, (Figure 38). The work function of the first surface steadied at 4.19 eV and the final surface at 3.91 eV.

The tungsten filament surrounding the palladium thimbles was heated, in the absence of hydrogen, and no change in ϕ was detected during two hours.

For this tube the dummy unit consisted of pyrex glass only. The lead and soda glasses had been removed prior to evacuation and the length of pyrex was processed exactly as before. Forty minutes after switching on the dummy heater an increase in ϕ of 0.09 eV was noted giving a final cathode work function of 4.00 eV.

At this stage an electrical fault caused a delay of three days and measurements were resumed after a fresh gold reference surface had been deposited.

The fourth silver surface had an initial work function of 3.98 eV which reduced to 3.92 eV in forty-five minutes, (Figure 39).

After the work function had remained steady for

about two hours, a small amount of oxygen was admitted by careful decomposition of the barium peroxide, and when the Alpert gauge reading had indicated a pressure increase from 5×10^{-8} mm.Hg. to 5×10^{-7} mm.Hg oxygen production was stopped.

Within nine minutes of producing the gas the work function had decreased to 3.84 eV, but during the following six hours it increased to 4.05 eV.

Deposition of a fifth silver surface led to a steady value of ϕ of 4.19 eV but this became 3.79 eV after a fresh gold reference surface had been put down.

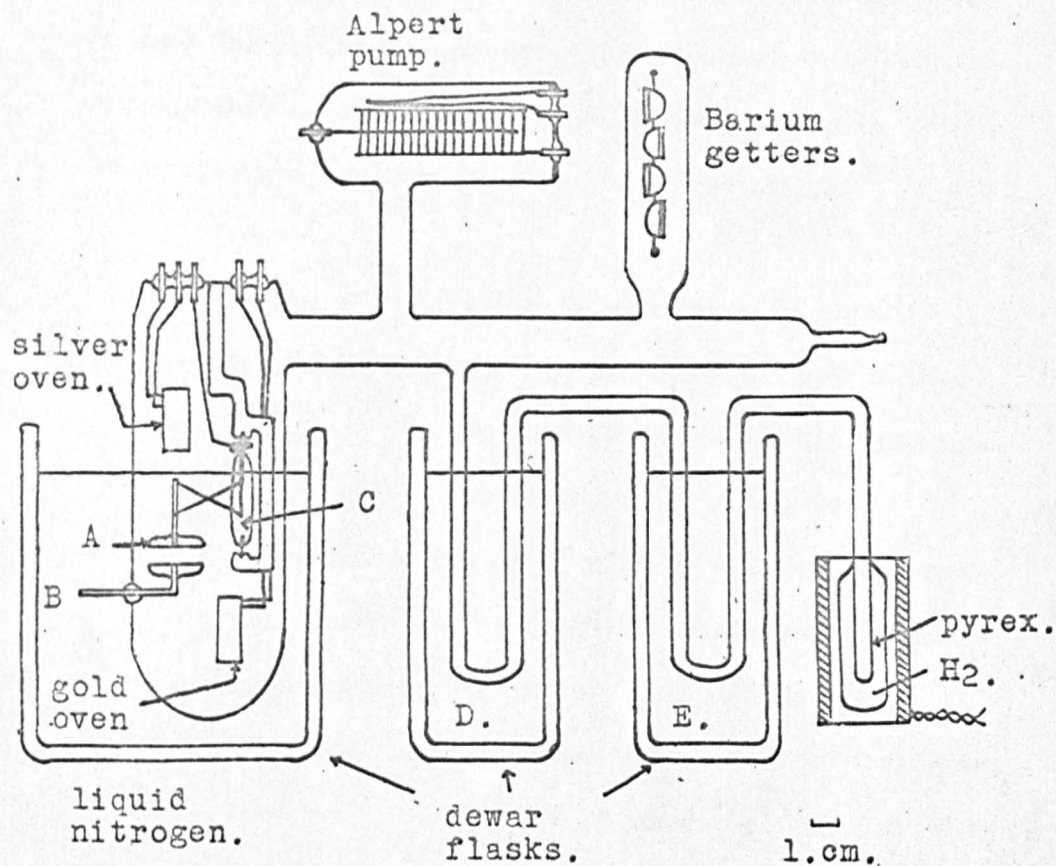
A set of sparking potential measurements was obtained for the final surface and for the gap distance of 0.5 cm., and are shown in (Figure 33). Values of (ω/α) corresponding to the different values of (E/p) were calculated from the Paschen curve and are displayed in (Figure 34).

4.5. Tube 4.

Measurements obtained with tubes 1, 2 and 3 have indicated that some change takes place in the cathode during the first forty minutes after its deposition and that a change in work function can be caused by heating part of the glass system, i.e. the dummy thimble unit. Tube 4 was designed and constructed with a new manifold to investigate these effects more closely.

The tube contained a gold kelvin electrode and a

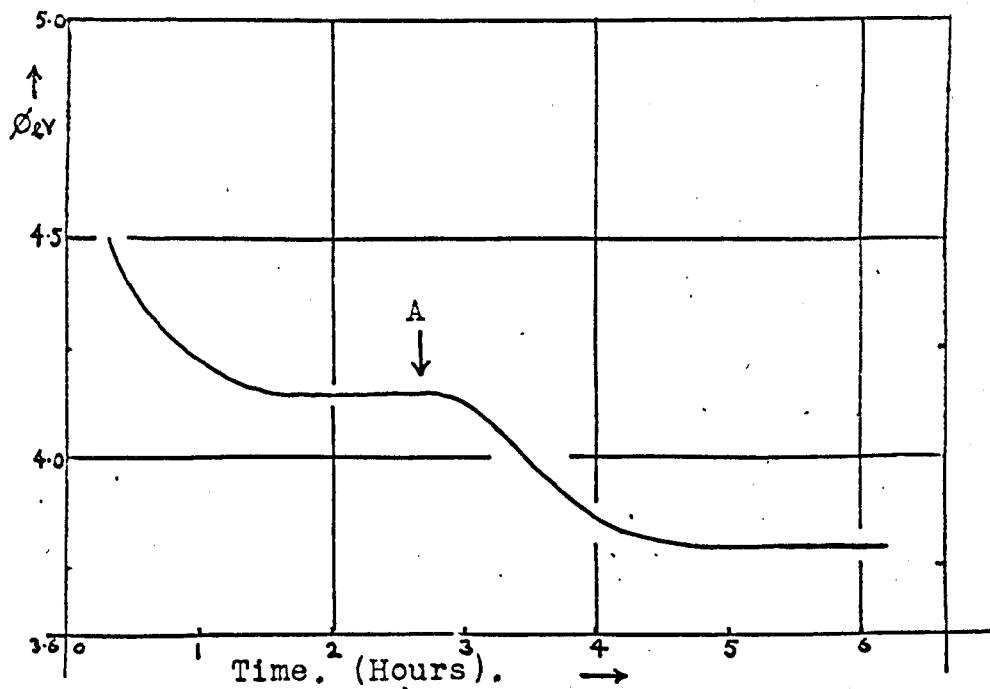
Design of Tube. (4) and Manifold.



- A.- Kelvin electrode.
- B.- Silver cathode.
- C.- Pivot.
- D.- Trap containing liquid nitrogen.
- E.- Trap containing carbon tetra-
chloride at -10°C .

Fig. 40.

Change in ϕ with Time. Tube. (4). (Cooled cathode).



A.- Coolant removed.

Fig. 41.

silver cathode which was supported by a thick tungsten rod sealed into the lower end of the glass envelope, (Figure 40). The whole tube could be immersed in liquid nitrogen and the tungsten rod acted as a heat conductor between the cathode and the dewar flask. This rod was also the electrical connection to the cathode surface.

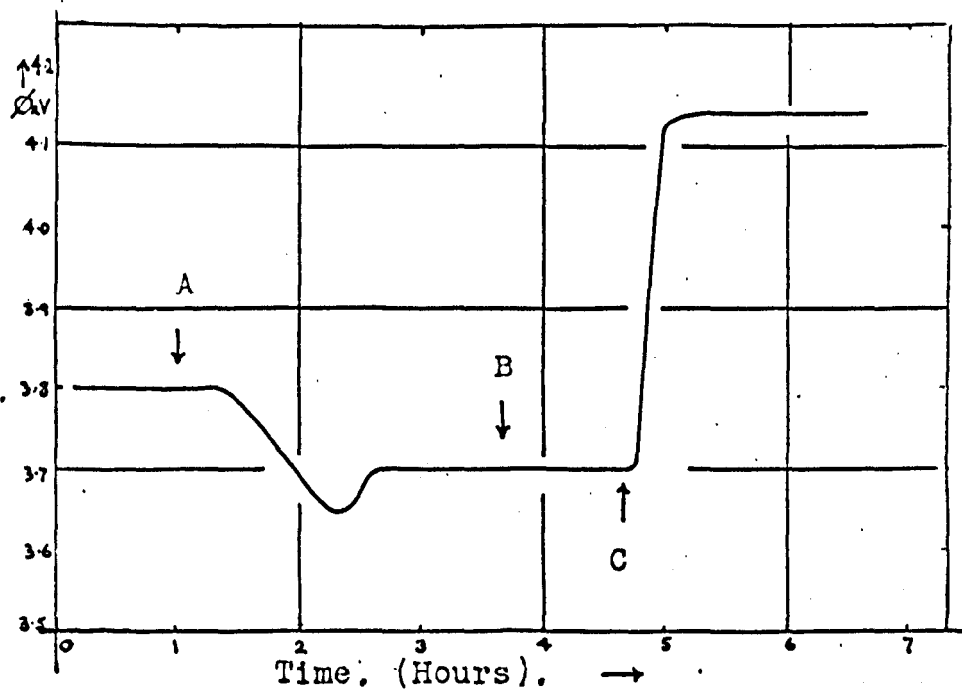
The dummy palladium thimble unit consisted of a sealed pyrex tube surrounded by a larger pyrex tube containing hydrogen at a pressure of about 10 mm.Hg. The whole unit could be heated to between 200°C and 350°C by means of a small cylindrical oven as before. Between the dummy unit and the experimental tube were two condensing traps, the one nearest the tube being immersed in liquid nitrogen at -196°C and the other being immersed in carbon tetrachloride at -10°C. This construction made it possible to fractionally condense any vapours given off during heating of the pyrex tube.

A residual gas pressure of 10^{-8} mm.Hg was obtained after normal processing. The experimental tube was immersed in liquid nitrogen for four hours until thermal equilibrium occurred, and the gold reference surface was quickly deposited so that steady conditions prevailed after a further hour of cooling.

Immediately after deposition the silver work function was 4.50 eV but this gradually fell during the next eighty minutes to a steady value of 4.14 eV, (Figure 41).

Change in ϕ with Time.

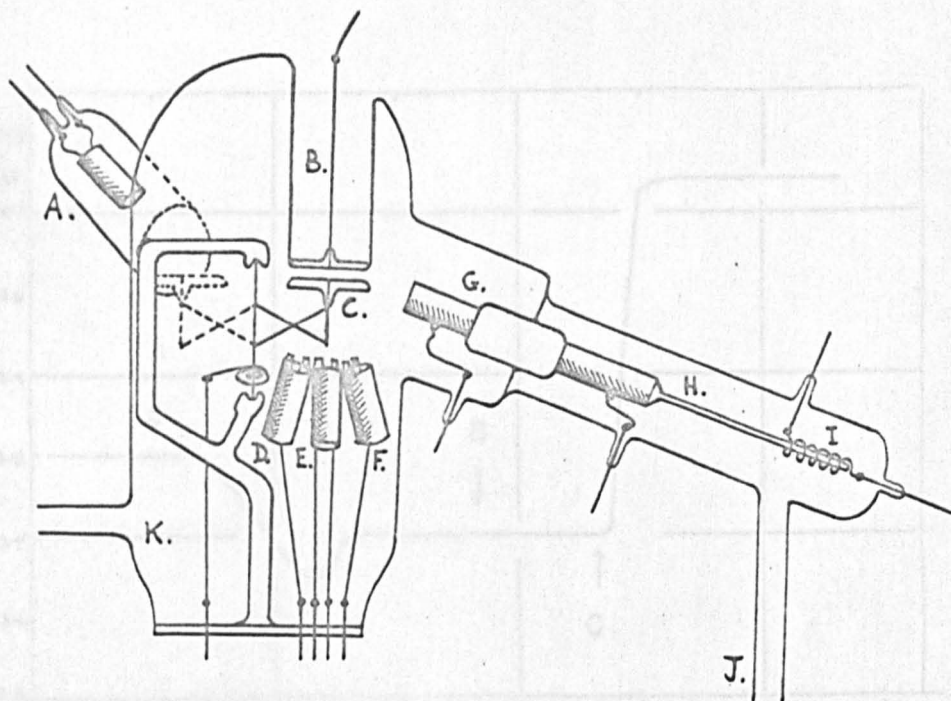
Tube. (4).



A.- Pyrex side-arm heated.
B.- Liquid nitrogen removed.
C.- Carbon tetrachloride removed.

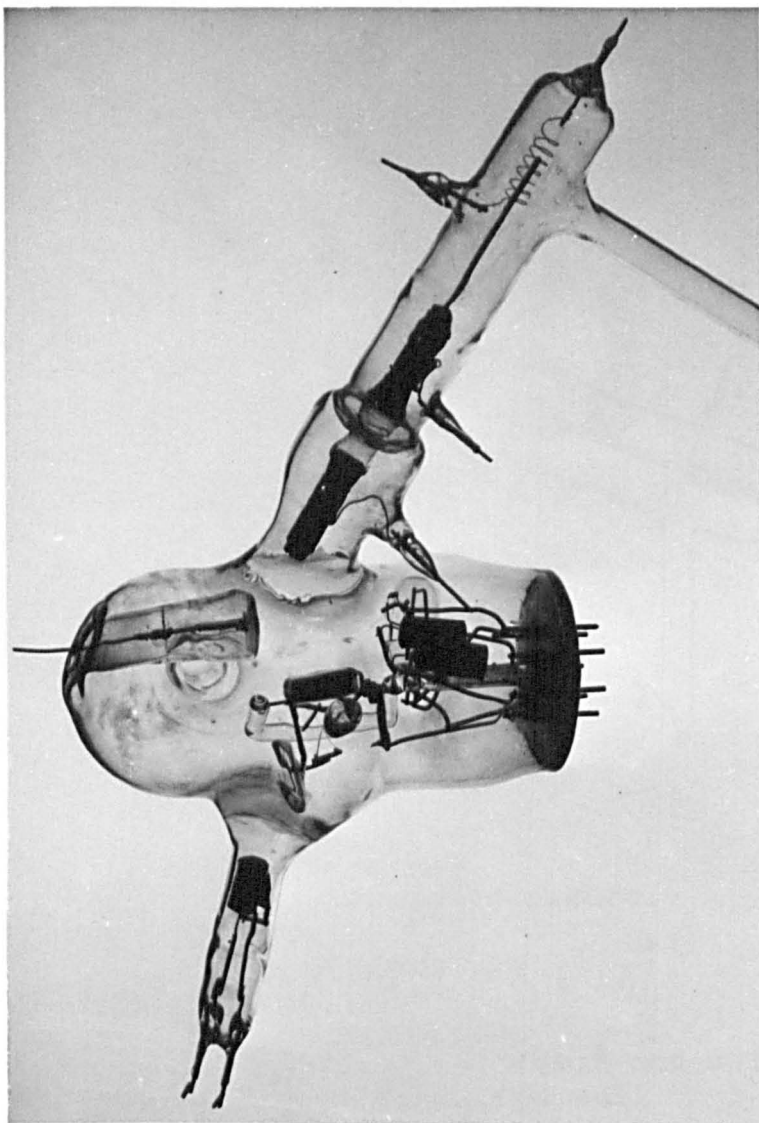
Fig. 42.

Design Details of Tube. (5).



- A.- Gold evaporater.
- B.- Hollow cathode structure.
- C.- Cathode.
- D.- Copper evaporater.
- E.- Tin evaporater.
- F.- Barium evaporater.
- G.- Positive ion collector and drift tube.
- H.- Palladium diffusion unit.
- I.- Tungsten heater.
- J.- Hydrogen inlet.
- K.- Evacuation port.

Fig. 43.



Tube. (5).

Fig. 44.

During a period of two hours, after the dewar flask had been removed and all ice etc. cleaned away from the tube, the work function gradually fell to 3.80 eV. Similar figures were obtained from a repeat experiment using fresh metal films.

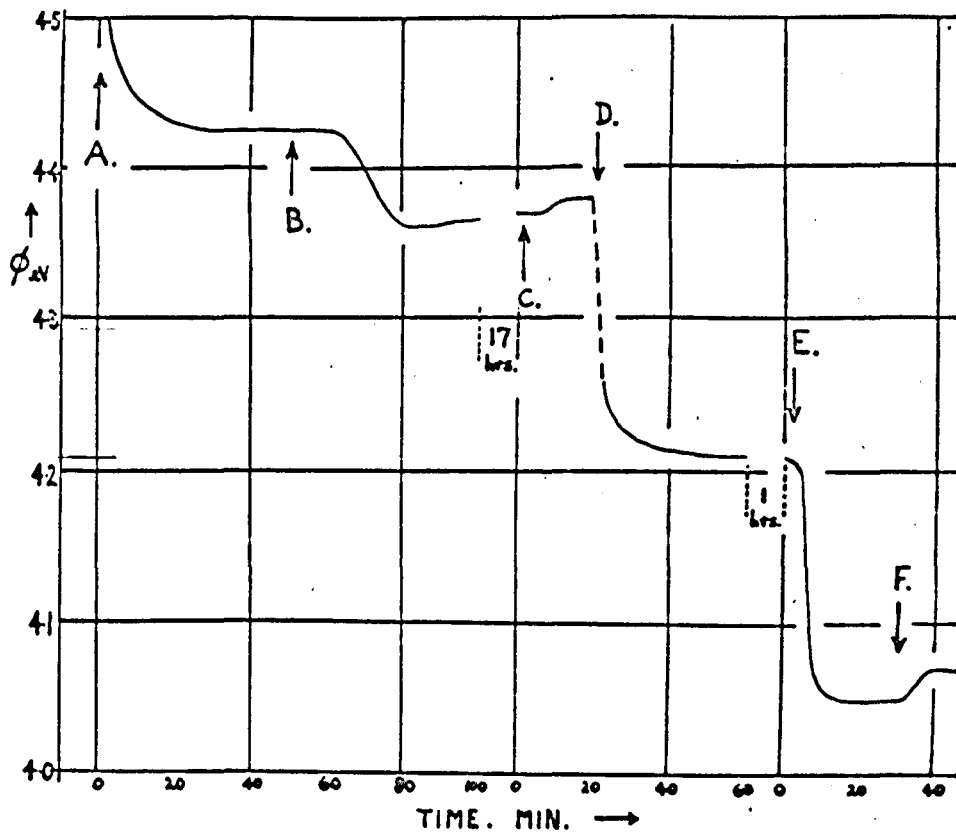
When the electrode surfaces had again become steady the pyrex tube was heated to between 300°C and 350°C. The rise in temperature was accompanied by a decrease in ϕ of 0.15 eV, and a steady figure of 3.70 eV was attained after one hour, (Figure 42). There was no detectable change in ϕ as the liquid nitrogen trap was warmed to room temperature, but ϕ increased by 0.44 eV in ten minutes as the carbon tetrachloride trap was warmed.

These changes were subsequently confirmed when, for a fresh cathode surface, the pyrex was heated to 250°C. The magnitudes of the changes were correspondingly lower.

4.6.

Tube 5.

Tube number five was designed to follow the work function history of a composite cathode under more efficiently controlled temperature conditions. The glass cathode substrate was the polished end of a re-entrant side-arm of the main envelope which could be rapidly cooled by filling with liquid nitrogen, (Figures 43, 44). Three separate metal evaporators were disposed symmetrically under the cathode and enabled films of copper, tin and barium to be



- A.- Thick, cooled copper film deposited.
- B.- Coolant removed.
- C.- Coolant replaced.
- D.- Thin tin film deposited.
- E.- Coolant removed.
- F.- Coolant replaced.

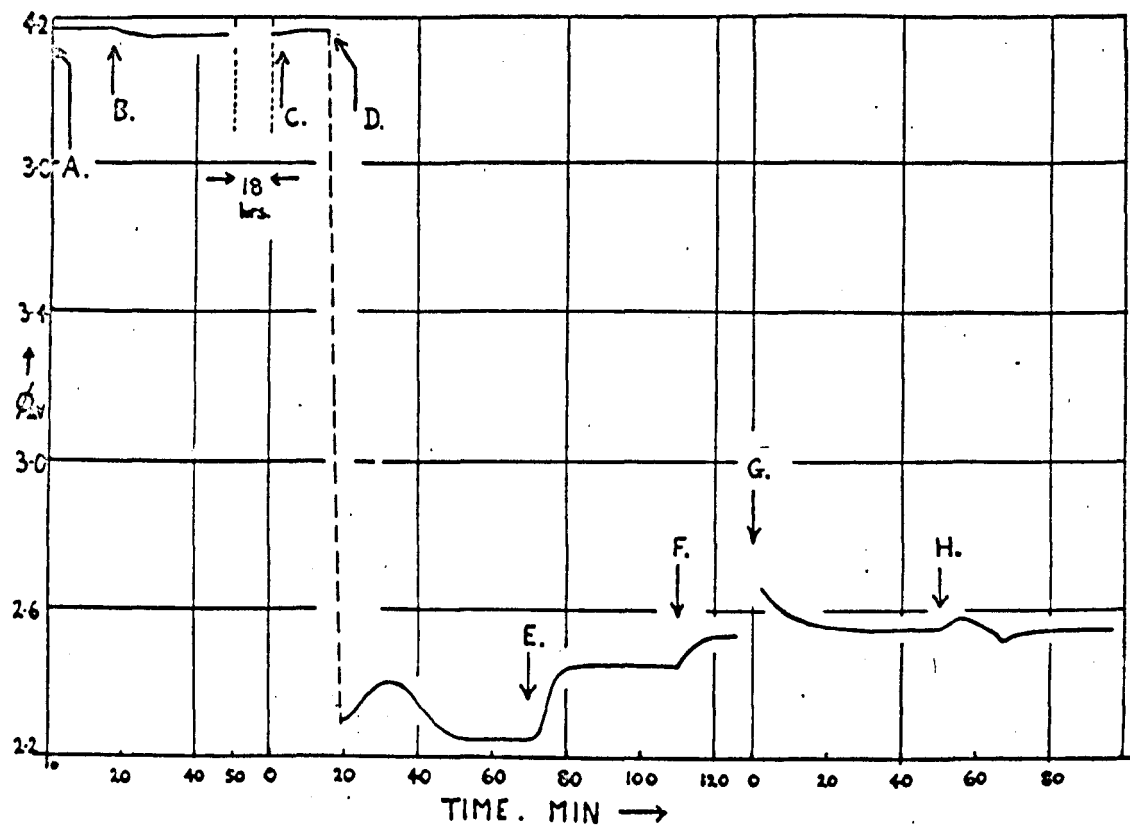
Fig. 45.

deposited. The barium was evaporated from a commercially produced getter which could be fired by ohmic heating.

The final cathode was used to try to detect any positive ion emission from heated palladium by trapping any such ions on the surface and observing any change in the contact potential difference. The positive ions could be produced in a gun arrangement, (Figures 43, 44), which was used either to direct the beam on to the cathode or to collect and measure the ion current directly.

Unfortunately the internal arrangement of this tube was such that it was difficult to estimate film thicknesses. It was possible to make a distinction between thick and thin films where the thin films would be less than about 800 Angstrom units deep by regulating the evaporation time and observing deposits on the walls of the tube.

The initial copper surface was deposited thickly because difficulty had been experienced during outgassing and it was likely that the copper bead would become detached from its support during repeated heating. The work function of this cooled copper film was measured 45 seconds after the evaporator had been switched off and was found to be 4.50 eV. This decreased in 40 minutes to 4.43 eV, (Figure 45), and removal of the coolant led to a further decrease giving a steady value of 4.36 eV.



- A.- Thick tin film deposited.
- B.- Coolant removed.
- C.- Coolant replaced.
- D.- Thin barium film deposited.
- E.- Coolant removed.
- F.- Coolant replaced.
- G.- Thick barium film deposited.
- H.- Coolant removed.

Fig. 46.

Seventeen hours later the work function was found to be 4.37 eV and cooling of this cathode, in preparation for the deposition of a thin tin film caused a small increase to 4.38 eV.

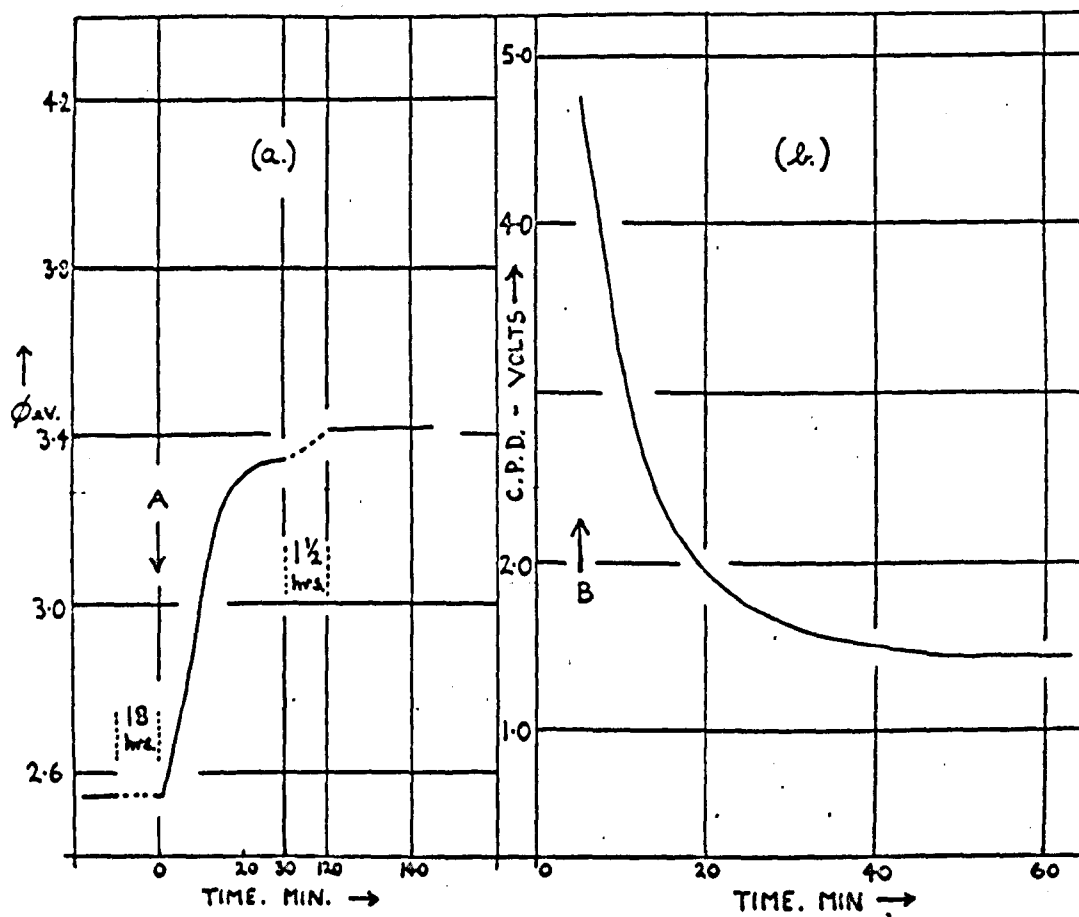
Deposition, and subsequent warming to room temperature, of a thin film of tin caused similar decreases as those observed for copper, the cold and warm values of ϕ being 4.21 eV and 4.05 eV respectively. A 0.02 eV rise in ϕ was noted on further cooling prior to deposition of a thick tin film, and the cold and warm values of ϕ for this final tin film were 4.18 eV and 4.15 eV, which represented an increase of 0.10 eV above the value for the thin tin film, (Figure 46).

The residual gas pressure at this stage had risen to 10^{-8} mm.Hg due to gas evolution from the copper and tin beads, but this fell to 8×10^{-9} mm.Hg overnight during getter and Alpert pumping.

As the cathode was re-cooled in readiness for barium deposition a small increase in ϕ of 0.01 eV was detected. (This particular change is obscured in Figure 46 by a scale effect.)

The work function of the thin, cooled barium film was measured three minutes after deposition and initially rose from 2.30 eV to 2.41 eV. This was followed by a reduction to 2.25 eV, the stable surface being formed after about thirty-five minutes. Removal of the coolant was

Change in ϕ and C.P.D. with Time. Tube. (5).



A.- Barium cathode exposed to hydrogen.
 B.- Discharge passed. (10^{-7} amp for 10sec.).

Fig. 47.

followed within five minutes by a rise in ϕ of 0.20 eV to a steady value of 2.45 eV, and re-cooling twenty minutes later caused a small rise to 2.525 eV, (Figure 46).

Deposition of a thick, cooled barium surface increased the work function only slightly to 2.55 eV, and removal of the coolant was followed by a small pulse increase and decrease leading to a steady value of 2.54 eV which was only 0.01 eV lower than that for the previously cooled surface.

Previous workers in this laboratory, (74, 75), have used barium electrodes in the presence of hydrogen and have reported that an originally vacuum deposited and optically reflecting metallic film has apparently disappeared on the admission of hydrogen. Since their measurements were obtained from what might have been a changing surface it was thought necessary to repeat the effect and follow any associated changes in work function.

The admission of hydrogen, up to a pressure of 2 mm.Hg, was accompanied by a rapid rise in the work function of the barium surface, (Figure 47(a)). After thirty minutes the rate of change began to decrease and a steady value of 3.42 eV was obtained after a further hour, the total change amounting to an increase of 0.88 eV.

In order to test for the production of positive ions in the palladium diffusion process it was necessary to

confirm that the presence of ions could be detected, under these conditions, by changes in contact potential difference.

The reaction between hydrogen and barium would probably have caused the formation of a high resistance surface layer. It was, therefore, only necessary to pass a discharge between the cathode and the nickel evaporation shield above it and observe any changes in contact potential difference. The changes seen immediately after passing a discharge of 10^{-7} amps for ten seconds are shown in Figure 47(b). A total contact potential difference change of 3.3 volts was measured four minutes after passing the discharge and this fell approximately exponentially to zero in about fifty minutes corresponding to a cathode work function of 3.22 eV.

The positive ion gun structure, referred to earlier, consisted of a normal palladium tube mounted on a copper housekeeper seal and a similar copper tube which was mounted co-axially but about 1 cm behind it. The palladium thimble was in the hydrogen system and could be heated by a tungsten coil surrounding it. The copper drift tube was sealed so that it formed the only communication channel between the palladium and the vacuum system.

The complete unit was fixed into the experimental tube so that its axis was directed towards the cathode at as steep an angle as possible, (about 40°), and the end of the

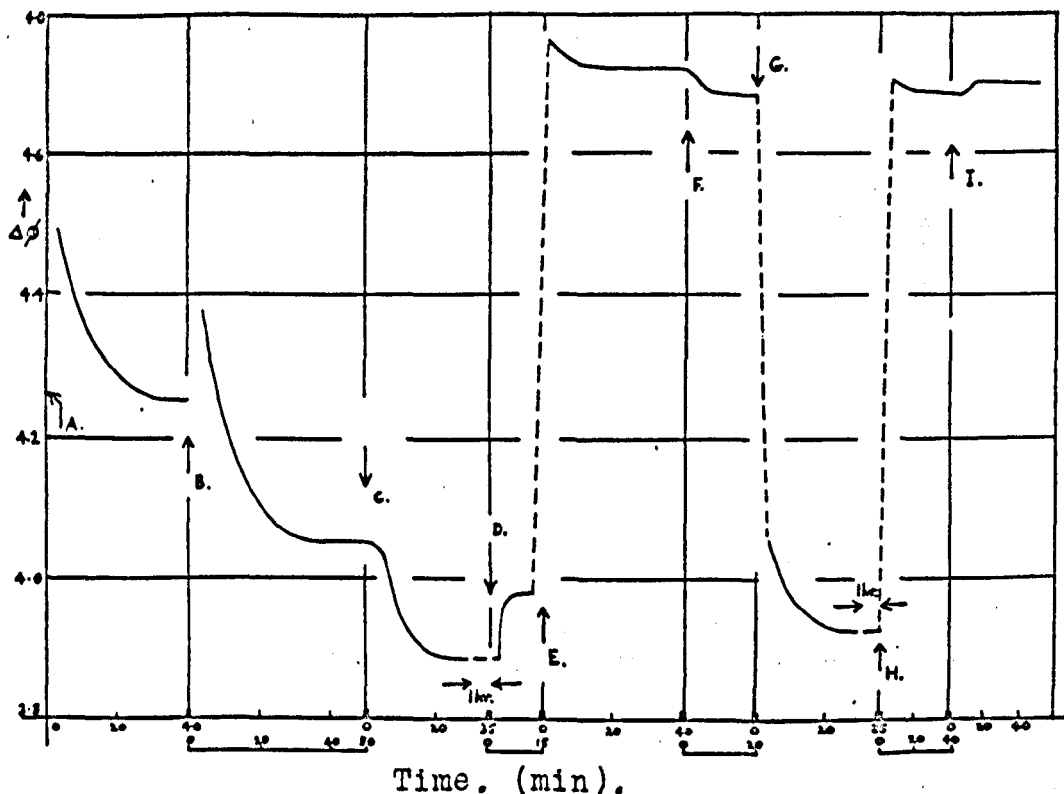
drift tube was about 2 cm. from the cathode centre. Electrical contact could be made to both the palladium tube and the drift tube by means of tungsten-glass seals.

Care was taken to ensure thorough outgassing of the copper tubes during preparation and they were subjected to a hydrogen glow discharge for several hours.

It was possible, using the electrometer circuit shown in Figure 48, to measure currents of the order of 10^{-14} amps between the copper tubes. The high resistances R_1 and R_2 ($\approx 10^{13}$ ohms) were in the grid circuits of a BDM.10 type of double tetrode valve. At balance there was no difference between the two anode currents but if a small potential was developed across R_1 , due to a current in the circuit linking the copper tubes, then a large out of balance current would be indicated by the galvanometer G. The calibration curve for this instrument is shown in Appendix III.

Before taking measurements the manifold was reopened to the high vacuum system, by breaking a pig's tail seal, and the hydrogen pumped away. The residual gas pressure before testing was about 10^{-7} mm.Hg.

Great care was taken in this experiment and the only detectable current was a pulse rising to about 10^{-11} amps and lasting for about five seconds which occurred ten seconds after commencing each diffusion process. This pulse was independent of palladium temperature in the range



- A.- Thin, cooled silver film deposited.
- B.- Thick, cooled silver film deposited.
- C.- Coolant removed.
- D.- Coolant replaced.
- E.- Thick gold film deposited. (cathode).
- F.- Coolant removed.
- G.- Thick silver film deposited.
- H.- Thick gold film deposited. (cathode).
- I.- Cathode warmed. (water added at 85°C).

Fig. 49.

studied, i.e. up to about 300°C , and independent of the collecting potential between - 30V and - 500 V. For collecting potentials greater than - 30V the pulse decreased and could not be detected at - 5V. The pulse also decreased with decreasing time interval between experiments but appeared to be maximum and constant for times greater than about ten minutes.

No changes in the contact potential difference between cathode and kelvin electrode were observed throughout the experiment.

4.7. Tube 6.

This tube was designed to re-investigate the changes in ϕ with thickness of a silver cathode under more efficiently controlled temperature conditions, i.e. with the re-entrant, hollow type of cathode structure described in section 4.6. It was also possible to superimpose a gold cathode film in order to look for any changes that might have taken place on the gold reference electrode throughout the experiment.

The results obtained are shown in Figure 49.

The work function of the initial, cooled, thin silver film followed the usual decrease after deposition and steadied at 4.25 eV. Immediate deposition of a thick film on this surface caused a sharp rise in ϕ , to 4.38 eV, and this also fell during forty-five minutes to 4.05 eV. Removal of the coolant was followed by a sharp decrease in ϕ to 3.89 eV.

The residual gas pressure was 9×10^{-9} mm.Hg at this stage.

An hour later the cathode was again cooled and ϕ was seen to rise by 0.09 eV to 3.98 eV.

Deposition of a thick gold film raised the apparent work function to 4.72 eV and this fell to 4.68 eV on warming to room temperature.

Unfortunately this deposition caused an increase in residual gas pressure to 5×10^{-8} mm.Hg.

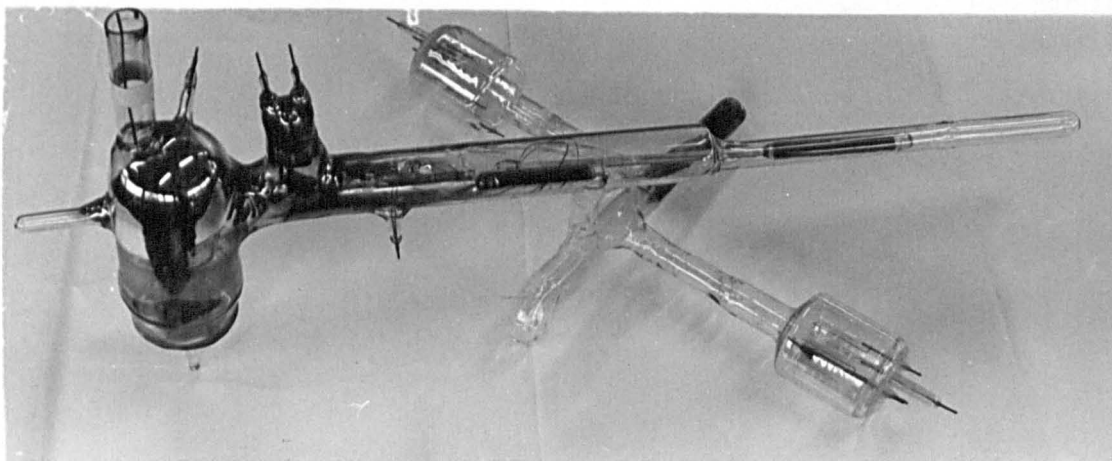
A further silver deposition at room temperature gave a work function of 3.93 eV, and this surface was finally covered by gold having a steady work function of 4.68 eV.

When hot water was poured into the cathode, and maintained at 85°C using a tungsten wire immersion heater, the contact potential difference gradually reduced and was zero after an hour, indicating an apparent work function of 4.70 eV.

4.8. Tube 7.

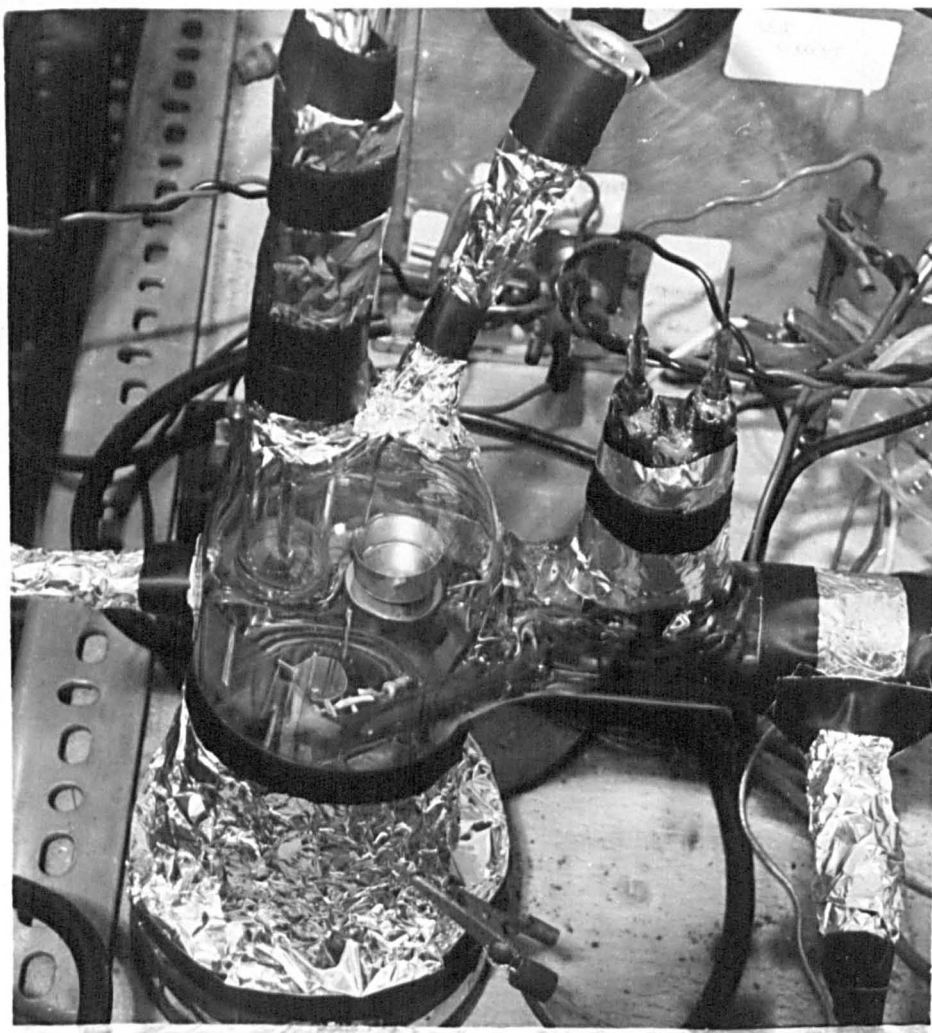
This final tube was designed to investigate the effects of annealing in the temperature range -196°C to 250°C and the effects of different substrates on the cathode work function under greatly improved vacuum conditions.

Two cathodes were used, one being of the re-entrant hollow type and the other being an 'O' nickel button. Their surfaces, which were in the same plane, could be simultaneously



Tube. (7). and Manifold.

Fig. 50.



Electrode and Furnace Layout. Tube. (7).

Fig. 51.

exposed to evaporation from a silver bead and the gold kelvin electrode could be moved into place from a side arm in the envelope, (Figure 50).

Gold evaporation, to form the kelvin surface, was performed in the side arm and the whole kelvin assembly could be delicately moved along glass rails by means of an external solenoid and positioned under either cathode, (Figure 51).

The volume of the ultra-high vacuum system was kept as low as possible (≈ 1500 cc) and the whole was carefully outgassed for two weeks.

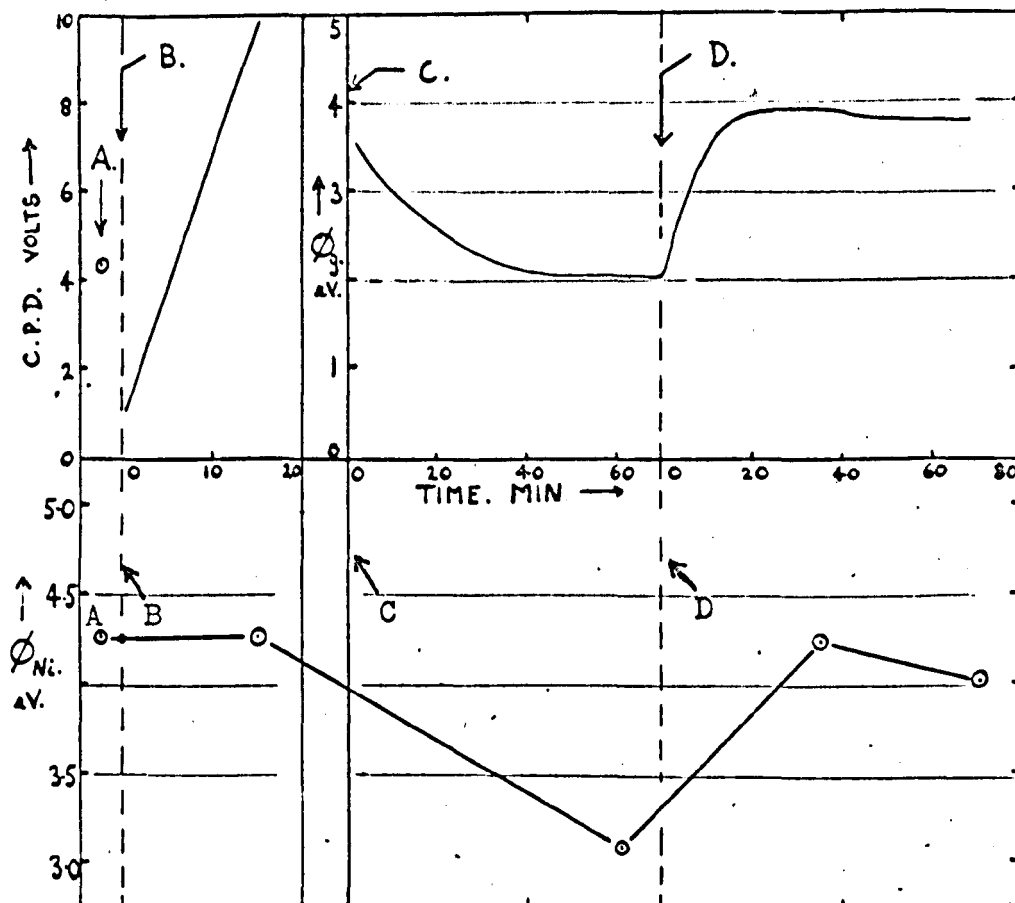
At final seal-off the system consisted of the experimental tube, an arm containing barium getters and two commercially produced Alpert pumps.

After gauge pumping for two days the pressure was 3×10^{-10} mm.Hg and at no time during the experimental period did this rise above 5×10^{-10} mm.Hg.

After evacuation the work function of the nickel cathode was 4.26 eV but the work function of the glass electrode, i.e. the tungsten lead-through painted with aquadag, appeared to be 0.36 eV corresponding to a contact potential difference of 4.34 V.

On filling the glass electrode with liquid nitrogen, in preparation for the first silver evaporation, the contact potential difference reduced immediately to zero and

Change in ϕ and C.P.D. with Time. Tube. (7).



- A.- Initial C.P.D.- (glass substrate).
 Initial work function. (nickel).
 B.- Coolant added.
 C.- Very thin silver film deposited.
 D.- Coolant removed.

Fig. 52.

rose linearly to 10 volts in fifteen minutes.

It was noted, however, that over-vigorous movements of the kelvin electrode had caused the gold surface to touch the glass repeatedly during this period and care was taken in subsequent measurements.

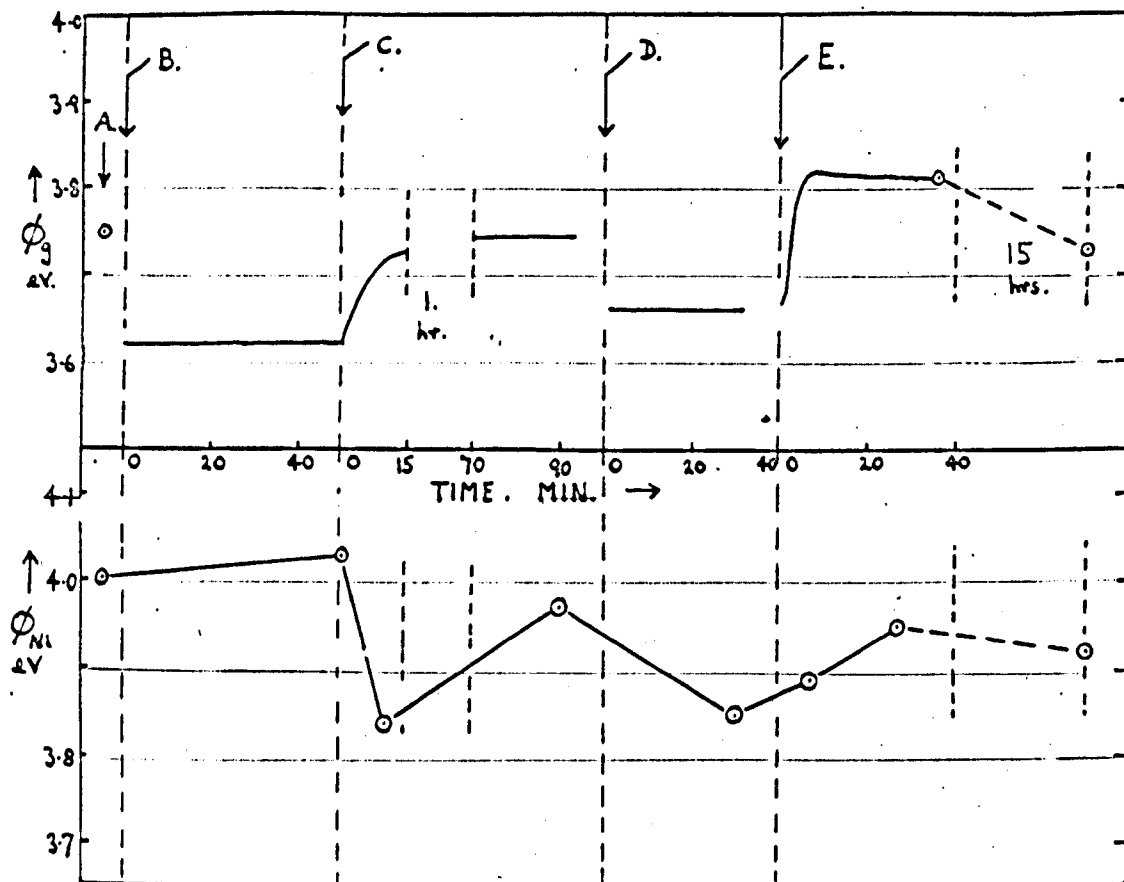
The work function of the nickel surface remained constant during cooling, as was expected since the two cathodes were thermally isolated.

The first deposition was of a very thin film, probably $\ll 400 \text{ \AA}$, and the cooled glass substrate yielded an original work function of 3.51 eV. This fell in about an hour to a steady value of 2.14 eV, (Figure 52). The corresponding final value for the nickel electrode was 3.15 eV.

Unfortunately, it was not possible to follow continuous changes for both surfaces and it was decided to follow the changes in the glass substrate electrode and to take intermittent measurements on the nickel electrode.

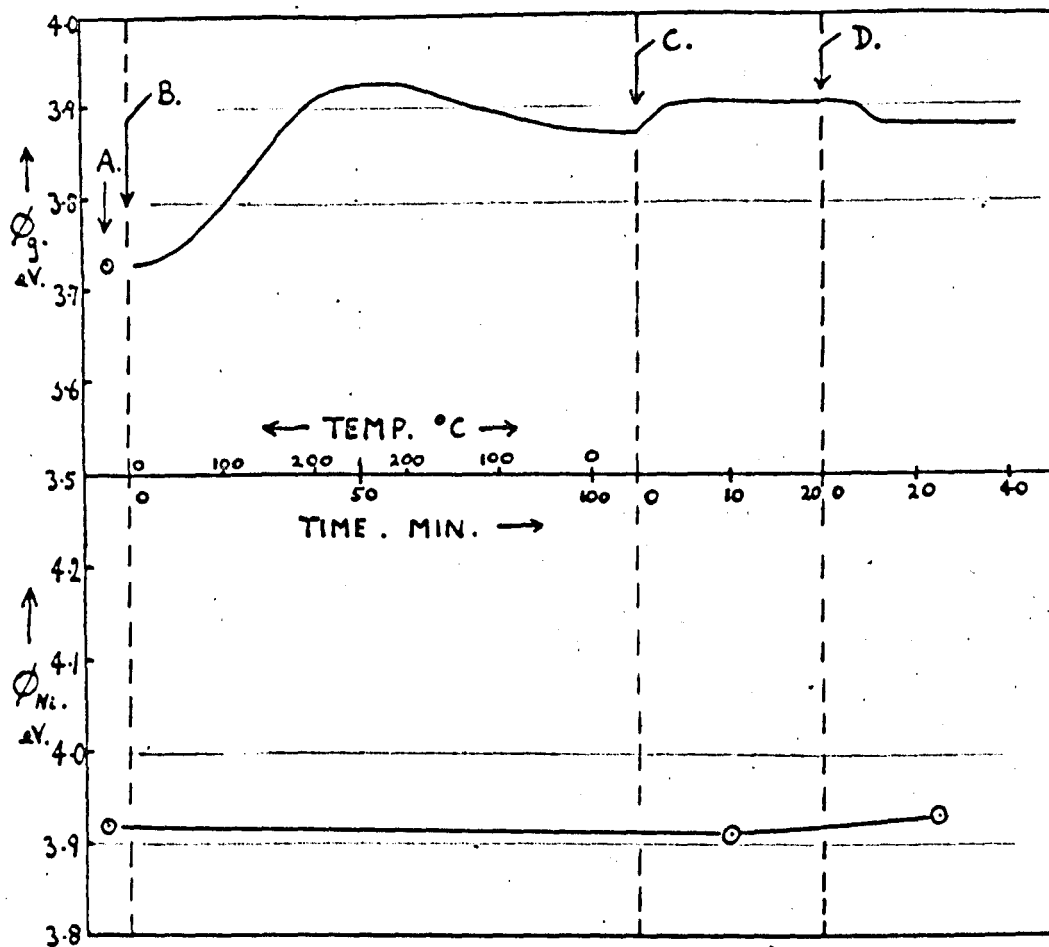
Warming to room temperature, by removing the coolant, was accompanied by a rise in ϕ_{glass} to 3.75 eV, the change taking about seventy minutes. During this change ϕ_{nickel} reached a maximum of 4.24 eV in thirty-five minutes and a final value of 4.01 eV after seventy-one minutes.

The second silver deposition gave rise to a cooled film of total thickness about 1500 \AA and a work function which remained steady at 3.62 eV for fifty minutes. The value for



- A.- Initial work functions.
- B.- Second silver deposition. (cold).
- C.- Coolant removed.
- D.- Third silver deposition. (cold).
- E.- Coolant removed.

Fig. 53.



- A.- Initial work functions.
- B.- Annealing process started.
- C.- Liquid nitrogen added.
- D.- Liquid nitrogen removed.

Fig. 54.

the nickel surface was 4.03 eV measured at the end of this time, (Figure 53).

Removal of the coolant again caused an increase in ϕ_{glass} to 3.74 eV over a similar period of time. The value of ϕ_{nickel} , however, decreased to 3.84 eV after ten minutes and rose again after ninety minutes to 3.97 eV.

A third deposition, this time of a thick film, caused similar changes, the steady ϕ_{glass} being 3.66 eV and the final ϕ_{nickel} being 3.85 eV.

A steep increase in ϕ_{glass} of 0.15 eV was observed on warming and the final value of ϕ_{nickel} became 3.95 eV. Both work functions decreased overnight, a period of fifteen hours, the former to 3.73 eV and the latter to 3.92 eV.

In order to follow any changes in ϕ caused by raising the temperature of the metal film the hollow cathode was filled with silicone oil and heated by means of a tungsten wire immersion heater.

The changes observed are plotted in Figure 54 as changes in work function against temperature over the complete thermal cycle, i.e. the maximum temperature being midway along the axis. For purposes of comparison it was arranged that the heating time should be approximately equal to the cooling time, and the temperature axis can therefore give some idea of the time scale. Maximum temperature was reached after about fifty

minutes and room temperature was regained after about one hundred minutes.

The highest work function, (3.92 eV) was obtained just after maximum temperature, (250°C), and the final value of ϕ_{glass} was 3.87 eV. It was not possible to obtain values of ϕ_{nickel} during this test.

The final experiment consisted of recording work function changes during re-cooling and warming of the thick silver film.. An increase in ϕ_{glass} of 0.02 eV was detected on cooling and this was followed by a decrease of 0.02 eV on warming, both changes requiring less than ten minutes each. The values of ϕ_{nickel} cold and ϕ_{nickel} warm were 3.91 eV and 3.93 eV respectively.

CHAPTER V

DISCUSSION OF RESULTS AND CONCLUSIONS

5.1. Introduction

The experiments described in the preceding sections have all been directed towards an investigation of the factors influencing the work functions of evaporated metal cathodes of the type used in this laboratory in the study of low current gas discharges.

All the experimental tubes were concerned with the insulating layers which appear to be formed on cathodes very soon after their deposition, and the changes in work function which accompany this process.

At residual gas pressures not lower than 10^{-9} mm.Hg. it can be expected that adsorbed monolayers will form in times not longer than about 40 minutes, (20). Since pressures lower than this were not attainable initially, and since the changes observed are of this time scale, it must be inferred that adsorption processes are contributing to the changes.

It is also likely that as a metal film is built on a substrate by condensation many lattice defects will be frozen into the bulk metal. Such defects would not be rigidly frozen at room temperature and many of them would be able to diffuse to the film surface. This process would

lead to a change in work function since the surface would then contain a greater number and a wider range of types of adsorption site.

A lowering of the substrate temperature should fix any defects more rigidly, with a consequent retardation of this 'annealing' process, whereas an elevation of the substrate temperature should accelerate relief to a more perfect lattice and a different work function.

Unfortunately, lowering of the substrate temperature leads to more effective adsorption, the accommodation coefficients for the gases on the surface being increased and the cooled system becoming a weak cryogenic pump. Elevated temperatures will lead to a greater decomposition of the glass components which will increase the number and variety of adsorbable particles.

If a series of films is deposited at residual gas pressures of the order of 10^{-9} mm.Hg and at intervals greater than about 40 minutes, a complicated film will result having a sandwich type of structure, i.e. metal plus adsorbed layer plus metal plus adsorbed layer, etc. Such a surface should have a work function different from that of a single film of the metal of equivalent thickness and the extent of the difference may give some idea of the depth within the film beyond which changes in structure will not affect the work function of the surface.

The rigorous outgassing and hydrogen furnacing schedules employed in tube construction indicate that the greatest partial pressure of residual gases will be that due to hydrogen.

For copper and silver electrodes any hydrogen adsorption will be physical adsorption, (97), and will result in a dipole layer having its positive side outwards and causing a reduction in ϕ , (see Figure 7).

For thin electrode films, i.e. those which are optically transparent, it is probable that the metal does not form a continuous film, (81, 120), but that it exists in the form of islands which link as the film thickness is increased. Discontinuities must also be introduced by the surface roughness of the substrate, which for pyrex glass is described by a roughness factor of at least 2.5, (84).

Immediately after the deposition of such films, when the numbers of dislocations and other lattice defects is high, the surface will consist of a large number of metallic aggregates whose constituent atoms are mobile enough to allow diffusion of the defects to take place.

After a few minutes many of the defects will have reached the surfaces of the islands and the result will be a large number of randomly oriented crystallites. The measured work function of such a system will be the average of the large number of slightly different work functions of

the various crystal faces and will depend on the extent of coverage of the substrate or, in the case of glass substrates, on the extent of coverage of the point of electrical contact. A substrate of high work function will 'show through' the thin film and increase the measured average value.

Von Engel has reported, in his work on secondary electron emission, (121), that electrons are emitted from glass by electron bombardment, such electrons having received sufficient energy to enable them to surmount the surface barrier. It may be possible, therefore, to assess a certain high value of 'work function' for glass. Such a quantity is difficult to interpret and may have no physical significance, but for thin metal films on pyrex substrates it may help to explain some of the unexpectedly high values of ϕ obtained.

5.2. Glass Decomposition and the Admission of Hydrogen

The increases in work function observed with tubes 1, 2 and 3, as the 'dummy' palladium thimble unit was heated must be interpreted as being due to the formation of adsorbed layers of gas and decomposition products from the heated glass components, (c.f. 82).

The gases likely to be evolved are (a) hydrogen, previously chemisorbed during the flushing process, (122), (b) water vapour still present due to limitations on outgassing temperature, (viz the presence of lead glass), and liberated in glass decomposition, and, (c) oxygen also from glass

decomposition. Large particles of alkali metal compounds may be driven from the glass but these are unlikely to reach the cathode surface.

Allen and Mitchell, (97), have shown that copper, gold and silver films do not chemisorb hydrogen at room temperature and since physical adsorption would lead to a reduction in ϕ it is evident that hydrogen is not causing the observed increases of from 0.08 eV to 0.15 eV, (Figures 31, 35, 37, 38).

For the adsorption of water vapour on clean metals it is likely that the predominant force will be Van der Waals attraction and that the oxygen side of the molecule will be on the metal, (126). This would cause a dipole layer having its positive side outwards and would lead to a reduction in ϕ , (Figure 7). If the metal is covered initially with an adsorbed layer of hydrogen the introduction of water vapour would also lead to a reduction in ϕ since the hydrogen would be attracted to the negative end of the water dipole, i.e. the oxygen atom. In the case of a metal initially possessing an oxide monolayer, however, the effect would be an increase in ϕ since the oxide would present a negative charge which would attract the hydrogen atoms of the water and form a dipole layer having its negative side outwards, (126).

Oxygen, which is not chemisorbed by gold, would chemisorb on copper and silver films, (97), also causing an

increase in ϕ since it would be adsorbed as O^{-2} . The radius of the O^{-2} ion is 1.40 \AA and this indicates that a completely saturated monolayer would contain about 1.6×10^{15} ions/sq.cm.

The change in work function of a surface due to the presence of a dipole layer, containing n dipoles/sq.cm. each having charges of e coulombs separated by d cm., is given by $\Delta\phi = 4\pi ne^2d$ and application of this relationship to the case of O^{-2} ions indicates that a change in ϕ of 0.1 eV would require 2.7×10^{12} ions/sq.cm. This implies that each ion would dominate an area having a diameter of about 70 \AA .

The observed changes in ϕ took place within about 15 minutes and this would require a partial pressure of oxygen of the order of 10^{-8} mm.Hg.

When oxygen was admitted to tube 3 an increase in ϕ was observed of the same magnitude as the change caused by heating the dummy thimble, but this increase was preceded by a short 'pulse' decrease in ϕ , (Figure 39). This could have been due to an already high partial pressure of hydrogen causing the initial formation of a water vapour dipole layer which was followed by preferential chemisorption of oxygen, (Figure 6(b)). The activation energy for the reaction between hydrogen and oxygen to form the water molecules would have been provided by the oxygen producer, i.e. the filament causing the thermal decomposition of barium peroxide, and the presence of minute quantities of water vapour from

the glass or in its surface would have catalysed the reaction. The original physically adsorbed hydrogen layer, formed during the first 40 minutes after film deposition, would have been incomplete and a water vapour layer superimposed on it would have caused a decrease in ϕ

The changes in ϕ of a fresh metal film, when hydrogen was admitted by heating the palladium thimbles with an external oven, (Figure 35), are of the same magnitude as those caused by heating the dummy thimble and by admitting oxygen. They are probably due to outgassing and decomposition of the glass near the thimbles. The metal films would possess thin adsorbed layers soon after deposition but the work function would be initially raised by the formation of oxygen and water vapour layers from gases driven from the glass near the palladium. With the palladium at a sufficiently high temperature hydrogen would begin to diffuse through it and would displace the large adsorbed water vapour molecules, (preferential adsorption, Figure 6(b)), and cause the observed decrease in ϕ .

This explanation is supported by the changes followed (Figure 31), when the palladium was heated after the dummy unit had been operated for the same surface. A water vapour dipole layer would be formed at first and this would be gradually replaced by hydrogen.

The failure to detect any changes in ϕ when hydrogen

was admitted using the modified heater, i.e. by heating the metal directly, (Figures 37, 38), appears to support the conclusion that the adsorbed gases originated from the heated glassware. The presence of hydrogen, however, should have caused a decrease in ϕ due to the formation of a physically adsorbed layer but this was not observed. The effect may have been obscured by the formation of a complete hydrogen layer in the forty minutes following film deposition.

The attempt to fractionally condense the gases and vapours evolved from heated pyrex, (tube 4), yielded some useful information but such an analysis should have been made with a mass spectrometer, (Figure 42).

As the pyrex was heated, ϕ decreased by about 0.1 eV, a change which could have been produced by the release of adsorbed hydrogen. This hydrogen would not have been trapped by the liquid nitrogen. No change in ϕ was detected as the liquid nitrogen trap was removed, indicating that no materials with boiling points between -196°C and -10°C had been condensed. It is possible that oxygen, liberated from the pyrex, would have been condensed in the liquid nitrogen trap and adsorbed on the inside wall of the trap. This process would have been reversible on warming, if the adsorption had been physical, but chemisorbed oxygen would not have reappeared. It is more likely that such a small quantity of gas, evolved at 350°C and having a boiling point so near

to that of liquid nitrogen, would have only been delayed in passing through the trap with hydrogen. The initial cathode changes in Figure 42 may, then, have been due to physical adsorption of hydrogen followed by a small amount of oxygen chemisorption, the relative amounts of each being determined by the extent of initial hydrogen coverage of the cathode.

The sharp increase in ϕ of 0.45 eV as the carbon tetrachloride trap (at -10°C) was removed must have been caused by the release of water vapour which physically adsorbed on the insulating layer already present on the cathode. This change was much bigger than the changes seen on heating the dummy thimble units but this can be explained by the difference in temperatures of the two tests. The dummy units were baked at 250°C whereas the pyrex in tube 4 was heated to 350°C .

Conclusion

The foregoing discussion has shown that the changes in work function observed when admitting hydrogen to the experimental system can be satisfactorily explained on the basis of gas evolution from heated glassware and physical adsorption of hydrogen. The effects of glass decomposition were eliminated by a simple modification to the method of heating but it must be inferred that the use of glass vacuum equipment is undesirable in the study of clean surfaces for systems containing heated components. The main

limitation appears to be the low melting point of glass, and its consequent low outgassing temperature.

5.3. The Effects of Discharges

The Paschen curves obtained for copper and silver cathodes with the first and third tubes are shown in Figure 33. The curves for the variation of ω/α with E/p , in the range of E/p between 150 and 400, were calculated from the Paschen curves using Myatt's values of α , (37), and are shown in Figure 34. Although many determinations of α have been made in hydrogen Myatt's values were used since they were obtained for similar surfaces under similar conditions of gas purity and they are, therefore, likely to apply to the gas specimens used in this work.

The Paschen minima occur at 312 volts in the case of copper and 295 volts for silver. The work function of the copper in hydrogen was 4.46 eV immediately before sparking but the exact figure for silver was not obtainable at a similar stage. The figure before admitting hydrogen was 3.79 eV and comparison of this with the figure obtained for tube 2 in hydrogen shows that ϕ may have been higher during sparking. This would explain the low figure of 25 volts change in V_m obtained per electron volt change in ϕ (c.f. 50, 61, 67, 68).

The secondary emission curves show a marked dependence on ϕ at higher values of E/p , and very little

dependence for values of the order of 150.

The passage, in hydrogen, of a discharge of 10^{-7} amps for 10 seconds was used to confirm the existence of a cathode insulating layer (tube 1, Figure 32(a)), by following the changes in work function produced by positive ions on the cathode, (66, 68). The copper cathode of this tube would have possessed a fairly thick insulating layer since the changes caused by the admission of hydrogen had just been examined. The time constant for the decay of the observed change was, however, of the same order as for the changes seen by earlier workers, (66, 68).

Assuming that all the positive ions produced in the discharge were present on the insulating layer the number of ions would have been $6.25 \times 10^{+12}$. For a cathode of radius 1cm. this represents $2 \times 10^{+12}$ ions/sq.cm. The drop in ϕ caused by the ions was 0.42 eV and if we assume that only one quarter of the total number of ions remained on the insulating layer then this compares with the figures calculated earlier for 0^{-2} ions.

The time to half value for the decay (Figure 32(a)), was seven minutes and an estimate of the resistance of the insulating layer may be made from the equation $Q = Q_0(1 - e^{-t/RC})$.

The capacitance of the system, of area A, is given by $C = \frac{KA}{4\pi d}$ where the thickness of the layer of dielectric constant

κ is d cm. Assuming a figure of 6 for the dielectric constant and a film thickness of 6×10^{-8} cm the value of resistance becomes 22 Megohms.

Illumination of the ion layer with ultra-violet light caused its neutralization by photoelectrons from the metal, (Figure 32(b)).

Confirmation of the existence of a similar high resistance layer on the complicated cathode in tube 5 was also obtained by passing a discharge, (Figure 47(b)). In this case a change in contact potential difference of 3.25 volts was measured for a discharge of 10^{-6} coulombs, which decayed to a constant value in fifty minutes. Application of the equation for the discharge of a capacitor through a high resistance, as before, indicates a value of about 25 megohms for the resistance of the insulating layer.

Conclusion

The dependence of gas processes on the work function was illustrated by Paschen and secondary emission curves and a figure of 25 volts change in V_m per electron volt change in ϕ was derived from them. This figure must be regarded as low but indicates that a change in ϕ of 0.1 eV, which may be caused by the formation of an adsorbed layer, will change the sparking potential by at least 2.5 volts.

The layers of insulating material formed on clean metal surfaces, which mainly originate from heated glass

components, have resistivities of the order of 12×10^{14} ohms per centimetre cube.

5.4. The Production of Positive Ions from Hydrogenated Palladium

The property described in the previous section, where the presence of a layer of positive ions was indicated by a change in contact potential difference, was used in tube 5 as a means of detecting any positive ion emission during the diffusion of hydrogen through heated palladium.

The sensitivity of the method was such that a contact potential difference of 3.25 V corresponded to a discharge of 10^{-6} coulombs, (Figure 47(b)), and, assuming that all the positive ions of the discharge eventually rested on the insulating layer, the number of positive ions present must have been 6.25×10^{12} . It was possible to detect a contact potential difference of 0.005 volts, that is a total number of 9.6×10^9 ions. Such a charge could be delivered by 1.5×10^{-9} coulombs at a current of either 1.5×10^{-10} amps running for 10 seconds, or 1.5×10^{-11} amps running for $1\frac{1}{2}$ minutes.

If it is assumed that less than 1% of any ions produced eventually rested on the cathode, a positive ion current of 10^{-9} amps could have been detected. No contact potential difference change was detected or expected since no positive ion emission had been found by direct measurement.

No satisfactory explanation can be found for the

pulse of 10^{-11} amps detected 10 seconds after each switching on of the palladium heater. Any circuit effect should have either reversed on switching off the heater or have continued throughout the test. The one-way pulse observed must have corresponded to the thermal desorption of material from the palladium, an effect which would slowly reverse on cooling and which would take place after each heating. Such desorption must have been of physically adsorbed hydrogen, for which the ionization potential is about 15 volts.

No explanation can be found for the thermal desorption of positive ions, when the original adsorption must have been of molecular gas, except that hydrogen is electro-negative with respect to palladium, (hydrogen = 2.1, palladium = 2.2), and would have tended to donate its electron to the metal.

Conclusion

It seems that under the conditions described there was no proton emission greater than 10^{-14} amps.

The significant difference between this work and that described in Chapter II has been the temperature of the metal and it may be that previous workers have been collecting thermionically emitted ions. The fact that hydrogen is electronegative with respect to palladium may be the key to this problem in that there may be a substantial apparent reduction in the ionization potential of hydrogen

at a palladium surface.

5.5. The Stability of the Reference Surface

In order to test for changes in the gold reference surface during any of the experiments described in Chapter IV fresh gold films were deposited on both cathodes and kelvin electrodes.

In tube 6, (Figure 49), a fresh gold cathode was deposited having a thickness of about 4,000 Å. If both surfaces had been the same, the contact potential difference should have been zero but the steady work function of the cooled cathode surface was indicated as 4.72 eV, (Figure 49), that is a negative potential of 0.02 volts relative to the cathode had to be applied to the kelvin electrode for balance. Since gold does not chemisorb either hydrogen or oxygen the change seen immediately after depositing the fresh, cooled gold film must have been due to physical adsorption. Removal of the coolant led to a drop in ϕ of 0.04 eV to a value below that assumed for the reference surface. Such a process can be explained, as before, by further cathode adsorption of gas desorbed from the previously cooled glassware.

The remaining significant difference between the two gold films was their age. The discrepancy of 0.02 eV cannot be attributed to long term adsorption of many layers of gas since this would mean that the difference in ϕ should

have increased as the fresh film acquired further layers of its own. It is likely however, that some metal annealing process may have taken place slowly in the kelvin film leaving a more perfect lattice structure having a higher work function.

in order to confirm these observed changes, and to investigate the effect of artificially 'ageing' a metal film by raising its temperature, the cathode was first re-silvered with a thick film and a further gold film was then deposited. These depositions were carried out at room temperature and the final surface had a work function exactly the same as that for the previous test.

The effect of adding water at 85°C to the hollow cathode was a rapid rise in ϕ to a contact potential difference of zero, indicating that both surfaces were the same and adding weight to the hypothesis of metal annealing. Such a change could have been caused by the physical adsorption, on the already contaminated cathode, of water vapour driven from the glass cathode support by the increased temperature. It is unlikely, however, that sufficient water vapour would have been evolved at such a low temperature, (82).

The deposition of a fresh kelvin surface in tube 3, (Figure 39), caused an apparent decrease in ϕ of 0.40 eV but this must have been due to a former increase in ϕ of the kelvin electrode. The history of this tube was complicated

by the admission of oxygen which, together with the substantial amount of hydrogen evolved from the metal beads, must have formed a considerable amount of water vapour. Over the period of 10 hours before the fresh gold surface was formed a water vapour layer could have been built up on the kelvin electrode. The dipole moment of a water molecule is 1.85 debyes and this indicates that a change in ϕ of 0.40 eV would have required 5.8×10^{13} dipoles/sq.cm., i.e. each dipole would dominate an area having a diameter of about 15 Å.

Conclusion

The only processes likely to cause a change in the work function of the gold reference surface are those of physical adsorption and annealing of the metal film. The first of these may be eliminated by operating at a sufficiently low gas pressure and the second may be reduced by raising the temperature of the film for a short time. Comparison of these results for gold with those described for silver in section 5.9. shows that the temperature for efficient annealing should be at least 250°C.

5.6. Effects of Variations in Film Thickness

The apparent decrease in ϕ with thickness of the copper and silver films in tubes 1 and 3, shown in Figures 31 and 38, can be explained by the processes described in section 5.1., i.e. the processes of (a) physical adsorption in times of 40 minutes, (b) the building of a complicated sandwich

layer cathode, and, (c) progressive covering of the electrical contact to the surface, (see Section 5.9.).

The residual gas pressures were of the order of 10^{-9} mm.Hg. and the films were deposited at room temperature on to glass substrates having tungsten-aquadag electrical contacts. The decreases in ϕ immediately after deposition took place in times of between 40 and 60 minutes.

In the case of copper the lowest work function observed was 4.305 eV corresponding to a total thickness of about 1700 Å but this may not have been the minimum value observable, (there is a difference of 0.05 eV between the last two depositions). For silver the lowest value was 3.91 eV.

For comparison the results observed for equivalent thickness at one deposition, and under similar conditions, show a final value of 4.36 eV for copper, (Figure 45), and 4.45 eV for silver, (Figure 37). These results show that the presence of the sandwich layers reduced the work function of the copper film by 0.06 eV and the silver film by 0.54 eV.

From Figure 38 it can be seen that there is little difference in ϕ between the last two silver depositions and if the minimum value corresponds to a thickness of 1700 Å and the first film is about 600 Å thick, then the maximum depth within the film which affects the work function must be approximately 1100 Å.

Since the ionic crystal radius for silver is 1.26 Å

this indicates a depth of about 450 atomic layers, which appears to be in accordance with expectations, (85).

Conclusion

Silver films behave independently of the nature of the substrate for film thicknesses greater than about 1100 \AA . If the film contains a major discontinuity, for example in the form of a layer of trapped gas, the work function will be lowered if the discontinuity is within a certain critical distance of the surface.

The minimum work function of a regular sandwich cathode occurs for a thickness beyond which further layers cease to affect the value of ϕ . For silver this thickness corresponds to about 450 atomic layers.

This technique of investigating the structure of evaporated films could become very useful particularly in studying the effects of substrates under pressures of the order of 10^{-11} mm.Hg .

5.7. Effects of Cathode Cooling

In order to try to separate the effects of metal annealing and adsorption taking place for a freshly deposited metal film, a cathode was used, (tube 4), which could be cooled with liquid nitrogen. Any annealing should have been retarded and any adsorption should have been accelerated.

Unfortunately, the design of this tube was such that the whole envelope was immersed in liquid nitrogen and

presented a considerable area for surface cryogenic pumping.

The result obtained for silver indicates that the low temperature held up a component of the decay curve, (Figure 41), and that warming allowed the process to continue.

The residual gas pressure in this tube prior to cooling was of the order of 10^{-9} mm.Hg. and a monolayer would have been formed in about 40 minutes at room temperature. At the temperature of liquid nitrogen the rate of adsorption is increased by a factor of about 10 and a monolayer would have been formed in about four minutes.

Most of the adsorbable gases in the tube would have been taken up by the envelope on cooling and the pressure reduced to about 10^{-10} mm.Hg.

The cathode substrate would have cooled more slowly than the envelope (because of limited conduction along the tungsten rod support), and would not have been covered by such a thick gas layer.

On deposition of the film the rate of formation of the initial gas layer, which would most probably have been of physically adsorbed hydrogen evolved from the metal bead, would correspond to a pressure of about 10^{-10} mm.Hg. and a temperature of -196°C , and would form a monolayer in about 40 minutes.

The second part of the curve, (Figure 41), may be explained as being due to a combination of annealing and

further adsorption.

As the tube was warmed the metal annealing process would lead to a surface containing many imperfections and having a high roughness factor. (The film may in fact become porous, (83)). Warming of the envelope would also cause the desorption of a large quantity of hydrogen taken up during cooling. The net effect of these processes would be a further reduction in ϕ .

Similar changes, as those just described for tube 4, were observed with tube 6. The silver deposition was made when the substrate had been satisfactorily cooled with liquid nitrogen. At this stage the background pressure must have been less than 10^{-9} mm.Hg and the large area of cooled glass forming the re-entrant cathode tube must have held much adsorbed hydrogen.

The usual decay curve was followed, (Figure 49), for both the thin and thick cooled films corresponding to the formation of a monolayer of physically adsorbed hydrogen. The final cooled film although containing a sandwich layer, can be regarded as a single film since the second deposition was of a film considerably greater than 2000 \AA in thickness, (Section 5.6.).

Removal of the coolant caused a further decrease in ϕ of 0.16 eV compared to the similar change of 0.34 eV observed with tube 4. This change can be attributed to further

cathode adsorption of the hydrogen desorbed by the warming glass and such a process could operate if the hydrogen was adsorbed more readily on the metal than on the glass. The process would be assisted by any metal annealing.

The factor of 2 difference between the figures for tubes 4 and 6 is probably due to the difference between the areas of each tube cooled by liquid nitrogen and therefore able to adsorb and subsequently desorb hydrogen.

When the work function of the warm surface had remained constant for more than an hour the cathode was re-cooled with liquid nitrogen. This would have caused the re-adsorption of much of the previously desorbed hydrogen and would have given rise to a thick gas layer on the cathode. The change in temperature of about 212°C would have thermally contracted the silver film with a possible change in ϕ , but this change would probably not have amounted to more than about 0.02 eV. (For tungsten the thermal coefficient of ϕ is $6.5 \times 10^{-5} \text{ eV}/^{\circ}\text{C}$. (80).) The observed change of 0.09 eV must have been mainly due to the formation of a thick adsorbed hydrogen layer.

Conclusion

The attempt to retard any annealing process by cooling was complicated by enhanced adsorption at the low temperature and desorption on warming. The observed changes can be accounted for by these processes and the explanations

are supported by comparison with the results obtained at much lower gas pressure, (section 5.9.). It was not possible to separate any thermal dependence of ϕ because the adsorption effects led to much greater changes.

5.8. The Superimposition of Different Metals

A deliberate attempt was made with tube 5 to build a strained cathode by superimposing metals of different crystal structure. The metals chosen were (a) copper, which has a face centred cubic structure, (b) tin, which has a tetragonal structure at room temperature, and, (c) barium, which has a body centred cubic structure. The tin deposition at -196°C would be of the α , face centred cubic, grey allotrope having a density of 5.75 gm/cc but warming to above 18°C would cause the spontaneous phase transition to the β , white form of density 7.28 gm/cc. There would be a corresponding increase in work function during this transition. The previous work function measurements on these metals, those reported by Rivi re, (80), Anderson, (123), and Michaelson, (124), were obtained under similar conditions to those described in this thesis, and will be assumed correct for purposes of comparison. The published values are:-

copper	4.52 eV
tin (β)	4.11 eV
barium	2.52 eV

The first work function figure obtained was for a thick, cooled copper film and was measured within one minute of deposition, (Figure 45). The figure of 4.50 eV compares well with the quoted figure of 4.52 eV for clean copper.

The familiar decrease in ϕ was seen in the first 40 minutes and warming to room temperature caused a further decrease to 4.37 eV.

The first steady value must have represented equilibrium for the physical adsorption of hydrogen at 10^{-9} mm.Hg, and the second steady value must have represented the equilibrium at a higher pressure due to desorption from the glassware on warming. This would correspond to preferential adsorption by the metal.

Re-cooling in readiness for the deposition of tin was accompanied by a rise in ϕ of 0.015 eV due probably to thermal contraction of the film with consequent reduction in the lattice spacing.

If it had been possible to deposit an extremely thin layer, or even a monolayer, of tin on the copper an increase in ϕ would have been expected since tin is electronegative with respect to copper and would have tended to accept electrons from the copper thus presenting a barrier to the passage of electrons.

The quoted work function of tin, however, is 4.11 eV, that is less than that for copper. Deposition

of a film having a full band structure would, therefore, have led to a decrease in work function. (The figure of 4.11 eV quoted above for β tin must be higher than that for α tin because of the possible phase transition.)

Deposition of the cold, thin tin film will have led to a surface which may not have been continuous but which, because of the difference between the crystal structures of film and substrate, will have consisted of many disoriented crystallite islands each of sufficient thickness to have a band structure. The net result, after normal physical adsorption of hydrogen by the fresh metal surface, would have been the observed decrease in ϕ , (Figure 45).

Removal of the coolant would not have caused the tin phase change because the transition temperature of 18°C was never exceeded but the mobility of the tin atoms on the surface would have been greatly increased, (120), and much of the disorientation of the crystallites would have been removed. This would have resulted in a preferential orientation of the tin lattices with consequent lowering or raising of the average work function.

Tin reacts slowly, even at elevated temperatures, with hydrogen to form traces of SnH_4 and it must be concluded that any adsorption of hydrogen, even at room temperature, will be physical adsorption and will decrease the work function.

The final value of 4.05 eV is less than the quoted figure, (4.11 eV) and the discrepancy may be due to either the presence of lattice defects within the crystallites or the presence of a hydrogen sandwich layer less than 500 Å below the surface.

The rise in ϕ of 0.02 eV on re-cooling must have been caused by a temperature dependence of ϕ .

The second tin film was more than 3000 Å thick and the deposition was accompanied by a rise in pressure to 10^{-8} mm.Hg. The gas evolved must have been hydrogen although the tin bead was prepared under vacuum because much would have been taken up during the outgassing and flushing processes. Such an increase in pressure will have caused the formation of a monolayer in less than 4 minutes and it is not surprising that a steady work function was observed, (Figure 46). The value after warming to room temperature was 4.15 eV, i.e. 0.10 eV greater than for the first film, indicating that the minimum thickness for obscuration of the substrate had been exceeded.

From a consideration of the relative electro-negativities of barium and tin it was expected that a very thin layer of barium on tin would have caused an increase in ϕ . However, it was again found to be very difficult to control and measure the film thickness, and the abrupt decrease in ϕ of 1.85 eV on deposition must have been

caused by a layer of barium about 500 Å in thickness.

Barium is usually employed in ultra-high-vacuum systems as a getter because of its high chemical reactivity. Barium can chemisorb large quantities of hydrogen, (125), and since such adsorbed hydrogen would be in the form of the metal hydride it would behave as a negative ion layer and the work function should be increased, (c.f. Sachtler, 96).

The immediate increase in ϕ of 0.1 eV on deposition may have been due to reaction of the barium with the hydrogen already physically adsorbed on the cooled tin substrate and present in the tube at a residual pressure $\approx 5 \times 10^{-9}$ mm.Hg. The following decrease to the steady value of 2.25 eV may then have been due to diffusion of the hydrogen into the bulk of the metal film thus disturbing the already imperfect lattice structure.

Removal of the coolant would have caused the release of physically adsorbed hydrogen from the glassware and this would have immediately been chemically taken up by the barium to produce the observed increase in ϕ to 2.45 eV.

The interpretation of the changes taking place after the deposition of the thick barium film is complicated by the fact that it was not possible to outgas the barium source thoroughly because of the low temperature of barium emission. The getter source had to be heated strongly to deposit the thick film and foreign gases must have been

evolved from the support system. The final surface, however, exhibited a work function of 2.52 eV which is in exact agreement with the published values. This must imply that the published values, (123), were not those of the pure metal but rather those of the metal possessing a fairly thick chemisorbed layer.

Admission of hydrogen caused a sharp increase in ϕ to 3.41 eV which coincided with the apparent disappearance of the barium film from the tube envelope. The complete change required about 20 minutes and this must have corresponded to the time required for the hydrogen to diffuse to the middle of the film. The final cathode surface must have been of barium hydride on a tin substrate and must have behaved as a tin cathode possessing a thick, physically adsorbed dipole layer. This would explain the unexpectedly low work function of the composite surface.

A further possible explanation is that the barium hydride forms a thick layer of high dielectric constant but that this layer is powdery and not continuous. Such a film would expose parts of the substrate which must possess thick physically adsorbed hydrogen layers and the average work function of the surface would be low.

Conclusion

Unfortunately the relatively high residual gas pressure, (10^{-9} mm.Hg) caused adsorption effects which

again largely masked the annealing effects looked for in this experiment. However, the changes observed can all be satisfactorily explained by the processes of physical adsorption, in the cases of copper and tin cathodes, and chemisorption in the case of barium coupled with changes in microcrystalline structure of the surfaces on warming, (c.f. Section 5.9.).

It was not possible to arrange for the cooling of the cathode films without causing great changes in adsorption characteristics and it is clear that such an investigation must be made with much improved vacuum conditions.

5.9. Effects of Reduced Residual Gas Pressure

All the results obtained with tube 7 were for vacuum conditions at least an order of magnitude lower than for the other tubes.

The first measurements were made on the substrates of the two cathodes, the nickel substrate having a work function of 4.26 eV and the glass substrate (or the aquadag covered contact point on it) having a work function of 4.34 eV.

Cooling of the glass substrate led to a steady increase in the contact potential different, (Figure 52), indicating an apparent reduction in ϕ . After 15 minutes, however, the contact potential difference had risen to 10

volts and the change must have been due to the adsorption of positive ions produced in the ionization gauges.

The decay in work function after the deposition of the first exceedingly thin silver film, on the glass substrate, led to a steady value of 2.14 eV over a period of one hour. A pressure of 10^{-10} mm.Hg. would have caused the formation of a monolayer in times of about 7 hours and it was expected that if the fall in work function immediately after film deposition is due to physical adsorption then this change would be much retarded at the lower pressure. It seems, therefore, that the initial drop in ϕ must have been caused by some structural change in the thin film. In this case a re-orientation of the silver atoms into some preferred direction could have accounted for the change. This view is supported by the fact that the effect was not seen after subsequent depositions, an effect that would have been produced by epitaxial growth on the already oriented first film. This first film must have been only a few atomic layers thick since the work function of the nickel substrate was reduced to a value lower than that for either metal. This can be explained by the fact that nickel is electronegative with respect to silver and will tend to accept electrons from the thin silver leaving a positively charged outer layer and causing the observed decrease in ϕ .

Warming to room temperature must have increased

the mobility of the silver atoms to such an extent that globulation occurred with consequent diminution of the surface coverage. Under these conditions the silver would have behaved more like a bulk metal and the measured work function would have been the average of the amount of bulk metal and the amount of substrate presented. The increased temperature would have also allowed the diffusion of lattice defects in the crystal globules and the sharp rise of 1.61 eV would have been caused by both processes acting simultaneously.

The second and third silver depositions, (Figure 53), gave similar curves in the case of the glass substrate but the increases on warming were reduced to about 0.15 eV, probably because the substrate was completely covered and the change was caused entirely by the diffusion of bulk crystal defects.

In the case of the nickel substrate the decrease in ϕ , seen after warming the second film, was towards the value for a complete silver film and it can be inferred that the cold deposited material was drawn into the existing globules by some surface tension effect, thus leaving much of the substrate uncovered. (The nickel substrate was effectively much larger than the contact on the glass substrate and there may also have been some scale effect.) Warming may then have allowed more complete coverage of the nickel.

The work functions at this stage were 3.81 eV for the glass substrate and 3.95 eV for the nickel substrate and the difference seems to indicate that the substrate or its microstructure were still influencing the work function.

Both surfaces appear to have acquired monolayers of physically adsorbed hydrogen during the 15 hours following the third deposition, the work function of the glass electrode being lowered by 0.08 eV and the nickel electrode by 0.03 eV.

Raising the temperature of the glass electrode to 250°C, (Figure 54), assisted the annealing process and must have caused the thermal desorption of most of the gas taken up by the surface overnight. The final figure of 3.87 eV represented an increase of 0.14 eV due to desorption and annealing. Subtraction of the change caused by adsorption, (assuming this to be equal and opposite to the change caused by desorption), leaves a change of 0.06 eV that must have been due to annealing of most of the lattice defects and strains. The peak value of 3.92 eV may have been due to a dependence of ϕ on temperature.

Such a temperature dependence of ϕ was investigated in the final test when the silver film was cooled and warmed in the space of 45 minutes. The total change in ϕ was 0.020 eV for the temperature range of 212°C. This shows a temperature coefficient for silver of 9.5×10^{-5} eV/°C which is satisfactorily in accord with

expectations.

The final work functions of the two cathodes differed by 0.05 eV. This difference may have been due to differing orientations of each crystal lattice and differing substrate microstructures since the films were similar in every other respect.

Conclusion

The operation of tube 7 at a reduced residual gas pressure eliminated most of the troublesome adsorption effects experienced with other tubes. The observed changes in ϕ must, therefore, be interpreted as changes in crystal structure either by re-orientation or by diffusion of lattice imperfections. For exceedingly thin films ($<100 \text{ \AA}$) it is probable that there is a certain amount of globulation, caused by surface tension forces, which leads to increased substrate exposure.

It appears that evaporated films at room temperature have work functions that are lower than those of well annealed metals due to the presence of lattice faults. It has been shown that an increase in the work function of silver of 0.06 eV was caused by annealing to 250°C.

The final tube was also used to estimate the thermal coefficient for the work function of silver and a figure of $9.5 \times 10^{-5} \pm 11\%$ electron volts per degree centigrade was obtained.

5.10. Suggestions for Further Work

The present work has underlined the importance of ultra-high vacua in the study of surface changes, particularly work function changes.

Future investigations should proceed along two separate lines, (a) the effects of structural changes within the metal films at various temperatures and under residual gas pressures of the order of 10^{-11} mm.Hg, and (b) the effects of adsorption of single pure gases on clean metal surfaces.

It is clear, from the present work, that glass vacuum equipment is unsuitable for this type of study, due to limitations of outgassing temperature and doubtful stability. This could be shown conclusively by the use of a mass spectrometer to analyse the decomposition products present even after prolonged outgassing. Such an investigation is also necessary in view of the fact that metal deposition has been predominantly on to glass electrode substrates and since it is probable that sufficient energy is given to the substrate by the condensing metal to cause surface decomposition.

An investigation of the structural changes in thin films would require the use of an electron microscope or an electron diffraction technique to observe the migration properties of the metal atoms over a large range of temperatures. Any globulation or diffusion of lattice

defects could be readily detected by such techniques.

The effects of the adsorption of pure gases could be used to determine any quantitative relationships between the pressure of the gas and its temperature, the relative electronegativities of gas and metal, the dipole moments, (for asymmetric gas molecules), and changes in the work function of the metal produced by gas adsorption. Such a relationship may clarify the processes taking place when hydrogenated palladium is heated in a vacuum. Since hydrogen is electronegative with respect to both palladium and gold it may be possible to observe positive ion emission from gold when hydrogen is thermally desorbed from its surface.

The relationship between the thickness of a metal film and its work function should be investigated for a greater range of thicknesses by either introducing a gas layer into a film and observing its effect on the work function for various depths within the film or by progressively covering a substrate of different work function. These investigations may be complicated by structural changes due to the lack of epitaxy but the effects could be practically eliminated by suitable choice of materials. Either investigation requires a sensitive method of measuring film thicknesses. A possible method is now available whereby a resonating quartz crystal is loaded on one face by

metal deposition and the change in resonant frequency measured. The technique assumes that metal evaporation is directionally uniform over the range covering the specimen and the crystal, and it is possible to estimate thicknesses to within one angstrom unit.

The kelvin method of measuring work functions has been used throughout the present work and could be applied satisfactorily in a further study. The technique could be improved, however, by using electrically maintained oscillations. This could be achieved by mechanical resonance from a system outside the experimental tube.

REFERENCES

1. F.M. Penning and C.C.J. Addink: *Physica* 1. (1934), 1007.
2. H.S.W. Massey: Report on Conference on Ionized Gases.
Roy.Soc., 1953.
3. J.B. Hasted: Report on Conference on Ionized Gases.
Roy.Soc., 1953.
4. F. Horton and D.M. Millest: *Proc.Roy.Soc. A.*,
185, 381, 1946.
5. J. Freckel: *Z.Phys.* 51. 232, 1928.
6. Schottky, W.: *Phys.Z.* 15, 526, 1914.
7. G. Herrman, and Wagner, S.: "The Oxide Coated Cathode".
Chapman and Hall, 1951, pp. 16.
8. L. Kapitza: *Phil.Mag.* 45, 989, 1923.
9. M.L.E. Oliphant and P.B. Moon.: *Proc.Roy.Soc. A*,
127, 388, 1930.
10. G. Schneider: *Ann.Physik.* 11, 357, 1931.
11. P.F. Little: *Handbuch der physik.* Springer-Verlag.
1956, pp. 651.
12. Hagstrum, D.H.: *Phys.Rev.*, 96, 2, pp. 336, 1954.
13. O.W. Richardson; *Phil.Mag.*, 28, 633, 1914.
14. S. Dushman; *Phys.Rev.* 21, 623, 1923.
15. L.W. Nordheim: *Proc.Roy.Soc. A*, 121, 626, 1928.
16. L.W. Nordheim: *Phys.Z.*, 30, 177, 1929.
17. W. Schottky: *Phys.Z.*, 15, 872, 1914.

18. Stern, Fowler, Gossling: Proc.Roy.Soc. A 124,
699, 1929.
19. J.D. Cobine: Gaseous Conductors. Constable 1958
p. 118.
20. R.N. Bloomer and M.E. Haine: Vacuum 3 p. 128, 1954.
21. D. Alpert: Physics Today. Volume 16. 8. 1963, p.22.
22. Degras, Petermann and Schram: Vacuum Symposium Trans.
Macmillan, 1963, 447.
23. G. Moore: J.App.Phys. 32. 1241, 1961.
24. J.S. Townsend: Theory of Ionization of Gases by
Collision. (Constable, London), 1910.
25. J.S. Townsend: Phil.Mag. 8, 738, 1904.
26. T.L.R. Ayres: Phil.Mag. 45 353, 1923.
27. D.H. Hale: Phys.Rev. 56 1199, 1939.
28. L.J. Varnerin and S.C. Brown: Phys.Rev. 79,
946, 1950.
29. R.W. Crompton, J.W. Dutton and S.C. Haydon:
Proc.Phys.Soc.Lond. B,69 2. 1956.
30. W. Hopwood, N.J. Peacock and A. Wilkes: Proc.Roy.Soc.,
A,235 334, 1956.
31. D.J. de Bittetto and L.H. Fisher: Phys.Rev. 104
1213, 1956.
32. K.G. Emeleus, R.W. Lunt and J.M. Meek: Proc.Roy.Soc.,
A,156, 394, 1936.

33. J.S. Townsend: Electrons in Gases. Hutchinson, 1947.
34. D.J. Rose: Phys.Rev. 104, 273, 1956.
35. H.A. Blevin, S.C. Haydon and T.M. Somerville:
Nature 179, 38. 1957.
36. J.G.C. Milne: Ph.D. thesis University of
Birmingham, 1958.
37. J. Myatt: Ph.D. thesis University of Birmingham,
1959.
38. J. Fletcher; Ph.D. thesis University of Keele,
1963.
39. D.H. Hale: Phys.Rev. 55, 815, 1939.
40. H.D. Hagstrum: Phys.Rev. 89, 338, 1953.
41. H.D. Hagstrum: Phys.Rev. 91, 541, 1953.
42. H.D. Hagstrum: Phys.Rev. 104, 309, 1956.
43. H.D. Hagstrum: Phys.Rev. 104, 317, 1956.
44. H.D. Hagstrum: Phys.Rev. 104, 1516, 1956.
45. F. Llewellyn-Jones: Phil.Mag. 28, 192, 1939.
46. L.B. Loeb: Basic processes of Gaseous Electronics,
University of California Press, 1955.
47. F. Llewellyn-Jones and J.P. Henderson: Phil.Mag.
28, 185, 1939.
48. D.H. Hale: Phys.Rev. 54, 241, 1938.
49. A.A. Kruithof, and F.M. Penning: Physica 3,4,
515, 430, 1936, 1937.
50. H. Jacobs and A.P. La Rocque: J.App.Phys. 74,
163, 1948.

51. F. Llewellyn-Jones and D.E. Davies: Proc.Phys.Soc.
B.64, 519, 1951.
52. W. De la Rue and H.W. Muller: Phil.Trans.Roy.Soc.
171, 109, 1880.
53. F. Paschen: Weid Ann 37, 69, 1889.
54. J.S. Townsend and S.P. McCallum: Phil.Mag. 17
678, 1934.
55. F. Llewellyn-Jones and C.G. Morgan: Proc.Phys.Soc.
64, 500, 1951.
56. D.K. Davies, J. Dutton and F. Llewellyn-Jones:
Proc.Phys.Soc.Lond. 72, 1061, 1958.
57. D.K. Davies, J. Dutton and F. Llewellyn-Jones:
Fourth International Conference on Ionization
Phenomena in Gases. Uppsala 1 210, 1959.
58. D.E. Davies, D. Smith and J. Myatt: Conference
on Ionization Phenomena in Gases. Munich, 1961.
59. W.R. Carr: Phil.Trans. A.201, 403, 1903.
60. J.S. Townsend: Electricity in Gases. Oxford Clarendon
Press, 1915, Chapter 9.
61. H. Jacobs and A.P. La Rocque: Phys.Rev. 18, 199, 1947.
62. D.H. Hale and W.S. Huxford: J.App.Phys. 18, 586, 1947.
63. W.E. Bowls: Phys.Rev. 53, 293, 1938.
64. F. Ehrenkranz: Phys.Rev. 55, 219, 1939.
65. F. Llewellyn-Jones and D.E. Davies: Proc.Phys.Soc.
B.64, 397, 1951.

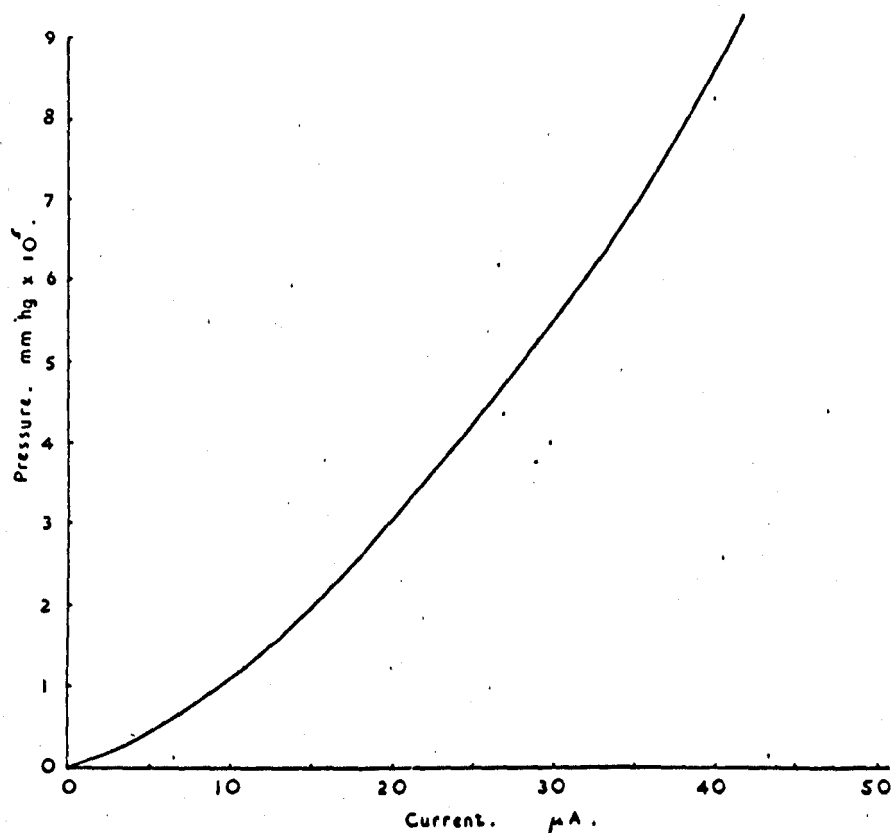
66. D.E. Davies and R.K. Fitch: Brit.J.App.Phys. 10
502, 1959.
67. D.E. Davies and B.J. Hopkins: Brit.J.App.Phys.
10, 498, 1959.
68. C.F. Gozna: Ph.D. thesis University of Birmingham,
1960.
69. F. Llewellyn-Jones and E.T. de La Perelle:
Proc.Phys.Soc. A.216, 267, 1953.
70. W. Rogowski: Arch. Electrotech. 16, 496, 1926.
20, 99, 1928.
71. C.G. Morgan: Phys.Rev. 104, 506, 1956.
72. J. Dutton, F. Llewellyn-Jones, S.C. Haydon and P.M.
Davidson: Proc.Roy.Soc. A.218, 206, 1953.
73. L.H. Fisher and B. Bederson: Phys.Rev. 81, 109, 1951.
74. G.A. Dawson: Ph.D. thesis University of Birmingham,
1963.
75. B.P. Betts: Uncompleted and unpublished work, Keele
1963.
76. P.A. Anderson: Phys.Rev. 115, 553, 1959.
77. E.W.J. Mitchell and J.W. Mitchell: Proc.Roy.Soc.
A.210, 70, 1951.
78. W.A. Zisman: Rev.Sci.Inst. 3, 367, 1932.
79. J.W. Mitchell: Private communication, University of
Bristol, 1959.
80. J.C. Rivière: Proc.Phys.Soc.Lond. B.70, 676, 1957.

81. R.E. Hayes, R.W. Alsford and D.I. Kennedy: Conference on Sorption properties of vacuum deposited metal films, Liverpool, April 1963.
82. D.G. Bills and A.A. Evett: J.App.Phys. 30, 564, 1959.
83. A.D. Crowell and A.L. Norberg: J.Chem.Phys. (U.S.A.). 37, 714, Aug. 1962.
84. J. Kivel, F.C. Albers, D.A. Olsen and R.E. Johnson: Journal of Phys.Chem. 67, 1963.
85. M.J. Morant and H. House: Proc.Phys.Soc. B. Vol. 69, p. 14, 1956.
86. T.J. Lewis: Proc.Phys.Soc. B. 67, 187, 1954.
87. H.E. Farnsworth and R.E. Schlier: J.Phys.Chem. Solids. 6, 271-6, 1958.
88. C. Herring and M.H. Nichols: Rev.Mod.Phys. 21, 183, 1949.
89. L.L. Blackmer and H.E. Farnsworth: Phys.Rev. 77 826, 1950.
90. Ying Chung Fu., and H.E. Farnsworth: Phys.Rev. 85, 485, 1952.
91. H.E. Farnsworth: Proc.Phys.Soc. 71, 703, 1958.
92. D.J. Moppett: Bulletin of Inst.Phys. and Phys.Soc. 292, 1961.
93. Garron, R.: C.R. Acad.Sci. Paris, 254, 243, 1962. 254, 4278, 1962; 255, 1107, 1962.

94. D.E. Davies, G.A. Dawson and C.F. Gozna: Conference
on Ionization Phenomena in Gases. Munich, 1961.
95. E.E. Donaldson and M. Rabinowitz: J.App.Phys.
Vol. 34, No. 2, 1963.
96. W.M.H. Sachtler: J.Chem.Phys. Vol.25, No. 4, 1956.
97. J.A. Allen and J.W. Mitchell: Disc.Faraday Soc.
Heterogeneous Catalysis, 361, 1950.
98. J.B. Taylor and I. Langmuir: Phys.Rev. 49, 878, 1936.
99. C.F. Gozna: M.Sc. Thesis, University of Birmingham,
1958.
100. D.J. Rose: J.App.Phys. 31, 643, 1960.
101. F. Llewellyn-Jones and C.G. Morgan: Proc.Roy.Soc.
A. Vol. 218, p.88, 1953.
102. R.H. Fowler, and L. Nordheim: Proc.Roy.Soc. A. 119
173, 1928.
103. F. Llewellyn-Jones: Brit.J.App.Phys. 1, 60, 1950.
104. H. Hulubei: Comptes Rendus 199, 1934.
105. M. Wolfke and J. Rolinski: Phys.Zeits. 30, 817,
1929.
106. F. Goldmann: Ann der Phys. 10, 460, 1931.
107. Y. Sugiura: Inst.Phys. and Chem.Research Tokyo.
16. No. 310, 1931.
108. R. Kollath: Zeits für Phys. 94. 397, 1935.
109. R.G. Stansfield: Proc.Camb.Phil.Soc. 34, 1938.
110. Bachman, C.H. and P.A. Silberg: J.App.Phys. 29
1266, 1958.

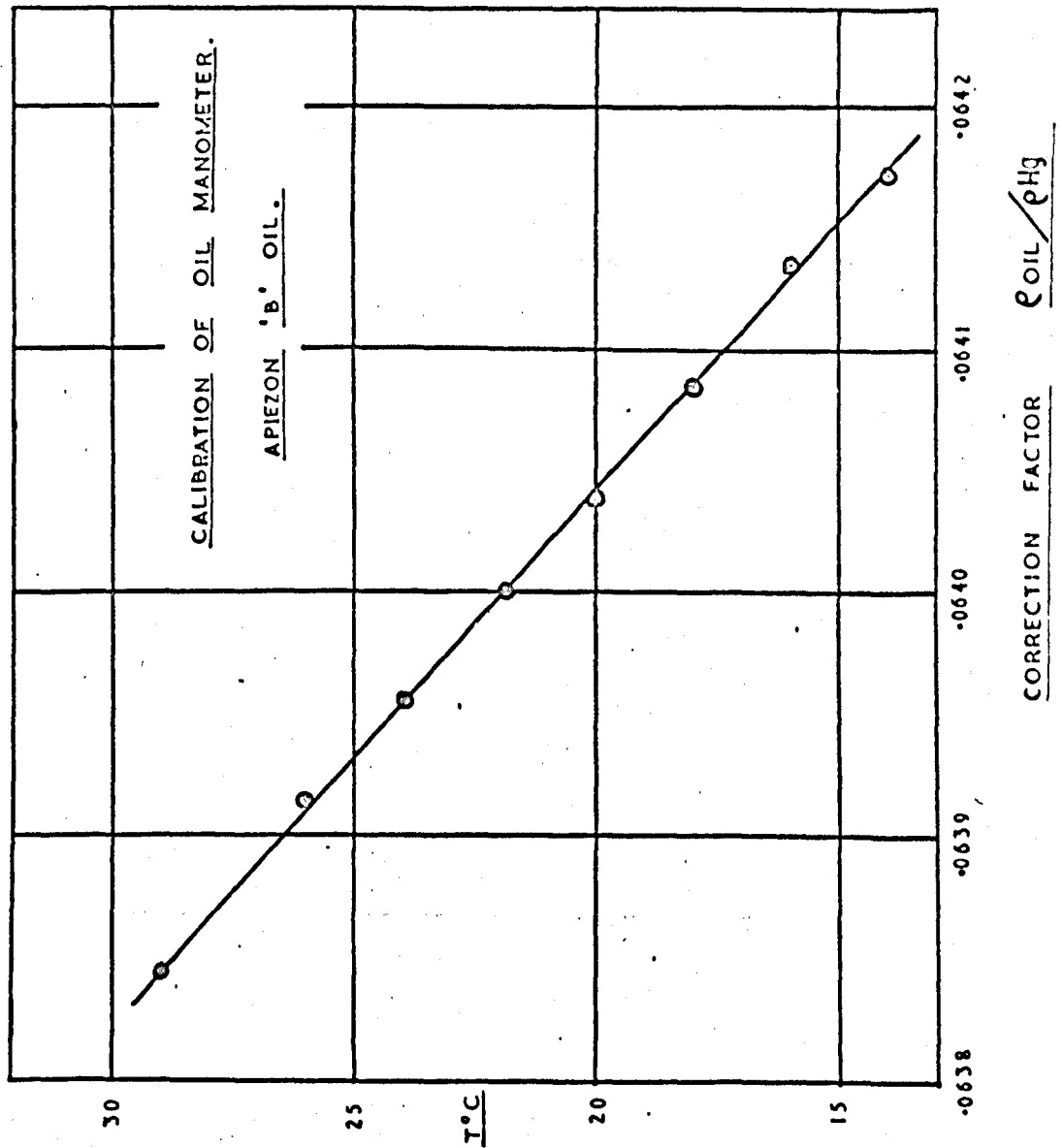
111. R.W. Crompton and M.T. Elford: J.Sci.Inst. 39, 480, 1962.
112. J.B. Hunter: Plat.Metal Review 4 130, 1960.
113. C.S. Bull: B'ham Coll.Adv.Tech. Private communication, 1962.
114. J. Yarwood: J.Sci.Inst. 34, 297, 1957.
115. R.T. Bayard and D. Alpert: Rev.Sci.Inst. 21, 571, 1950.
116. D. Alpert: J.App.Phys. 24, 7, 1953.
117. G. Carter and J.H. Leck: Proc.Roy.Soc. A. 260 303, 1961.
118. L. Holland: Vacuum deposition of Thin Films. Chapman and Hall, 1956.
119. W. Steckelmacher, et al.: Vacnique, Vol. 3, 11-12, 1963.
120. Pashley et al.: Proceedings of Conference on Electrical and Magnetic Properties of Thin Films London, December 1963.
121. A. Von Engel: Ionized Gases. Clarendon Press, 1955.
122. T.W. Hickmott: J.App.Phys. 31, No. 1, 128, 1960.
123. P.A. Anderson: Phys.Rev. 59, 12, 1941.
124. H.B. Michaelson: J.App.Phys. 21, 536, 1950.
125. T.A. Giorgi and F. Ricca: Second International Symposium on Residual Gases in Electron Tubes, Milan, 1963.
126. J.H. de Boer: Electron Emission and Asorption Phenomena, Cambridge, 1935.

Calibration Curve for Penning Gauge in Hydrogen.

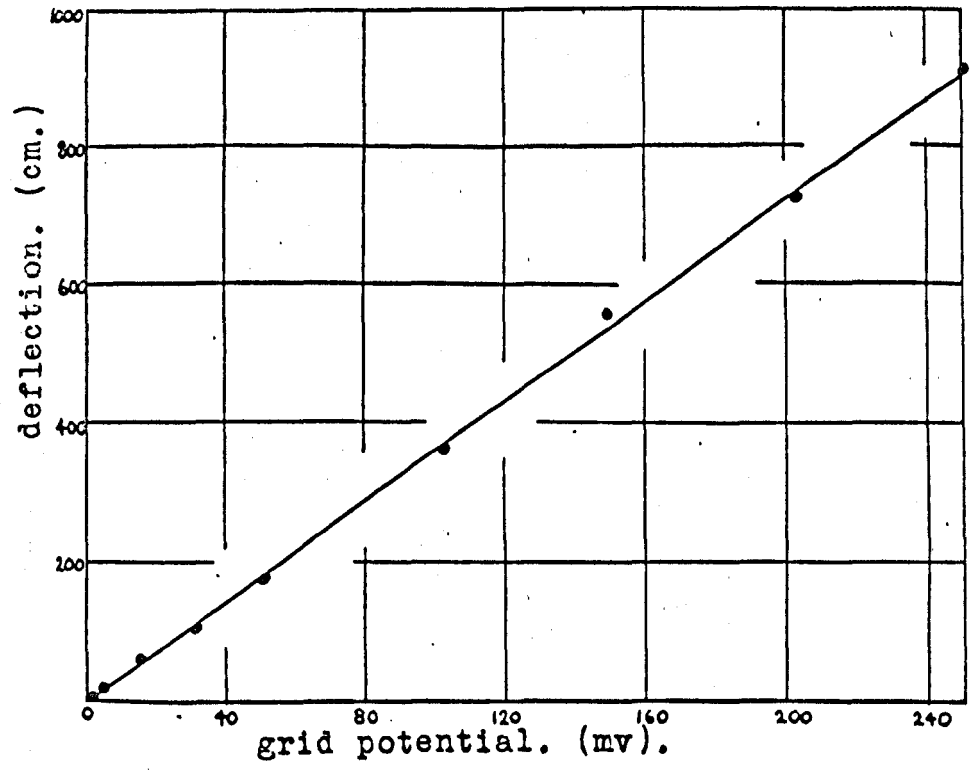


Appendix. (1).

Calibration of Oil Manometer.



. Appendix. (2).



Appendix. (3).

Results for Figures 33 and 34.

Paschen Curve for Copper Cathode in Hydrogen

Values of ω/α calculated using Myatt's values of α/p .

$P_0 d (\text{mm.Hg.cm.})$	$V_s (\text{Volts})$	$E/p_0 (\text{C/cm/mm.Hg.})$	ω/α
0.54	367	678	-
0.93	325	349	0.149
1.15	312	272	0.090
1.25	312	249	0.072
1.50	319	212	0.045
2.10	346	165	0.018

Variation of E/p_0 with α/p_0 as measured

by Myatt (1960)

E/p_0 (V/cm./mm.Hg.)	α/p_0 (cm ⁻¹ mm.Hg ⁻¹)	E/p_0 (V/cm.mm.Hg.)	α/p_0 (cm ⁻¹ mm.Hg ⁻¹)
60	0.47	220	2.11
70	0.68	240	2.14
80	0.86	260	2.16
90	1.05	280	2.18
100	1.22	300	2.19
120	1.50	325	2.19
140	1.75	350	2.19
160	1.89	375	2.19
180	2.01	400	2.20
200	2.06		

Physical Constants of the Metals Investigated

Element	Ionization potential (Volts)	Electro-negativity	type of crystal structure	Lattice spacing (Å)	density (gm/cc)	Work function (eV)
H	13.53	2.1	-	-	-	-
Cu	7.68	1.9	F.C.C.	3.615	8.93	4.52(R)
Sn(β)	7.30	1.8	T.	5.831	7.29	4.11(M)
Sn(α)	7.30	1.8	D.C.	6.470	5.80	-
Ba	5.19	0.9	B.C.C.	5.025	3.78	2.52(A)
Ag	7.54	1.9	F.C.C.	4.085	10.49	4.31(R)
Ni	7.61	1.8	F.C.C.	3.524	8.60	4.74(R)
Au	9.18	2.4	F.C.C.	4.078	18.88	4.70(R)
Pd	8.30	2.2	F.C.C.	3.890	12.16	4.49(M)
C	13.55	3.5	-	-	-	-

F.C.C. - Face centred cubic

T. - Tetragonal

D.C. - Diamond cubic

B.C.C. - Body centred cubic

R - Rivière

M - Michaelson

A - Anderson